UNIVERSITÀ DEGLI STUDI DI TORINO

**SCUOLA DI DOTTORATO IN SCIENZE
DELLA NATURA E TECNOLOGIE INNOVATIVE**

**DOTTORATO IN
SCIENZE AGRARIE, FORESTALI ED AGROALIMENTARI**

CICLO XXX

Metrology applied to agrometeorology and forecasting models for agro-food sciences technologies

Francesca Sanna

Docente guida:
Prof. Angela Calvo

Co-tutor:
Dr. Andrea Merlone

Coordinatore del ciclo:
Prof. Aldo Ferrero

ANNI:

2014; 2015; 2016; 2017

Summary

1. Introduction

Meteorological data have many applications in the prevention of natural adversities of climate origin, in programming and addressing the human activities, in the use of resources and in territorial planning. Besides weather networks, local agro-meteorological stations provide useful data in forecasting models to support management decisions at enterprise level, to contain costs and to reduce the impact of farming activities on environment. High quality traceable records of measured parameters are necessary for more accurate estimation and forecasting.

The phytopathologies are influenced by both culture conditions (varietal susceptibility, soil type, fertilizations, irrigations, etc.) and by seasonal meteorological trends. The cultivation techniques can change, to create an environment more favourable to the crop and unfavourable to the pathogen or pest (appropriate manner and sowing time, fertilizing appropriately proportioned, etc.), while it is not possible to act on the climate.

Climatic conditions can influence the onset of infestations and infections. The “on schedule” philosophy is inspired by the use of fungicides and insecticides to maintain consistent crop protection, starting treatment early in the season and continuing at regular intervals until the harvesting, without taking into account actual state. Increased environmental concern has led to this strategy being reconsidered, introducing methods to substantially reduce the use of chemicals, limiting their use only when absolutely necessary. The monitoring carried out in the field, for example, can avoid treatments executed in the absence of the pathogen or pest. These observations can be used to evaluate whether the disease or infestation can be maintained at levels

so low as not to warrant chemical interventions. The use of forecasting models can assist in this evaluation.

The success of any investigation or study depends upon the availability of reliable data. Meteorological data should be collected under standard conditions in accordance with established practices, both for observations and for the exposure of instruments. Weather stations should be equipped with standard approved instruments but robust traceability to the national standard is not always defined. In particular, agricultural weather stations are mostly not calibrated or on site calibrations by comparison are performed. Therefore, it is necessary to define protocols ensuring the traceability to national standards and that the calibration procedures are metrological correct, in order to improving the reliability of forecasting models.

1.1. Agrometeorology

The agrometeorology is the branch of meteorology that deals with the relationships of weather and climate to crop, livestock production and soil management. It is concerned with the meteorological, hydrological, pedological and biological factors that affect agricultural production and with the interaction between agriculture and the environment. Its objectives are to elucidate these relations and to assist farmers in preparing themselves by applying this supportive knowledge and information in agrometeorological practices and through agrometeorological services (WMO, 2010).

Agrometeorology of land surfaces extends from the soil layer of the deepest plant and tree roots (pedosphere), through the air layer near the ground in which crops and trees grow and animals live, to the higher levels of the atmosphere in which processes such as the transport and dispersal of dust, seeds and pollen take place. Its fields of interest range from agricultural production, including horticulture, animal husbandry, fisheries and other forms of outdoor and indoor production. Other important subjects are agroclimatic characterization, pests and diseases and their safe control, covered agriculture, quality of agricultural products, animal comfort aspects, plant cultivation and environmental impacts.

The first, most visible and impact signal of the human activity on the environment is represented by climate change, strictly linked to the emission of greenhouse gases. Agriculture accounts for 52% and 84% of global anthropogenic methane and nitrous oxide emission, respectively, released into the atmosphere and potentially causing hazard to man, animals, eco and agro-system (Maracchi *et al.*, 2008). Together with energy, land use is becoming a main problem: land is needed for food crops, for producing renewable biomass energy, for urban-industrial uses, transport, material extraction, refuse deposition,

but also for leisure, recreation and nature conservation. Despite of the advantages in the knowledge-based and technological models, a drastic revision of our concepts of economic model is impellent, although precision agriculture will allow to use crop models and monitoring technologies to apply correct input, adjusted to the environment, including meteorological variables (Mc Bratney *et al.*, 2005). Strategies in agricultural activities to help farmer to better and less riskily produce in a climate change scenario constitute a potentially great value for agriculture. At the same time, the adoption of environmentally sustainable practices in the field may reflect on climate, allowing agriculture itself to positively act to contrast climate change.

Agrometeorology can also play a significant role in reducing the negative impacts caused by pests and diseases. An appropriate, preferably integrated, pest management system using meteorological and microclimatological information can reduce pre and post-harvest losses appreciably. Agrometeorologists are now collaborating not only in the experimental stages but also during the operational stages of pest and disease control (Rossi *et al.*, 2012). Support systems for agrometeorological practices and services include data (and therefore quantification), research, training, education and policy environment. Mathematical models are increasingly used in operational agricultural meteorology to provide inputs to Decision Support Systems (DSSs). These models have relied on meteorological observations but now also benefit from operational numerical weather and climate predictions. These forecasts may be exploited to increase the utility of models for decision-makers, although this remains extremely difficult in practice (WMO, 2010). Detailed observations/monitoring and real-time dissemination of meteorological information, and derived indices and operational services, are important for tactical agrometeorological decisions in the short-term planning of agricultural operations

(Monteith and Unsworth, 2007). The practical application of this knowledge is linked to the availability and accuracy of weather and climate forecasts. The requirements range from accurate details of short-range weather forecasts (less than two days), to medium range forecasts (less than 10 days), to seasonal predictions of climate patterns.

Regardless of the type of decision, an ever-improving understanding of the effects of weather and climate on soils, plants, animals, trees and related production in farming systems is necessary for decision-makers (farmers and managers), to ensure timely and efficient use of meteorological and climatological information and of agrometeorological services for agriculture. Decision-making in agricultural operations for healthy crops or crops damaged by pests, diseases and/or other environmental disasters, needs weather forecasting and climate prediction with the required accuracies. However, the probabilistic character of forecasting remains one of its larger difficulty in wider applications. This is also due to the lack of the model input data accuracy of the observed meteorological parameters.

The observation of meteorological conditions of importance in agricultural production involves physical measurements, from the upper-level recordings of radiosonde equipment to the soil depth, where nutrient movements towards root systems occur. Quantification by physical methods is the basis for researching and understanding processes that explain phenomena determining growth, development and yields of important plant and animal species in agriculture. Observations of the physical and biological variables in the environment are essential in agricultural meteorology. Without quantitative data, planning, forecasting, research and services, agrometeorologists cannot properly assist agricultural producers to

meet the ever-increasing demands for food and agricultural products. Such data also need to assess the impacts of agricultural activities and processes on the environment and climate. When cause and effect relationships are better known, mechanistic modelling assembles such knowledge to provide mathematical representations of the processes involved. Empirical values for parameters and even empirical representations of sub-processes, to simulate phenomena, are still used, but error analyses are often weak (Monteith, 2000).

A number of crop monitoring systems are now being implemented worldwide. They have different degrees of complexities. More mechanistic models are now available, but many of these models need to be further refined and tested before being widespread applied. These models should, after all, address the composite problem of global climate, regional weather variability, agricultural productivity, decision-making and economic responses. Models can be useful only if they get real input data and if additional real observations are available to check the validity of model output (Sanna *et al.*, 2014). Parameters, such as humidity, temperature, solar radiation, wind, precipitation and soil moisture are very important in agrometeorology. Such measurements require specialized equipment, i.e. weather stations that provide information that is useful for operational agrometeorological purposes and in the management of risks and uncertainties.

Therefore, it is of utmost important that these instrumentations are well characterized (type, calibration, maintenance), their exposures defined (mounting, siting, etc.) and based on international guidelines, their observation, such as sampling, averaging, frequency of measurements, and recording, are associated with documented procedures traceable to the International System of Units (SI) and the measurement uncertainty well defined and evaluated.

1.2. Vine and vineyards

1.2.1. *Taxonomy and distribution area*

The vine belongs to the botanical species *Vitis vinifera* L. The cultivated varieties (vines) are classified in the subspecies *sativa*. The wild forms from which the domestic ones derive are instead classified in the subspecies *silvestris*. Other species of the genus *Vitis*, important for viticulture, are those of North American origin that, directly or more frequently through hybridization, have given rise to varieties for rootstocks (*V. rupestris*, *V. riparia* and *V. berlandieri*) or for the grape production (*V. labrusca* and *V. aestivalis*), while in the Southwestern states of the USA is also cultivated the *Muscadinia rotundifolia.*

In the European countries hybrid varieties are still marginally cultivated, which in the recent past has been considerable species in France, even though is no longer permitted for commercial vinification purposes. In Southeast Asian countries is cultivated the *V. amurensis*.

1.2.2. *Cultivation limits*

The vine is a perennial, deciduous woody plant of temperate climates. In order to complete its annual cycle, it needs an adequate cold winter period to which it is prepared by going into quiescence. The entry into quiescence follows a series of physiological adaptations to the low temperatures manifested by the lignification of the shoots and the fall of the leaves. Moreover, the resistance to winter colds is relatively limited compared to other plants of temperate climates; in the middle of vegetative rest, temperatures below -15 °C can already cause irreversible damage to the plants. This limits the distribution area to the regions with an average annual temperature of not less than 10 °C, within the durations of the

growing season and average daily temperatures above 10 °C for at least 200 days.

Relatively arid environments are suitable for the vine. It is a species that requires large amount of light (heliophilous) and therefore in nature it is always found in well-exposed sites, on the edge of the woods, in the clearings, along the hedges. From the cultural point of view, fruiting and good ripening of the grapes require a high availability of light.

1.2.3. *Morphology and development*

The vine is a plant with a potentially perennial life cycle but in modern viticulture the age of the vineyard tends to decrease to 20-25 years, due to the loss of general efficiency of the plant, caused by a progressive loss of productive efficiency of the plants, to physiological and pathological causes, as well as for technical and economic obsolescence. In nature, the reproductive system of the vine is mixed. The new individuals derive both by generative way, through the seeds, and by vegetative way, thanks to the ability of the shoots of one and two years to emit roots and to become autonomous, if separated from the mother plant. In the cultivated vine, the seed is not used for the multiplication of the plant, except for genetic improvement purposes.

The plant consists of a root system (hypogeal part) branched into the ground and of a cauline system that instead articulates above the ground (epigeal part); in turn made up of the woody structures (skeleton) and the herbaceous ones. The whole of the shoots system, constituted in turn by an axis on which the leaves are inserted, the lateral shoots, the clusters and the tendrils, represents the foliage of the plant. In most of the wine-growing regions of the world, the cultivated vines derive from the grafting between a variety of *V. vinifera* and a hybrid of American species, used as a

rootstock for resistance to *Daktulosphaira vitifoliae* attacks. This disease, also known as phylloxera, is an insect native to North America that has spread in Europe since the last quarter of the nineteenth century, destructive to the radical apparatus of the *V. vinifera.*

1.2.4. *Fruit: anatomy and development*

From a botanical point of view, the fruit of a vine is a berry. The fruit (pericarp) consists of the peel (exocarp), the pulp (mesocarp) and a thin internal epidermis that separates the pulp from the seminal lodges (endocarp). The growth of the berry is described by a curve in the form of a double sigmoid, which can be subdivided into at least three successive phases:

- phase 1 or herbaceous, the berry maintains vegetative characteristics, progressively accumulates tartaric acid and malic acid and the grape seed develops;
- phase 2 or stasis, the berry stops the growth and there is a reduction of the biosynthetic activities. The duration of the stasis can vary from a few days, in the early varieties, up to 20-30 days in the late ones;
- phase 3 or maturation, the veraison begins and the berry deeply modifies the mechanical and composition characteristics.

In its entirety, the maturation process involves the following aspects:

- growth of the berry, which doubles in weight and volume;
- modification of its mechanical consistency, following modifications of the cell wall structure and reduction of cellular turgor;
- accumulation of simple sugars (glucose and fructose) which at maturity can represent up to 20% of the fresh weight of the berry juice;

- reduction of acidity and increase in the pH of the juice. This is the consequence of the oxidation of malic acid, of the dilution and salification of both malic acid and tartaric acid;
- degradation of chlorophyll and appearance of yellowish coloration of carotenoids (white berry variety), or appearance of coloration, from grey-pink to intense blue (red berry variety), due to the accumulation of anthocyanins in the peel;
- accumulation of amino acids (especially proline and arginine) and low molecular weight proteins;
- partial inactivation of tannic molecules that are complexed with oligosaccharides and proteins;
- accumulation of aromatic molecules and their precursors.

1.2.5. *Phenology of the vine*

Phenology studies the annual cycle and how it is influenced by genetic differences and environmental variations, among which the climate and the meteorological course are more relevant. The annual cycle of the vine is articulated by the vegetative growth resumes (March-April) at the entrance to winter rest (November-December).

The phenological phases as for the BBCH scale (Biologische Bundesanstalt, Bundessortenamt und CHemical industry, 2001) are summarized in this section and these are better described in the following section 1.2.9.2.

The spring awakening of the plant is characterized by the progressive hydration of woody tissues which, at the same time, become less resistant to low temperatures. It following the hydrolysis of the starch stored as a reserve in simple sugars (glucose). Approximately one week after the rehydration, the buds start to swell (*bud swelling*), then a thick hair

produced inside the bud becomes visible to protect the meristematic apices (*wool stage*). The tip of the first leaflet becomes visible (*green shoot tips*). It follows the appearance of basal leaflets (*bud burst*) then the distension of the first leaflet and the lengthening of the internode subtended to it (*first leaf unfolded*).

At this stage the budding process must be considered completed. The inflorescence becomes visible when the fifth leaf is separated from the apex. At that stage, however, the secondary stalks are not yet distinguishable and the little flowers form a shapeless bunch (*inflorescences visible*).

Subsequently, the *inflorescences swelling* phase are characterized by the rachis extension and bunches separation from the apex. Then the secondary stalks separate and the florets become distinguishable (*inflorescences developed*). The bloom lasts for about 10-15 days depending on weather conditions. The single flower full bloom in 2-3 days (*first flowerhoods*), a bunch in a week, a plant in 10 days, a vineyard even in 15 days. The hot and sunny weather conditions accelerate the phenomenon, the cold and the rain slow it down.

The fruit set follows the bloom while continuing the growth of shoots. Also the growth of the berries begins, that during their development are classified by dimension in "*berries groat-sized*", then in "*berries pea-sized*". The further growth of the berries causes the closure of the bunch (*beginning of ripening*). In this phase, the shoots generally cease to grow. The berries then enter the stasis of growth before veraison (*berries ripe for harvest*).

During the ripening of the grape the lignification of the shoots begins, then the plant starts the winter rest with the senescence, the fall of the leaves

(abscission) and the ends of the non-lignified shoots. The lignified parts progressively dehydrate and wait for the warmth of spring to induce awakening. With the progress of the ripening of the branch, the gems pass from the state of *endo-dormancy*.

This transition implies the inability of the bud to germinate if not after having spent a certain period at low temperatures, such as at least 7 consecutive days with temperatures below 10 °C. Then the buds are capable of activating the processes of vegetative growth responding to active temperatures (greater than 7-8 °C). Dormancy in this phase is called *eco-dormancy*, i.e. due to environmental conditions.

1.2.6. *Photosynthetic activity*

As is known, photosynthesis is the conversion of water and carbon dioxide into simple sugars (glucose), which occurs in green tissues of plants thanks to the presence of chlorophyll. More generally, photosynthesis allows plants to convert the electromagnetic energy associated with light radiation into chemical energy contained in organic molecules, which in turn are the source of materials and energy used in life processes. The whole physiology of growth and fructification depends on the overall extent of photosynthesis.

There are both internal plant and environmental factors on which photosynthesis depends. The availability of light and temperature are the most important environmental factors; among those inside the plant, the degree of opening of the stomata, conditioned in turn by the water status of the plant; physiological age and nutritional status of the leaf; the presence of sink organs, such as fruits, shoot tips and roots, and the reserve tissues.

The photosynthetic intensity is typically expressed in micromoles of carbon dioxide (CO_2) assimilated per square meter of leaf per second (µmol m^{-2} s^{-1}). Solar radiation with photosynthetic efficacy is substantially that one of the wavelength in the visible spectrum, ranging from 400 to 700 nm, it is therefore called photosynthetically active radiation or PAR. The PAR in plant physiology is expressed in microns of photons per square meter of leaf per second (µmol m^{-2} s^{-1}). The response in terms of net photosynthesis (difference between gross photosynthesis and the total dark- and photo- respiratory losses of CO_2) of the single leaf as a function of PAR follows a curve characterized by an increasing section followed by a horizontal portion. In the growing stretch occurs an increase of net photosynthesis with increasing light intensity, in the horizontal section there is no longer increase in net photosynthesis as the light intensity increases (Wohlfahrt and Gu, 2015). The single vine leaf reaches this point around 800-1000 µmol m^{-2} s^{-1} of photons. On a sunny day in June in Mediterranean areas, the intensity of PAR reaches even 2000 µmol m^{-2} s^{-1}. This means that about 50% of the maximum radiation achievable in the best lighting conditions is sufficient to make the single leaf photosynthetic system work as fully as possible (Figure 1).

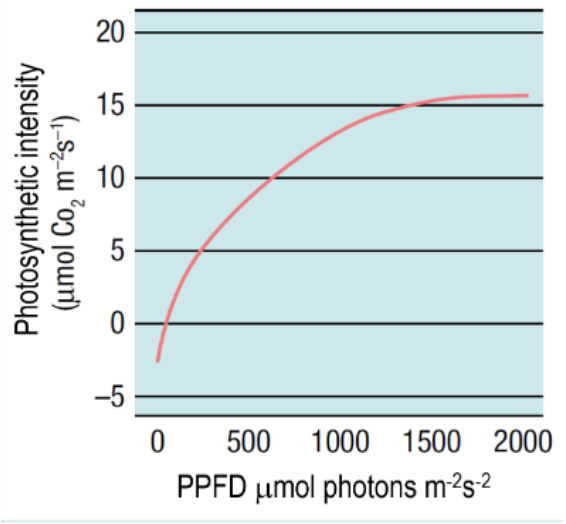

Fig. 1. Response intensity of net photosynthesis as the photosynthetic photon flux density (PPFD) change (Wohlfahrt and Gu, 2015)

The luminous intensity corresponding instead to the point of the curve below which

the net photosynthesis is negative, since the CO_2 released by transpiration exceeds that assimilated by photosynthesis, is called compensation point. In the vine corresponds to about 50 μmol of m^{-2} s^{-1} photons.

Temperature is another environmental factor of great importance in regulating photosynthesis. Likewise to PAR, the relationships between photosynthesis and temperature can be described with a curve, which presents an initial growing segment, a central horizontal and a final decreasing one. The curve identifies a minimum temperature (about 10 °C) below which the photosynthesis it is very low or zero, an optimal temperature range, between 25-30 °C, and a maximum temperature (about 45 °C) above which the net photosynthesis is cancelled (Greer and Weedon, 2012).

The degree of stomata opening is the main internal regulation factor of photosynthesis. In fact, CO_2 reaches the photosynthetic tissue through stomatal openings. If they are closed, photosynthesis stops due to lack of CO_2. The stomata opening is regulated by the light and the plant water status. The exchanges of CO_2 between the external atmosphere and inside of the leaf begin to be limiting photosynthesis only when the degree of stomatal opening is reduced to below 50%. At first the limitation is modest. However, it becomes more relevant when the degree of opening is reduced to below 25%. This means that even in conditions of slight water deficit (reduction of up to 50% of the stomatal opening) vine photosynthesis is not reduced. It is instead significantly reduced in the case of a strong deficit (reduction of more than 75% of the stomatal opening). The photosynthetic capacity of the leaf also depends on its physiological age and its nutritional status.

Among the mineral nutrients, the most correlated to the photosynthetic capacity of the leaf is nitrogen, the level of which conditions the chlorophyll content. In cases of lack of a mineral nutrient, such as the lack of iron, magnesium or manganese, which cause yellowing (chlorosis) or other damage to the leaves, the photosynthetic activity itself is reduced or completely compromised. The presence of sink organs that actively recall the elaborate sap (*discharge of the phloem*), such as the grapes ripening, maintains the photosynthetic activity of the leaves, which otherwise would be reduced.

1.2.7. *Nutritional aspects*

The grapes, as well as for the production of wine, are consumed as fresh fruit (table grapes), or preserved after drying (raisins); furthermore, the grapeseed oil is extracted from the seeds, rich in essential fatty acids (~ 68-100 g) and vitamin E (~ 19-100 g). A portion of grapes is good source of water, simple sugars (glucose and fructose), organic acids (tartaric), vitamins (in particular the C), mineral salts (with a good intake in Cu) and phenolic compounds (anthocyanins, flavones). The latter are present in very small quantities and the relationship between the various classes of phenolic compounds varies significantly among the different varieties of grape.

The synthesis of anthocyanin pigments and tannins in grapes depends on the sun exposure, high temperatures or other pedo-climatic conditions (Mori *et al.,* 2007). The colour of the peel is mainly due to the anthocyanins, while in the pulp the flavones are more abundant. These are phenol compounds (hydroxybenzene) with ester and glucosidic bonds with other molecules containing alcoholic groups. The grape skin also contained some odorous substances: essential oils and esters, which are

present in very small quantities but capable of giving to the fruit very pleasant aromas (for example esters of monoterpenic alcohols for the muscat aroma).

The residues of the processing of wine grapes (stalks, skins, grape-seeds) constitute the marc that, after fermentation and subsequent distillation, are used for the production of grappa (33.6 g/100 ml of ethyl alcohol). Grape seeds are considered to be rich sources of polyphenolic compounds, mainly monomeric catechin and epicatechin, gallic acid, and polymeric and oligomeric procyanidins. They have showed various biological effects, including antioxidant or antimicrobial (Baydar *et al.*, 2006).

All these substances characteristic of the plant, called phytochemicals, have assumed in the last decade a particular importance from a nutritional point of view, since it has been proved a protective effect against cardio-vascular and chronic-degenerative diseases (Dillard and German, 2000).

The phenolic compounds contained in grapes held, on the one hand, an essential role in the characterization of different red wines as responsible for their colour, fragrance (aromas) and above all taste (flavanols and tannins), on the other hand they have a great nutraceutical potential. A food is defined as "nutraceutical" (or functional) when it contains pharmacologically active compounds, which can prevent or treat one or more pathological forms, and/or improve certain physiological and metabolic functions of the organism.

1.2.8. *Diseases*

The grapevine downy mildew (*Plasmopara viticola*) and powdery mildew (*Uncinula necator*) are native to America and spreading to Europe since the import of rootstocks resistant to phylloxera (*Daktulosphaira vitifoliae*).

Attacks vary from year to year and, in favourable weather condition, the disease can also cause severe damage leading to loss of the entire crop.

P. viticola is one of the most important diseases affecting viticulture (Lafon and Clerjeau, 1988). The fungus survives the winter as oospores on fallen leaf litter in vineyard soils. In the spring, with soil wetness and favourable environmental conditions, such as temperature at 10 ºC or higher, at least 10 mm of precipitation over a 24-hour period and the vine shoots are 10 cm length (rule of "3 10" proposed by Baldacci, 1947), the oospores germinate producing sporangia. These in turn liberate the zoospores which are splashed by rain into the canopy causing the first infections (Figure 2).

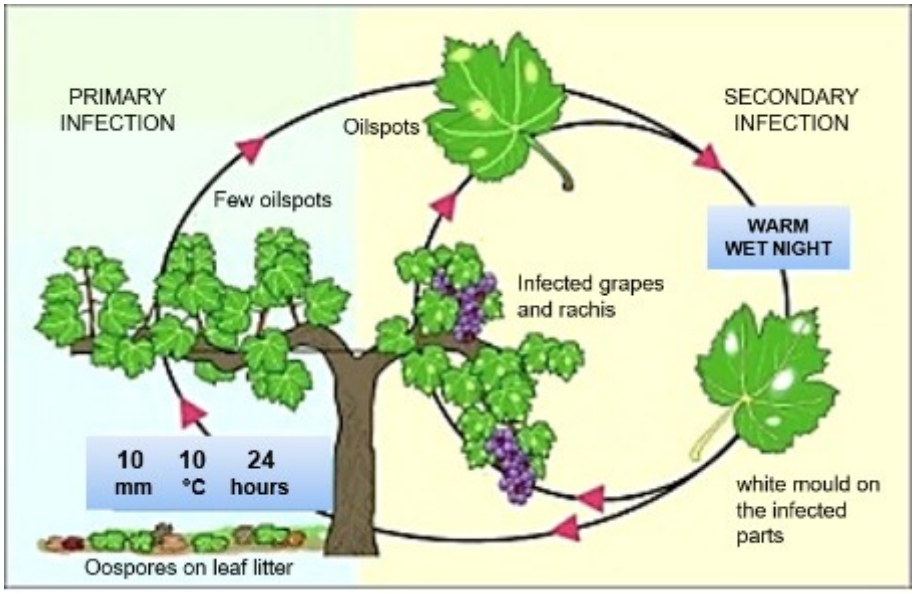

Fig. 2. Biological cycle of *P. viticola* primary and secondary infection (images by Magarey 1991, modified).

Following incubation, the disease reveals oneself in the form of white mould on the infected parts (figures 3a and 3b). Then, the microconidi are disperse from this mould that, with persistent rain, high humidity

(98%) and average temperatures higher than 13-14 °C, causing the development of the secondary infection (figures 3c).

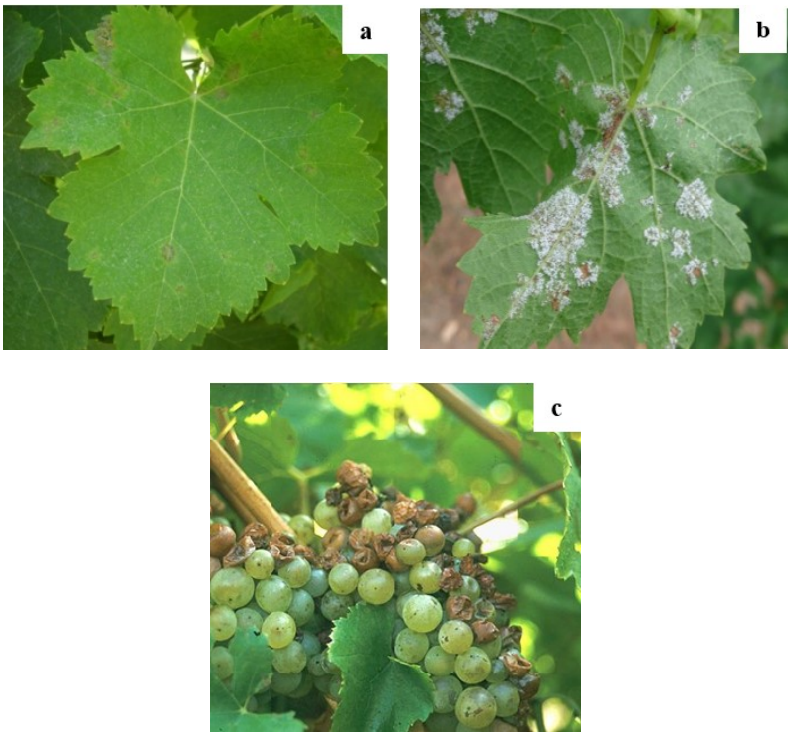

Fig. 3. Downy mildew symptoms (oil spots) on (a) abaxial leaf epidermis, (b) adaxial leaf epidermis and (c) secondary infection on grapes (photos by Francesca Sanna)

U. necator, contrary to other fungal diseases, does not need to develop in a liquid veil. The germination of the conidia can take place with less than 20% relative humidity and higher temperature favour the sporulation.

The development of parasitic fungus is also influenced of valley area and sun exposure. Vineyards or mountain cultures are positioned on slopes, sometimes close to forests and without any possible solar orientation, where a tree canopy influences climate conditions in the vicinity. The

presence of trees is expected to affect temperature, humidity and solar radiation measurements.

Moreover, in the family of dicotyledonous flowering plants *Vitaceae*, some plant defence mechanisms against fungal infections have been described (Adrian *et al.,* 1996). One of these mechanisms is the production of phytoalexins which can be induced by biotic or abiotic stresses, such as UV irradiation (Bavaresco *et al.,* 2007). The amount of radiation emitted, the duration of exposure and the correlation with the fungal infections are important parameters to be evaluated, to allow prompt actions against the pathogenic infections.

For a correct defence against pathogen attacks, it is necessary to know the incubation period in order to act promptly before infection conclusion. This requires an accurate knowledge of meteorological parameters such as temperature, precipitation and humidity.

1.2.8.1. Procedure of pathogen growth observation

In late spring, when the weather conditions start to improve, particular attention must be placed in the observation of chlorotic spots (oil spots) as possible symptoms of downy mildew or powdery mildew. In case of leaves with spots suspicious, they must be picked and incubated in a humid chamber and in the meantime submitted to the laboratory in a support (plastic bag or better Petri dish) with wet paper to keep the right humidity. Record the date, the sampling site and the phenological phase. The observed events should be recorded on paper ballot to be processed later.
In order to study the scalarity of primary infections, observed in the plots, all the leaves with infections in incubation are removed before the sporulation are able to initiate secondary infections. Within 24 hours, maximum 48, subsequent to the discovery of spots, repeats the survey in

order to eliminate any other sporulation referable to the same infectious event.

Ensure that the adjacent rows to the plot (vineyard treaty) there is no evasion of downy mildew in place or incoming possible sources of secondary infection.

Areas of observation, period and phenological recording

- In a vineyard selected to be representative of different vine-growing areas, for varieties, position, slopes, soil type, solar exposure and proximity of tree, identify a portion in which carry on the surveys. Choose at least 4 rows for a length of 20-30 meters and at least 10 strains. This portion will not be treated with fungicides until the end of the surveys;
- The period of observation starts on the bud break day;
- In the abovementioned period, record weekly the phenological phases using the BBCH scale, always indicating the prevalent phase (more than 50% of subjects).

Determination of the first emergence

- Observe weekly, with care, the whole area and identify early symptoms of downy mildew and powdery mildew on inflorescences, buds or leaves;
- In the presence of disease report affected organs (inflorescences, shoots and/or leaves);
- Identify 10 vines and of each label the fruiting canes for a total of 100 dormant buds;
- Observe and records all buds present on the fruiting canes labelled, dividing them into "long" (>10 cm in length) and "short" (<10 cm). Stop these evaluations when all the buds turn out to be long.

Subsequent investigation: sampling.

- Keep fruiting canes already labelled.

Subsequent investigation: weekly observations

- Shoots: Powdery mildew - distinguish the shoots in healthy and in “flag shape"
- Leaves: Downy mildew - distinguish between healthy and diseased leaves; recorder the date in witch are observed the first oil spot and the date in witch are observed the first sporulation of downy mildew disguised as a whitish mould on the lower side (fruiting bodies) of diseased leaves;
- Inflorescences/bunch: estimate the attacks by giving each inflorescence/bunch on the most appropriate severity of disease derived from the European Plant Protection Organization scale (EPPO, 2004; section 1.2.8.3).

1.2.8.2. BBCH phenological scale

For the recording of the phenological phase, the choice falls on the BBCH scale (figure 4), it is efficient to use, is mentioned in the descriptions of various crops, is a centesimal scale, structured to be used in the description of any monocot or dicot plant.

Each phenological scale is constituted by a set of stages, each of which describes a precise moment of development of a plant or one of its organs. A descriptive information on a particular phenological stage can contain a quantitative aspect.

The attribution of a specific phenological stage to a set of individuals will depend on:

- the prevalence of hierarchical stages, i.e. between any different growth stages under concomitant samples observed, is considered only that of last appearance;

- the numerical prevalence of individuals (is indicated the most recent stage that represent more than 50% of the units of observation)
- the reaching for the last phonological phase of a minimum threshold of units detected e.g. more than 25% of the population.

To represent the gradual development of individual subjects within a culture is good that at each observation are contains all the phenological phases present in the field, accompanied by the percentage of individuals that represent them (class of belonging).

The percentage can be estimated subjectively, referring to percentage values or numerical classes of belonging, or calculated exactly, as in the method of "maximum numerical limit" suggested by the World Meteorological Organization (Todorov, 1982).

With this method is specified analytically the number of plants that are found in different phenological phases, eliminating the subjectivity in the quantitative survey, and be limited to the assignment of the phenological stage of the individual subject.

00 - Dormancy: winter buds

05 - Wool stage

07 - Green shoot tips

08 - Bud burst

11 - First leaf unfolded

53 - Inflorescences visible

55 - Inflorescences swelling

57 - Inflorescences developed

60 - First flowerhoods

73 - Berries groat-sized

75 - Berries pea-sized

79 - Majority of berries touching

81 - Beginning of ripening

89 - Berries ripe for harvest

Fig. 4. Phenological phase description code as for the BBCH scale

1.2.8.3. EPPO Scale, severity of disease:

The EPPO Scale is included in the *Guidelines for the biological evaluation of pesticides* (2004), with the main purpose of harmonize the process of efficacy evaluation within the registration procedure of EPPO member countries by describing how field trials should be conducted in order to test the efficacy of plant protection products. A five-point scale (figures 5a and 5b) classified the degree of disease to the leaves and/or fruit surface:

1 – no visible damage on evaluated shrubs, leaves and/or fruits are healthy;

2 – sporadic spots on infected leaves and/or fruits, different in size and shape; number of spots between one and three;

3 – one third of the leaves and/or fruit surface covered with spots;

4 – half of the leaves and/or fruit surface covered with spots;

5 – spots covered nearly the entire surface of infected leaves and/or fruits

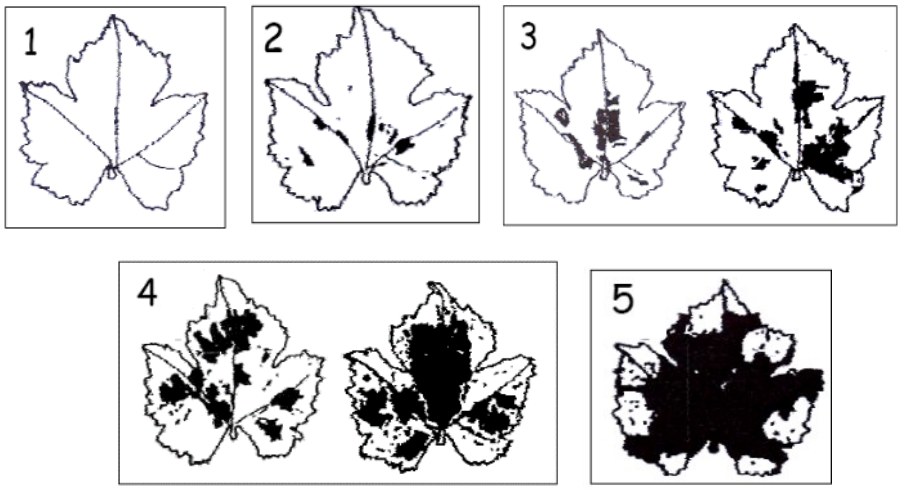

Fig. 5a. Severity of disease on grapevine leaves: 1 = Healthy; 2 = disease < 5%; 3 = disease 5–25%; 4 = disease 25-50 %; 5 = disease > 50 %

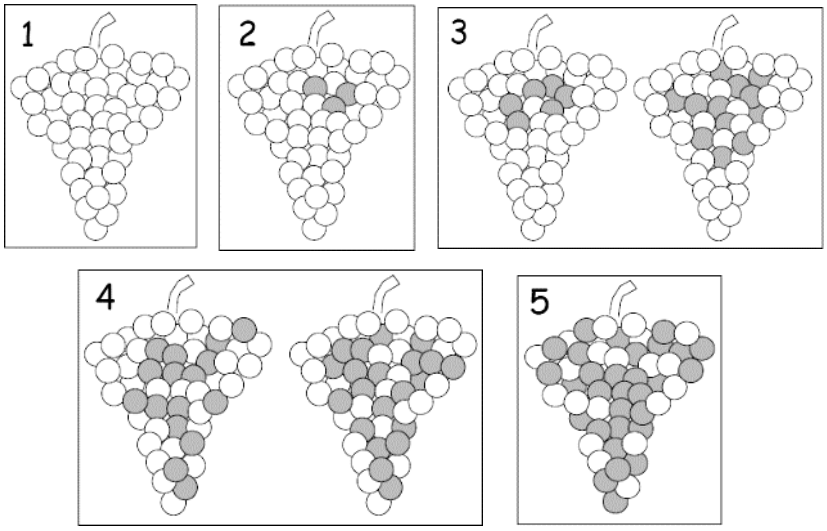

Fig. 5b. Severity of disease on grapevine fruits. 1 = Healthy; 2 = disease < 5%; 3 = disease 5–25%; 4 = disease 25-50 %; 5 = disease > 50 %

1.2.9. *Forecasting models*

During the past decades, several software tools were developed for agricultural research and decision making purposes. For example, crop and farm system modelling, pest and disease warning, algorithms for irrigation scheduling or agroclimatic indices can help farmers in decision making for crop management options and related farm technologies.

The epidemiological forecasting models are complex systems able to transform the relations between culture, adversity and the surrounding environment into mathematical equations, trying to represent in real-time, to the extent most likely possible, the performance of an epidemic phenomenon. Models are designed to alert farmers and technicians to the risk of a particular issue, so appropriate measures can be performed on time and in an optimal manner. In general, forecasting models are able to provide, through a software, information about the onset and evolution of

a disease or indicate a period of time in which it is highly improbable that the disease appears and indication of the best time to make or not treatment in the field, all depending on the meteorological data. The models simplify the situation extremely articulated so they should always be interpreted and calibrated to the peculiarities of a territory. Moreover, they can be extremely useful for the definition of guidelines for Integrated Pest Management (IPM).

In systemic models the epidemic trend is the result of the interactions that take place in the *climate-pathogen-host* system. The model breaks up the system into different phases, defining the necessary and sufficient conditions in order that they occur, increases the error of assessment leading in turn to incorrect interpretations. The various system components are then analysed by modulating their responses as a function of environmental parameters, taking into account their mutual effects and, finally, simulate the epidemical progression.

The simulation models "to compartments" are forecasting models developed specifically for the *P. viticola,* which consist of a series of sub-models (or compartments), related to each other, each of which represents the various stages of cycle infectious of the pathogen and the transmission of the disease.

Forecasting models have been proposed worldwide: the EPI (Etat Potential d'Infection) is a more complex model developed in France (Strizyk, 1983) that is based on the potential impact of the pathogen and its ability to cause infection and other model are proposed by Tran Manh Sung *et al.,* (1990) Magnien *et al.,* (1991) in the same nation. In Germany, Hill (1990) developed PRO (Plasmopara Risk Oppenheim) which helps growers to decide when downy mildew has reached a stage at which it will begin to

damage the crop. In Switzerland other tools are proposed by Blaise *et al.,* (1999) and Viret and Bloesch, (2002) while DMODEL, a downy mildew simulator was developed in Australia (Magarey *et al.,* 1991). DMCast (Downy Mildew Forecast), is a weather-driven model that provides estimations of both primary and secondary *P. viticola* infections in the USA (Park *et al.,* 1997) and a model simulating *P. viticola* infections based on fuzzy logic (Orlandini *et al.,* 2003). PLASMO, which simulates the limited survival of sporangia, the start of all possible infections and the duration of incubation periods, was developed in Italy (Rosa *et al.,* 1993). The UCSC (Università Cattolica del Sacro Cuore, Piacenza, Italy) has developed a mechanistic model which simulates the entire downy mildew disease cycle from oospore maturation through the onset of symptoms (Caffi *et al.,* 2007; Rossi *et al,* 2008). Other models include Vinemild, a quantitative model based on the biology of the pathogen and its reproductive capacity (Blaise *et al.*, 1999) and Vitimeteo Plasmopara, a qualitative model based on climatic conditions fostering infection and the readiness of oospores to germinate (Siegfried *et al*., 2004).

From the first forecasting models based on simple rule of thumb of the "3-10" proposed by Baldacci (1947), which predicts the latent period without considering the hours of leaf wetness and the meteorological trend, is reached to date at the modern mechanistic models. These latter take into account quantitative aspects of both sexual and asexual stages, the definition of primary inoculum season, the seasonal oospore dose, and its division into many coeval cohorts (Rossi *et al*., 2008). However, these models include many uncertainties and limitations resulting from unknown trends in future technology and human activities, a simplified representation of reality, lack of knowledge on system responses and lack of calibration data (Eitzinger *et al.*, 2008). Metrological investigations

are required to evaluate the target uncertainty on temperature and humidity measurements needed to improve the reliability and accuracy of forecasting model.

A more in-depth description of a commonly used forecasting model (EPI) is highlighted in Chapters 3 and 4.

1.3. Tomato and meteorological parameters

1.3.1. *Taxonomy and domestication of tomato*

The cultivated tomato (*Solanum lycopersicum* L.) belongs to the *Solanaceae* family. Its botanical group has relatively diversified recently (estimated around 7 million years ago) and it has subsequently colonized very different habitats along the west coast of Latin America from sea level to over 2500 m of altitude. The place where tomato domestication can be traced is uncertain. A theory indicates southern Mexico based on the spread of wild forms of round-small-berry tomato (also called cherry, included in the botanical form *S. lycopersicum* var. *cerasiforme*) and is supported by cultural, linguistic, historical and genetic-molecular evidence.

The set of genetic variations that, more or less consciously selected by man, have led to the adaptation of a species in a cultivated state goes under the name of domestication syndrome. In tomatoes it has been shown that these changes are due to a relatively small number of loci (i.e. genes) with different effects. The variation from the green to pigmented berry was one of the most evident manifestations of tomato domestication syndrome. A fundamental variation in the origin of the tomato regards the loss of incompatibility and allogamy in favour of a self-compatibility and self-fertilization capacity (autogamy). Another aspect of tomato domestication has been the notable increased in fruit size.

1.3.2. *Botanical and physiological characteristics*

Tomato is an herbaceous plant, with indeterminate growth that gives it the theoretically perennial habitus in relation to pedoclimatic conditions, but annual in cultivation. The cultivated tomato has a diploid form, with a genomic formula $2N = 2x$, with $x = 12$. The structure of the chromosomes

is quite similar from one species to another. Stem and leaves are pubescent, with hairs that produce aromatic secretions; the leaves are compound, alternate, stalked and irregularly pinnate. After a period of vegetative growth (8-12 leaves, or even less depending on particular environmental conditions such as low temperatures), the plant emits the first inflorescence that is not depending on the photoperiod control. Then a new inflorescence is issued every three internodes (leaves). The development of the tomato is sympodial: each segment ends with an inflorescence and the continued growth of the higher axillary bud (Figure 6). The inflorescence is pushed laterally and the indefinite repetition of this development gives an indeterminate growth habitus that requires an upright rearing with the support of guardians.

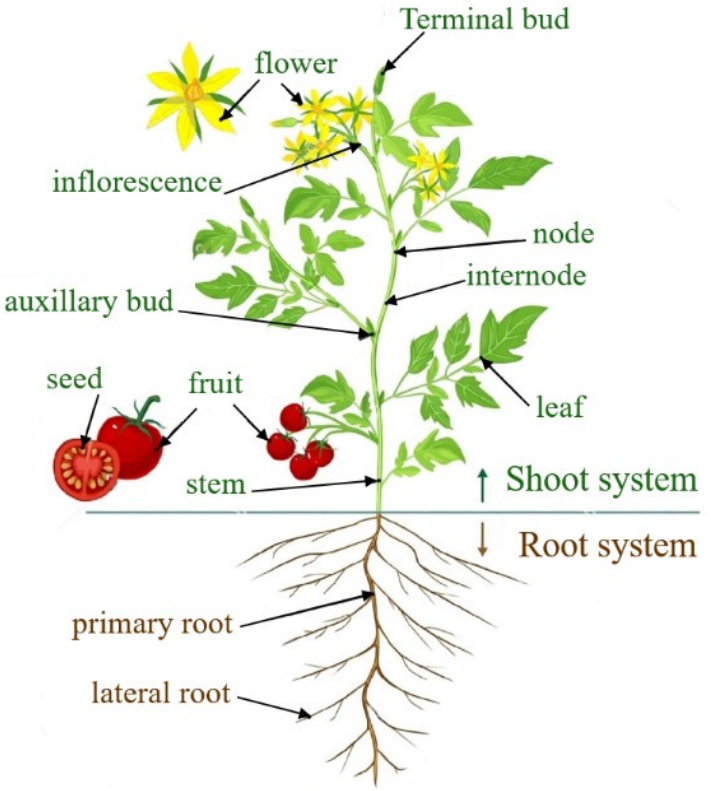

Fig. 6. Morphology of flowering tomato plant

The inflorescence is an axillary raceme or terminal composed of 4-12 flowers with scalar anthesis. The flower is generally pentamerous, with a yellow corolla. The stamens are typically welded together to form a cone terminating in a sterile apex; stylus and stigma are, in the cultivated varieties, generally enclosed by the cone of the anthers (stigma insert).

In consequence of the floral morphology and the complete self-compatibility, the fertilization in the tomato is mainly due to self-pollination. The self-pollination does not require the transfer of pollen from one flower to another, but it is still necessary for the flowers to be moved to facilitate the fall of the pollen on the stigma. For this purpose, wind is relied on in open field crops and on mechanical vibration or on the activity of pecker insects (usually bumblebees) in protected crops. In protected cultivation, the action of a pollinator agent is particularly important because the higher air humidity hinders the optimal dehiscence of the anthers.

The anthesis begins in the early hours of the morning and continues throughout the day; the first flowers to bloom are those placed at the base of the inflorescence. After fertilization, the petals dehydrate and fall, while the calix is persistent. The growth of the berry proceeds rather rapidly, requiring about 35-60 days to reach physiological maturation, depending on the type of the berry itself. The fruit is a red berry when ripe, although there are mutations of wild alleles that give yellow, orange, brown, purple colour. In addition to pigmentation, the ripening process is completed with the softening of the fruit and with the accumulation of sugars and acids, the ratio of which gives aroma and the typical slightly acidic flavour to the berry. Shape and size of the berry differ according to the cultivars, with wide variability. The seeds are flat, round, rough due to the presence of a

tegument with hairs, rich in lipids, and straw-yellow in colour. There are also brown seed varieties that are typical of wild species related to tomatoes. A thousand seeds weigh 2.5-3.5 grams.

The biological cycle of the common varieties ends with the desiccation of the leaves, the basal first, and ends with the desiccation of the stem. The entire biological cycle of the plant ranges from 140 to 180 days, a transplanted crop has a cycle of 100-120 days (the growth of the berry ranges from 35 to 60 days), during which the total water requirement is about 400 mm, according to the climate. A technique for controlling soil moisture is to use a tensiometer that measures the soil moisture tension as a centibar (cbar). In general, for the tomatoes, the soil moisture tension should be kept between 10 and 20 cbar. Irrigation should occur when the soil moisture pressure exceeds 20 cbar.

The optimal cultivation environments for tomatoes are those in warm and temperate-warm regions, since the climate and above all the temperature affect the plant's development. The photoperiod can modify the general morphology of the plant; intensity and quality of light seem to influence the flowering period, the degree of fruit set and the colour of the berries.

Tomato is a plant with high thermal demands. The minimum temperature for germination is 12 °C, for the flowering is 21 °C while the thermal limits for the culture are: 2 °C and 34 °C as minimum and maximum lethal temperature, respectively. The optimal temperature for growth of tomatoes is 22-25 °C and the minimum temperature should be greater than 13 °C. Temperatures higher than 32 °C day/21 °C night will be detrimental to most tomato cultivars (Figure 7).

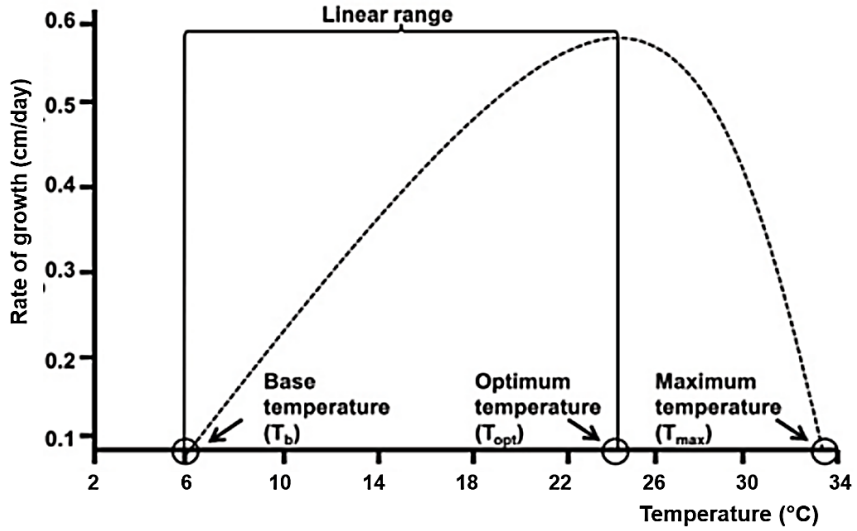

Fig. 7. Generic response of plant development to average day/night temperature (Van Ploeg and Heuvelink, 2005)

High temperature lead to a rapid development while excessive temperatures can cause flower abortion, pollen sterility and ripening disorders which severely reduces marketable yield of tomatoes. Yellow shoulder disorder (discoloured regions under the skin that show through and decrease the quality of the fruit) is exacerbated by very light intensity and air temperatures (Tsormpatsidis *et al.* 2008). The humid environments that favour diseases and rotting are not suited to tomatoes; the best ones are those with rather dry climate, i.e. soils with great water retention capacity or with the possibility of irrigation.

An extremely delicate phase is the control of the many parasites that can hit the plants in the greenhouse. Bacterial and fungal infections often develop as a consequence of the high humidity and condensation that occurs in the greenhouse during the cold and humid periods, that discourage the opening of the structure. Hence, the need to have good systems of forced ventilation and openings on the ridge or lateral, which,

combined with pest control treatments, allow a good control of diseases. Among the insects, aphids and thrips represent the most serious threat to indirect damage related to the transmission of viruses (Cucumber Mosaic Virus and Tomato Spotted Wilt Virus). Excellent results have been obtained with the use of nets that do not allow these parasites to pass inside the greenhouses.

1.3.3. *Nutritional characteristics*

The edible part of the *S. lycopersicum* is the fruit that is commonly considered as a vegetable. The composition and the ratios between the various constituents give the tomato a significant nutritional and dietary value. The nutraceutical component of the fruit varies according to the cultivar, the stage of maturation and depends also on numerous exogenous factors.

Tomato is a basic food of the Mediterranean diet, consumed both as fresh and processed product. It consists primarily of water (over 94%). In the aqueous component of the fruit, there are several mineral salts and trace elements, mainly K, P, Ca, but also Fe, Zn and Se. The tomatoes also contain discrete quantities vitamins, mainly C and A, but also B and E. The pigmentation of the fruit is determined by the concentration of carotenoids such as α-, β-carotene and lycopene, the latter responsible for the red colour. Lycopene is a bioactive molecule that possesses very strong antioxidant activity both *in vitro* and *in vivo* (Agarwal *et al.,* 2000).

Ripe tomato contains also some phenolic compounds, another class of molecules extensively studied for its antioxidant properties. Polyphenols are compounds produced by the secondary metabolism of plants, produced only in certain tissues and in particular stages of development. In tomato, limited amounts of some polyphenols are confined almost exclusively in

the peel (Toor and Savage, 2005). The most representative molecules of this class of antioxidants are flavonols: rutin, quercetin glycoside, and kampferol glycosides, whose concentration seems to decrease with the progress of maturation and is higher in tomatoes grown in the open field than those grown in greenhouses (Giovanelli *et al.,* 1999).

The macro and micronutrient composition of the tomato is strongly influenced by factors such as the type of cultivar, the agronomic practices, the exposure to sunlight and the characteristics of the soil that acting on the whole process of the food chain that goes from the ripening of the fruit to the conservation and consumption. For example, vitamin C and β-carotene continue to accumulate in tomatoes that ripen after harvesting but the accumulation of β-carotene is still lower than tomatoes ripening on the plant (Javanmardi and Kubota, 2006). The concentration of lycopene increases as the fruit matures, however the tomatoes grown in the greenhouse have lower lycopene concentrations than those grown in the fields. The temperature and light intensity exert a great influence on the lycopene and carotenoid content, in fact their synthesis is inhibited at temperatures below 12 °C or above 32 °C and is affected by the photoperiod during the maturity (Chattopadhyay *et al.,* 2013).

With regard to the influence of agricultural practices, the introduction of new varieties, the spread of greenhouse cultivation, the use of different types of cultivation systems (hydroponics, above ground, etc.), the insertion of resistance factors to parasitic adversities, fertilization and nitrogen level in the soil, influence the content of polyphenols as well as other macro and micronutrients.

Precisely for the richness in antioxidant compounds, some authors define the tomato a “functional food” (Ranieri *et al.,* 2004) that is able to perform

a beneficial and preventive action on human health, strengthening the body's protection against free radicals, etiologic agents of many diseases. Epidemiological studies have shown that consumption of raw tomato and its derived products is associated with a reduced risk of cancer and cardiovascular disease (Clinton, 1998; Giovannucci *et al.,* 2002). Given their importance for human health, antioxidants can be considered a valuable attribute of quality of tomatoes and it is important to minimize the losses of these compounds throughout the production cycle.

1.3.4. *Tomato and UV radiation*

Since the early 1970s, there has been keen interest in assessing the impact of stratospheric ozone reduction and the attendant increase in ultraviolet radiation on the growth and development of crop plants and natural ecosystems (Turunen *et al.,* 1999; Hao *et al.,* 2000; Krizek et al., 2005; Rozema *et al.,* 2005; Sullivan, 2007).

In general, UV radiation can be considered as a stress factor which is able to significantly affecting the characteristics of plant growth and to trigger a variety of physiological responses that lead to an accumulation of secondary metabolites which increase the plant resistance, but also important for human health given their antioxidant properties. In addition, the UV radiation is able to affect the sporulation of pathogenic fungi and reduce the prevalence of diseases caused by transmission of parasitic insects (Vakalounakis, 1991).

The quantity and the composition of secondary metabolites such as phenolic compounds present in foods are influenced by genotype (Howard *et al.,* 2003), storage conditions (Asami *et al.,* 2003), extraction procedure (Mukhopadhyay *et al.,* 2006), environmental conditions (Caldwell *et al.,* 2005) and solar UV radiation (Luthria *et al*. 2006). Studies aimed to

quantify the effects of UV radiation on crop quality have led to unclear results, often conflicting. Data are fragmented since they take into account only separately some aspects of the problem (physiological or production quality or entomological). Particularly the increase in UV-B radiation (280-315 nm) is a potential risk to the physiology and the plants growth, as it can damage DNA, proteins, cell membranes, and affect the physiologic function (Fedina *et al.*, 2009). However, subsequent research shown that comparatively low doses of radiation in plants inducing a metabolic response to stress resistance which leads to an increase of molecules at high antioxidant capacity (Schreiner *et al*., 2006).

Furthermore, the relationship between temperature and solar radiation induces non-negligible and joint effects. Low radiative intensity leads to weak growth and the phenomenon is accentuated the higher the temperature is. High average daily temperatures may cause delayed flower initiation, while low average daily temperatures may induce premature flower initiation and dormancy. The photoperiod is involved in this phenomenon.

Plants may produce secondary products to protect them against UV light damage, but these metabolites also play an important role in human health. Phenols, flavonoids and anthocyanins are responsible for antioxidant activity in fruits and vegetables (Wang *et al.,* 1996; Cao *et al*., 1997). Epidemiological studies have shown a positive relationship between fruit and vegetable consumption and reduced incidence of chronic and degenerative diseases (Prior *et al*., 1998).

Plants produce a wide range of flavonoids and related phenolic compounds which tend to accumulate in leaves of higher plants in response to UV radiation (Rozema *et al.,* 1997). It has been suggested that plants have

developed UV-absorbing compounds to protect them from damage to DNA or to physiological processes caused by UV radiation. These UV-absorbing compounds accumulate in the epidermis, preventing UV radiation from reaching the photosynthetic mesophyll (Braun and Tevini, 1993).

1.3.5. *Protected cultivation*

In recent years, irradiation with UV light (100-400 nm) has been tested as post-harvest treatment to reduce the colonization of fruit by pathogens or pests and to delay senescence in fruit and vegetables. These are generally relatively low doses of radiation, which induce in the fruit a metabolic response following the increased activity of the PAL, the enzyme phenylalanine ammonia lyase. The increase in PAL activity leads to the accumulation of newly formed metabolites (phytoalexins), toxic to pathogens, and to an increase in antioxidant molecules such as phenols and flavonoids (Schreiner and Huyskens-Keil, 2006).

Studies supporting the post-harvest effects on tomatoes treated with UV light have proven effectiveness in increasing the levels of lycopene and carotenoids (Liu *et al*., 2009), in reducing the damage from cold and delay ripening during cold storage (Liu *et al.,* 2012). Further studies have reported that low doses of UV can induce resistance to *Botrytis cinerea*, thanks to the accumulation of phytoalexin risitin, and delaying maturation, improving consistency and prolonging the shelf-life of tomatoes (Maharaj *et al.,* 1999; Charles *et al.,* 2008; Jagadeesh *et al,* 2011).

Obande *et al*. (2011) studied the effect of treatment with UV in pre-harvest on the maturation and resistance to pathogens of tomatoes grown in greenhouses, with particular attention to colour development and consistency. Researchers reported positive results and a dose-response

effect at higher dosages, but highlight the limitations due to optimization of treatments to determine both optimal quantity and timing. Del Corso and Lercari (1997) used UV sources to regulate the growth of tomato plants in greenhouses before transplanting outdoors. In fact, within a glass greenhouse the UV-B radiation (280 nm - 315 nm) is absent and the sudden transfer to the outside can induce strong stress to young plants. The treatment significantly reduces the height of the plant, the leaf area and the dry weight loss of the stem but the effects are strongly dose-dependent. Bacci *et al.* (1999) have shown that the daily treatment of tomato plants with UV-B leads to the early ripening of the fruits and the reduction of their size. The monitoring of UV radiation is therefore an important parameter as an indicator in determining the numerous chemical and biological effects on crops.

In light of the foregoing, it is evident that the application of physical elicitors, such as UV light, can induce changes in the plants' metabolism and influence the content of the antioxidant molecules on the fruits. Since the type of radiation that reaches the culture has effects on both the growth of the plant and the quality of the fruit, it is considered essential measuring the radiation that the plant intercepts to understand the effects on product quality. This aspect is extremely important when operating in protected cultivation, which involves a modification of the quantity and the spectral distribution of solar radiation within the cultivation environment, especially in light of the new problems due to atmospheric pollution that has changed the spectrum of solar radiation reaching the plants (Stapleton, 1992). To date, there are very few studies of the relationship between the microclimate generated in protected cultivation and the morphological-phenological and productive aspects of the tomato culture that takes into consideration also the qualitative aspects of the fruit, in terms of content

of health promoting compounds, and the maintenance of these in the post-harvest phase.

1.3.5.1. Greenhouse or tunnel

In 2016, world tomato production was around 38 million tonnes. The annual tomato production in Italy was about 111,400 hectares with an average production of 59.6 t/ha, destined for 17% for fresh consumption and for 83% for the canning industry for concentrates, peeled, shredded, past, etc. Significant economic importance has off-season production for fresh consumption with about 7,600 ha in greenhouse cultivations (source Istat, 2017).

When operating in protected cultivation (greenhouse or tunnel) the amount and the spectral distribution of solar radiation inside the cultivation undergoes a modification that depending on the type of cover used. The productivity of a protected crop is highly correlated to the amount of electromagnetic radiation received, which in turn depends on the amount of UV, PAR and IR radiation transmitted through the cover material of these structures (Krizek, 2004). On the other hand, instruments that measure solar radiation, the spectroradiometers, need constant maintenance and calibration, to obtain UV measurements of required quality (Hülsen and Gröbner, 2007). The calibration value has been underestimated or neglected for a long time. It has been shown that the introduction of the measurement uncertainty for the ground based spectroradiometric measurements increases significantly the reliability of the measured data (Schaepman, 1998).

Temperature management, moreover, is one of the most critical factors in successful production of many tunnel crops. The tunnels produced a warmer environment than standard field conditions, resulting in earlier and

higher yields especially for warm season vegetable crops. Economic analyses indicated that the tunnels could enhance profitability if growers used suitable production practices. While raising the minimum temperature is important, keeping the maximum temperature from exceeding a range optimum for crop growth is equally important. Since tunnels are passively vented through sidewalls and end-walls, air temperature and humidity can affect crop growth, nutrient and water uptake, pollination, fruit ripening and pest outbreaks (Tsormpatsidis *et al.* 2008). Proper design and venting of the high tunnel can prevent build-up of heat. Larger tunnels, which enclose a larger volume of air, do not increase in temperature as rapidly as smaller structures during the day.

Tunnels protect crops from wind, rain, snow, hail, insects and diseases. It is important to increase the minimum temperature, as well as to prevent the maximum temperature from exceeding the optimal range necessary for crop growth. The temperature inside the tunnels is about 5 °C higher than the external conditions. In addition, the tunnel provides frost protection of about 4 °C to the crop. In the summer, the high tunnel provides a rain shield and protection from storms, reducing disease pressure dramatically and eliminating fruit cracking. Later in the year, the tunnel again provides extra heat, extending fall production. While there is some loss of fruit set in the heat of the summer, reducing August production, fruit quality is still superior. For direct marketers, the high tunnel is becoming an essential tool for tomato production.

Tunnels usually used for cultivation take on a straight shape in the along the sides and of a half circle in the upper part. They are also equipped with a hinged door consisting of two frames (frames in galvanized tubes placed one above the other) that are held together laterally by a hinge. One of the

two frames stays fixed while the other can be opened like a normal door (Figure 8a). They do not require electrical connections for ventilation and extra heat.

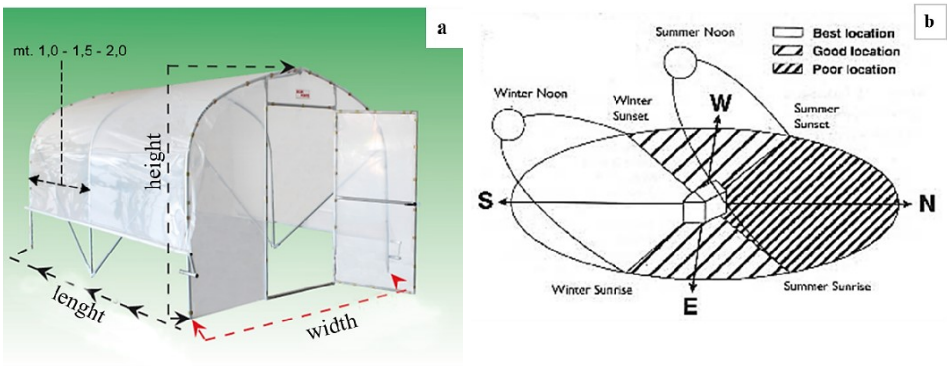

Fig. 8. a) The tunnel is composed of arcs, anchoring pipes, plastic cover, and hinged door. b) Tunnel orientation

The arcs may have a distance from one another ranging from 1 m to 2 m, the variation depends on climatic conditions, generally it is recommended 1.5 m. The arches are composed of three pieces: a semi-circular part that fits two feet. The recommended measurement for penetration of the feet into the ground is 20 to 50 cm, depending on the consistency of the soil.

The tunnels must be arranged in such a way as to prevent the structure from creating shading or being a source of irradiation towards the other. The optimum orientation is major side along the east-west direction (Figure 8b) (Fisher and Runkle, 2004). Since the tunnels are ventilated manually, they must be placed in an accessible position.

1.3.5.2. Covering materials

The world consumption of plastics in agriculture amounts annually to 6.5 million tons. The advantages in the use of plastic materials such as polyethylene (PE), polyvinyl chloride (PVC), and ethyl-vinyl acetate (EVA), rather than glass, are related to their economy, to their lightness

that requires more load-bearing structures easy to handle and with limited maintenance requirements. On the other hand, they have the disadvantage of having a definitely more limited duration compared to rigid materials such as glass (Dilara and Briassoulis, 2000). Today, most greenhouses on the market are made of PE/EVA multi-layer co-extruded films. The addition of EVA imparts superior elasticity, mechanical strength and UV resistance (Briassoulis *et al.,* 1997). Likewise, transparent polyethylene films containing additives capable of blocking UV radiation and, therefore, allowing high transmission of visible light are very common.

Photoselective films represent the latest level of evolution of cover films. This group includes various types of plastic capable of blocking certain wavelength bands of solar radiation. Transparent PE films are characterized by high levels of PAR transmission, containing additives capable of blocking UV radiation below 380 nm or passing those between 290 nm and 400 nm (Krizek *et al.,* 2005). They were experimented in tomato culture with positive effects on the quality of the product in terms of increasing the phenolic component (Luthria *et al.,* 2006).

A second type is a neutral film, produced with low-density polyethylene (LDPE) and with variable percentages of linear polyethylene (LLDPE) which optimize its mechanical performances. The absence of UV stabilizers recommends its use to cover greenhouses or tunnels exclusively for crops that have a short production cycle (Benhamida *et al.,* 2010). According to the UNI-EN 13206 (2017), the neutral film is classified in terms of duration in the "N" class.

Transparent thermal film based on ethylene-vinyl acetate (EVA) is another type of covering material that provides excellent transmission of solar rays, an excellent thermal effect and a high reduction of thermal inversion inside

the greenhouse, accumulating heat during the day and preventing it from escaping during the night hours. The film is recommended for covering greenhouses and tunnels for winter crops in low-light areas. The EVA film is used, in greenhouses and in double-coverage tunnels, as a cavity for winter and spring crops in very cold areas, reducing the risk of night frosts. The EVA film (class “N”) can be produced with UV stabilizers to obtain the same durations of the films additivated (class “A”), super-additivated (class “B”) and long life (class “D”). It is also possible to embed to the EVA film with an “anti-drip” additive, which by encouraging the flow of the condensation layer, prevents the formation of drops safeguarding the transparency of the film and the health of the cultivated plants.

1.4. Metrology for agriculture

Metrology, as defined by the *Bureau International des Poids et Mesures* (BIPM), is "*the science of measurement, embracing both experimental and theoretical determinations at any level of uncertainty in any field of science and technology"* (BIPM, 2004). Its activities include the definition of units of measurement, which may be internationally accepted, the realisation of these units of measurement in practice, the traceability, the evaluation of the components of uncertainty and the study of the characteristics of the instruments. Among the various fields of activity, the scientific or fundamental metrology sector deals with issues related to tools and methods, taking care also of terminology problems and the applied, technical or industrial metrology sector deals with the issues related to the study, production, dissemination of techniques, calibration methods and practices, up to the control of measurements for industrial products.

The reliability of accurate measurements is a relevant element and varies depending on the need to meet different requirements in several sectors, including agriculture, civil protection, entertainment and weather forecast (Santana *et al.* 2015). In the agro-food sector in particular, the reliability of the measures effectively directs the actions of technological innovation of the chemical, physical, and biological parameters that determine the healthiness, nutritional and organoleptic properties of the products, leading to an increase of the added value. The quality of the measurements related with security issues also plays a key role, as it depends on the prevention and protection strategies, the supervisory and control actions and the consequent decision-making processes. In general, the quality of the measurements is

determined by the development of metrology for the specific sector. Calibration is a primary tool for quality control, it is done by using properly evaluated methods and procedures.

Despite the great development of technologies and the measuring instruments increase in sensitive and performance, the availability of reliable analytical methodologies in the agro-food sector is still poor. This is also due to a delay in the development of metrology for measurements in this area and for the difficulties related to the identification and choice of parameters to be measured. Considering the lack of metrological approach in the agro-food sector, it is necessary to improve the research and to strengthen the metrological infrastructure in this field. Quality control helps minimizing the risks of product characteristics failing to meet the security, standards or regulatory requirements applying to consumers' health and to the environment (Osseni *et al*. 2015).

In order both to reduce the negative impact of agriculture, livestock breeding and forestry on the environment and to enhance positive effects (such as carbon storage, soil and plant cover stabilization, the reduction of runoff and erosion and disease containment), agricultural practices, adapted to the changing climate conditions, must be initiated (Charki, 2016). This requires developing qualitative and quantitative measurement mechanisms exchanged between relevant stakeholders in order to ensure sustainability. Reliable data allows the effective measurement of the agriculture's impact and helps designing agricultural policies targeting environmental protection. To avoid possible failures against security as well as environmental, social and economic interests, it is necessary to enforce robust assessment systems adapted to the new climate conditions

and the growing demand for qualitative products. The reliability of data quality controls of agricultural products is strongly correlated to the availability of skills in the evaluation system. For instance, calibration laboratories should carry out measurements according to well-proven technical prescriptions and produce results leading to the granting of conformity assessments (Lewis and Cooke, 2013). The strengthening of capacities to control agricultural products needs to be linked to a harmonized assessment system based on reliable, long-lasting measurements (Himbert, 2009).

1.4.1. *Measurement uncertainty*

The objective of a measurement is to determine the value of a particular quantity is achieved by a comparison between the quantities. In general, the result of a measurement is an approximation (estimate) of the value of a measurand, that is the value of the particular quantity to be measured, and therefore it is complete only when a statement of the uncertainty of this estimate accompanies it.

The concept of uncertainty as a quantifiable attribute is relatively recent in the history of measurement, even though the concept of error and error analysis are present since a long time in the practice of measurement science. It is important not to confuse the terms “error” and “uncertainty”. Error is the difference between the measured value and the true value of the thing being measured, while uncertainty is a quantification of the doubt about the measurement result.

As reported in the Guide to the expression of Uncertainty in Measurement (GUM), the uncertainty is a “*parameter, associated with the result of a measurement, that characterizes the dispersion of the values that could reasonably be attributed to the measurand*” (BIPM, JCGM 100:2008).

The GUM, publishes by BIPM, asses that the word “uncertainty” means doubt, and thus in its broadest sense “uncertainty of measurement” means doubt about the validity of the result of a measurement. Therefore, we cannot take as valid the value measured by an instrument if this parameter is not associate with it. The parameter mentioned in the definition of the GUM, as well as in the International Vocabulary of Metrology (VIM - BIPM JCGM, 100:2012), it can be, for example, a standard deviation called *standard uncertainty u(x)* or it can be the half-width of an interval having a probability of coverage established.

When reporting the result of a measurement it is essential to provide some quantitative information on its uncertainty in order to compare the results of different measures, assign the accuracy of the result and know the significance of the differences between different results.

Generally, measurement uncertainty includes many components. Some of these are evaluated by means of “Type A evaluations”, starting from the statistical distributions of the values coming from a series of measurements, characterized by the estimated variances s_i^2 (or the estimated standard deviations s_i) and the number of degrees of freedom v_i. The other components, which are assessed by “Type B evaluations”, that are evaluated with other method, should be characterized by quantities u_j^2, which can be considered as approximations to the corresponding variances. The quantities u_j^2 may be treated like variances and the quantities u_j like standard deviations estimated based on probability density functions derived from experience or other information.

The *combined standard uncertainty uc(y)* is the standard uncertainty of the result of a measurement when that result is obtained from the values of others quantities, equal to the positive square root of a sum of terms, the

terms being the variances or covariances of these other quantities weighted according to how the measurement result varies with changes in these quantities. The *expanded uncertainty U(c)*, indeed, is the quantity defining an interval about the result of a measurement that may be expected to encompass a large fraction of the distribution of values that could reasonably be attributed to the measurand. In order to obtain an *U(c)*, the combined standard uncertainty is multiplied by the *coverage factor k,* a numerical factor typically in the range 2 to 3.

In cases where a normal distribution (Gaussian) can be attributed to the measurand and the *u(x)* associated with the output quantity is sufficiently reliable, a coverage factor $k = 2$ can be used. The *U(c)* thus obtained corresponds approximately to a level of confidence of 95%. These conditions are met in most of the cases observed in instrument calibration. After performing a measurement, having identified and assessed all the known or hypothesized components of uncertainty and made any necessary corrections, however, remains an uncertainty about the correctness of the result, i.e. a doubt as to how well this represents the value of the measured quantity.

1.4.2. *Sensors calibration*

A calibration is a process used to compare the measuring, and test instruments to a recognized reference standard of known certified accuracy and uncertainty. The term calibration means the act of comparison, and does not include any subsequent adjustment of the instrument. Fundamental to a systematic program of instrument calibration and periodic recalibration is the idea that the instruments do not maintain their accuracy of measure along the time. Extended use, design, environment, and time are some of the factors that degrade the instrument performance

and its accuracy. A calibration system is designed to assure the verification, maintenance, and validation of the instrument's desired accuracy and traceability to the reference standard (Juran, 1974).

There are important concepts in calibration. Accuracy is defined as an agreement between the measured value and the true value. The precision instead is the closeness of multiple measurements values. Thus, an instrument can be precise but not accurate. Measurement accuracy, on the other hand, is not a quantity but a qualitative term, and it is not assigned a numeric value. A measurement is considered as more accurate as lower are the measurement uncertainty that characterize it.

Measurement repeatability refers to the degree of agreement between the results of successive measurements of the same measurand carried out in order to comply with all the following conditions: same measurement mode, same observer; same instrument for measurement; same place; same conditions of use; repetition within a short period of time. It can be expressed quantitatively in terms of dispersion of results (standard deviation). Finally, the measurement reproducibility is the degree of agreement between the measurement results of the same measurand when the individual measurements are carried out by changing various conditions, such as the measurement method, the observer, the measuring instrument, the location, the conditions of use and time. Reproducibility can also be expressed quantitatively in terms of dispersion of results.

In the case of temperature sensor' calibration, almost all thermometers used in practice belong either to the group of radiation thermometers or of contact thermometers. The operation of the contact thermometer is based on a sensor that by thermal contact is brought to the temperature of the object to be measured and whose temperature is then determined by

measurement of another quantity showing a dependence on temperature. In this sense, calibration of a contact thermometer means the metrological determination of the relation between the temperature of the sensor and the output quantity of the thermometer. Contact thermometers are, for instance, the resistance thermometers and their operational relies on the fact that the electrical resistance of metal conductors and semiconductors is temperature-dependent. The temperature measurement is thus traced back to the measurement of an electrical resistance.

Today, platinum is almost the most metal used as material for resistance thermometers (Platinum Resistance Thermometer or PRT). Best known are those with a resistance of 100 Ω at 0 °C, also called Pt100 thermometers. The range of their use extends from −200 °C to 600 °C.

Fig. 9. A Pt100 secondary reference standard connected to a resistance measuring bridge of high accuracy

The instruments used in this research activities for the in-field observations were Pt100 sensors combine in a single body with the relative humidity sensors (thermos-hygrometers). The two sensors were mounted on the top of a support made of plastic material due to minimize heat transfer from

the base towards the sensing elements. The sensor body is inserted inside a natural ventilation shield made of a pile of wedge shaped plates drilled in the middle and air circulation is guaranteed by thermodynamic characteristics of the structure (see chapters 3, 4 and 5 for further details).

The temperature sensors were calibrated with Pt100s, working reference standards (Figure 9), directly and documentably traceable to secondary reference standard used on INRiM primary laboratory (Figure 11) and to national reference standard (triple-point-of-water cell, primary reference standard), where the measurand consists by the ratio between the electrical resistance of the thermometer measured at the fixed points temperatures of the International Temperature Scale (ITS-90) (Preston-Tomas, 1990), with respect to the electrical resistance measured at triple point of water.

Prior to calibration, the thermometer is brought to a known temperature and the output parameter, e.g. the electrical resistance, is determined. A distinction is made between fixed point methods and comparison methods. In the fixed point method, the temperature of the respective fixed point (e.g. triple point of water) is realized, whereas in the case of the comparison method, the sensor in calibration and the reference standard are brought as exactly as possible to the same temperature, using a thermostated baths (Figure 10a) or a suitable furnace or also a climatic chamber (Figure 10b), and the measurements are compared with each other. Reference standard thermometers must have been traceably calibrated. For the measurement of the sensors in calibration and the reference standards, suitable electrical measuring devices (ohmmeter, resistance measuring bridge (Figure 9), standard resistors) are used, which also have been traceably calibrated. For the calibration in defined fixed

points of the applicable temperature scale, the preparation of the fixed point cells must take place in accordance with the ITS-90.

Fig. 10. Thermostatic bath (a) and climatic chamber (b) with inside the sensors in calibration, the reference sensor and copper comparing blocks

Within the scope of the determination of the measurement uncertainty, the spatial and temporal temperature distributions of the thermostat used for calibration (thermostatic bath, climatic chamber or furnace) are quantitatively determined and taken into account. For the determination of these distributions, calibrated thermometers of identical type are positioned on the boundaries of the working space (horizontal, vertical) of the thermostat. After thermal stabilization, the temperatures measured with the thermometers are continuously recorded (over a period longer than 20 min). The maximum resulting temperature difference between the thermometers is considered as a component of the uncertainty budget, with a rectangular distribution. Temperature gradients in thermostatic baths or climatic chamber can be reduced by providing a metallic comparator block

with boreholes to accommodate the reference standards and the sensors in calibration.

Before the calibration of a sensor, it is necessary to perform the initial check of it at the melting point of ice (0 °C), in a Dewar flask filled with crushed ice obtained from deionized water. The data are recorded in resistance (R_0). The thermometers are inserted into the ice for a length sufficient for the sensitive element to achieve thermal equilibrium with the ice. At least 5 readings of the thermometer in calibration must be performed and the values recorded are compared with those of the previous calibration, if available (Crovini *et al*. 1982). Then, the calibration continues by inserting the reference standard sensor and those in calibration in the thermostatic bath or climatic chamber in the zone of better thermal uniformity and stabilization is expected.

Sensitive elements of all sensors must be at the same depth. Also in this case, and after stabilization of the system, at least 5 readings of the signal of all the thermometers are carried out and the aforementioned operations are repeated for all the other calibration points established, by examining before moving to the next calibration point, the repeatability of the data obtained. The check at 0 °C is repeated and from this measure, averaged with the values of the initial check, the R_0 value of resistance to the melting point of the ice is obtained with its uncertainty. The initial and final readings on the reference sensor give an indication of the temperature stability of the bath or of the climatic chamber.

A calibration cycle can be performed either starting from the highest or the lowest temperature. In general, the calibration takes place on a minimum of 4 points (including the melting point of the ice) if the temperature interval is lower than 250 °C, up to 7 points for wider intervals.

Also for agricultural purpose, it is necessary to take into consideration the meteorological trends of the area under examination and to consider the intervals of temperatures and humidity that are recorded annually. In the specific case of this research, and in order to cover the whole range for atmospheric measurements, the selected set points were: −20 °C, −10 °C, 0 °C, 10 °C, 25 °C, and 45 °C for temperature sensors; 30 %rh, 60 %rh, 75 %rh and 90 %rh for relative humidity sensors, plus a second point at 60 %rh for the evaluation of the hysteresis.

The thermometers thus calibrated are characterized by determining the constants of the curve, which represents the trend of the signal as a function of temperature (t). The curve is represented numerically by a polynomial function of the type represented in equation 1:

$$y = a_0 + a_1 t + a_2 t + a_2 t^2 \ldots a_p t^p \qquad \text{(Eq. 1)}$$

were:

y = represents R/R_0,

R = is the resistance of the sensor in calibration

R_0 = is value of resistance to the melting point of the ice

The data processing will allow to derive the coefficients $a_0, a_1, \ldots a_p$ of the polynomial, the variance-covariance matrix and the calibration table starting from the points obtained experimentally with the method of least squares (Rippin, 1978).

Eq. 3 turns, as reported by IEC 60751 (2008), in equations 2 and 3:

- 2nd order polynomial for values above 0 °C:

$$R/R_0 = 1 + At + Bt^2 \qquad \text{(Eq. 2)}$$

- 4th order polynomial for values below 0 °C:

$$R/R_0 = 1 + At + Bt^2 + C\,(t - 100)\,t^3 \qquad \text{(Eq. 3)}$$

For thermoresistances to be used below 0 °C it is recommended to extrapolate the curve obtained above 0° C for values up to -40 °C and to determine the coefficient *C* for temperatures <-40 °C (Actis and Crovini, 1982).

The calibration uncertainty evaluation is obtained taking into account the contributions due at least to the following causes, assuming a statistical distribution in compliance with the applicable technical regulation:

- uncertainty of the reference sensor, obtainable from the calibration certificate;
- reference sensor stability, obtainable from the experimental data;
- interpolation on the reference sensor (by experimental data);
- comparator stability (by experimental data or by the manufacturer);
- temperature uniformity of the comparator (by experimental data or by the manufacturer);
- resolution of the sensor in calibration (by the manufacturer).

The interpolation uncertainty derives from the dispersion of the measures that causes uncertainty on the estimate of the interpolating polynomial coefficients (u_{int}). The u_{int} is obtained by calculating the square root of the quadratic sum of the "residuals" (M_i), i.e. the differences between the measured values and those calculated with the interpolating polynomial (converted into degrees Celsius), divided by degrees of freedom (equation 4):

$$u_{int} = \sqrt{\frac{\sum_i M_i^2}{n-m}} \qquad \text{(Eq. 4)}$$

with: $M_i = (y_{mi} - y_{ci})/(dy/dt_{ci})$

where:

y_{mi} = minimum value calculated at the *i*-th point

y_{ci} = value calculated at the *i*-th point

dy/dt_{ci} = value calculated from the derivative at the *i*-th point

n = number of calibration points

m = number of calculated coefficients of the polynomial interpolator, that is equal to 2 for the thermoresistances since they are determined by statistical means (least squares). The degrees of freedom of the interpolation process are *n* - *m*.

$$U(c) = k \cdot u = 2 \cdot \sqrt{\sum_i u(x)_i^2} \qquad \text{(Eq. 5)}$$

The equation 5 represents the expanded uncertainty *U(c)* expressed at the level of confidence of about 95% with a coverage factor $k = 2$ and it is equal to two times the square root of the quadratic sum of the *u(x)* of the single contributions considered.

1.4.2.1. Measurement model and uncertainty evaluation

It is necessary to clearly define what we intend to measure (measurand, *Y*) that is generally not measured directly, but through other *N* quantities. It is therefore essential to express mathematically the relation between the value of the measurand and the input quantities (*X*) from which *Y* depends (Equation. 6):

$$Y = f(X_1, X_2, \ldots, X_N) \qquad \text{(Eq. 6)}$$

The input estimated value x_i of each input variable X_i is determined with statistical analysis of series of observations or other methods. The result is an estimated *y* obtained using input estimates for the quantity X_i (Equation 7):

$$y = f(x_1, x_2, \ldots, x_N) \qquad \text{(Eq. 7)}$$

The *u(x)* is then evaluated for each x_i, any correlations and the results of the measurements are calculated from the functional relation *f* using the

values of x_i. The values of x_i and $u(x_i)$ derived from a distribution of possible values of the X_i. This probability distribution can be based on empirical frequencies (Type A evaluation, it is a retrospective evaluation) or on initial distributions (Type B evaluation, this is an a priori evaluation). A further step is the determination of *uc(y)*, determined in turn by $u(x_i)$ by applying the law of propagation of uncertainty, or the covariance associated with x_i. After calculating the *U(c)* by multiplying the *uc(y)* with the covering factor, the result of the measurement *y* is reported with its *uc(y)* or with its *U(c)*.

It is necessary to list all the possible sources of uncertainty. All the parameters that appear in the definition of the measurand will be characterized by a value of uncertainty and are therefore potential sources of uncertainty.

1.4.3. *Traceability*

Traceability involves the chain of measurements and accuracy transfers that connect the national standards of measurements, as maintained by National Metrology Institutes (NMI), with the measurements made in research, manufacturing and marketplace. It is important to provide that at each link in the chain or transfer from the reference standards at NMI or other secondary standards (Figure 11), consideration is given to the calibration uncertainty associated with that particular transfer. In addition, the measuring instrument must be calibrated by a reference standard that is itself traceable. Traceability is thus defined as the property of the result of a measurement or the value of a standard whereby it can be related to stated references, usually national or international, through an unbroken chain of comparisons all having stated uncertainties.

Fig. 11. Quartz sheath, long stemmed Capsule Standard PRT (C-SPRT) 25 Ω, reference standard used in primary laboratories and particular of the sensing element

The concept of traceability is important because it makes possible the comparison of the accuracy of measurements worldwide according to a standardized procedure for estimating measurement uncertainty.

When these various levels of calibration have been documented, a chain of traceable calibrations is created. Within a chain of traceability, the units of measurement with the highest accuracy are realized by international measurement standards which values is usually determined by comparison of national standards of the highest quality, or in the case of the kilogram by the mass of the International Prototype. Then, the national measurement standard serves as a reference for calibration of reference standards of lower accuracy. These reference standards are kept in a NMI or in an accredited calibration laboratory for calibrations not requiring the highest accuracy. Again, the result and the uncertainty will be stated.

2. Objectives of the thesis

Local agrometeorological stations must have the priority to provide useful data for the phytosanitary sector to support management decisions, contain costs and reduce the impact of agricultural activities on the environment. High quality traceable meteorological parameters are required for more accurate estimation and prediction. For these reasons, the metrology can be usefully applied for measurements of agrometeorological quantities in support to the DSSs and epidemiological forecasting models such as the grapevine downy mildew (*P. viticola*), a vineyards' disease strictly dependent on temperature, humidity and rain.

For a correct defence against pathogenic attacks, it is necessary to know the incubation period to act promptly before completion. This requires an accurate knowledge of meteorological parameters. Metrological studies are required to evaluate the measurement and calibration uncertainty components, necessary to improve the reliability and accuracy of epidemiological forecasting models. Different forecast models have been developed worldwide, these models have greatly improved the quality of output data; however, the meteorological data used as input values of the models usually derive from sensors not calibrated or calibrated without reference to the SI and without the inclusion of measurement uncertainties. Typically, these models do not consider the quality of input data (Sanna *et al.,* 2014).

The main objective of this research was the improvement of meteorological observations in the agricultural field through the dissemination of techniques and calibration methods using devices developed within the MeteoMet project (Merlone *et al.,* 2018) in collaboration with INRiM (National Institute of Metrological Research).

The structures available on the research site under management at IMAMOTER (National Research Council) were an ideal place for the study, as they are already dedicated to research activities with direct links to real applications. The evaluation of the potential improvement of the epidemiological forecasting models obtainable through the inclusion in the input values of accurate and traceable data with calibration uncertainty was another objective.

This research activity also concerned the quality of table tomatoes cultivated in tunnels, given the characteristics of health benefits of the crop and the strategic role of the cultivation in the Italian and world economy. The following aspects were evaluated:

- the solar radiation and microclimate measurements, using calibrated instruments and traceable data, within different cultivation environments for obtaining key parameters related to the effects both on final products and on environment;
- monitoring of the optical and radiometric properties of the films used as covering material, in order to study the evolution of the filtering capacity during film life time;
- the identification of the morphological processes of culture in response to the type of plastic film adopted by phenological and meteorological parameters observations.

Moreover, this research aimed to achieve a metrological approach applied to sustainable agricultural meteorological studies. The installation in the agricultural sites of calibrated and traceable automatic weather stations, the evaluation of the uncertainty in meteorological measurements may bring to optimize the use of pesticides with a positive impact on the environment, health and crops, towards a better management of agricultural risks.

3. Evaluation of EPI forecasting model for grapevine infection with inclusion of uncertainty in input value and traceable calibration.

Francesca Sanna[1,3,4*], Quirico Antonio Cossu[2], Guido Roggero[3], Simone Bellagarda[3], Andrea Merlone[3]

[1] *DiSAFA Dipartimento di Scienze Agrarie, Forestali e Alimentari, Università degli Studi di Torino, Largo Paolo Braccini, 2, 10095 Grugliasco (TO), Italy*
[2] *ARPAS Sardegna - Agenzia Regionale per la Protezione dell'Ambiente della Sardegna Dipartimento di Sassari.*
[3] *INRiM - Istituto Nazionale di Ricerca Metrologica, Torino.*
4 IMAMOTER-CNR - Istituto per le Macchine Agricole e Movimento Terra – Consiglio Nazionale Ricerche, Torino.

**Corresponding author: francesca.sanna@unito.it*

Published in: Italian Journal of Agrometeorology 2014, 19 (3) p. 33-44. Doi: 10.13140/2.1.2524.0644

Abstract: Forecasting models are useful tools to predict and manage epidemiological grapevine infection such as downy mildew (*Plasmopara viticola*). These models have improved the quality of the output data, but none of them considered the quality of the input data in terms of evaluation of measurement uncertainty of the sensors, the traceability and the weather conditions measuring system.

Air temperature and relative humidity sensors used in this study were calibrated by means of the transportable climatic chamber developed by INRiM, directly traceable to reference sensor, a Platinum Resistance Thermometer calibrated at the fixed points of the ITS-90 scale. The outcomes data collected during 2011 and 2012, with inclusion of measurement uncertainties, were used as input values for the diseases simulation by employing the EPI model.

The simulations with inclusion of more accurate data and measurement uncertainty foresee with better accuracy the period of infection and the moment to make treatments in the vineyard respect the simulation without inclusion of uncertainty, up to 7 days. In this study, the meteorological observations in field were improved by applying a metrological approach and calibration methods for automatic weather stations in homogeneous agricultural sites.

Keywords: Metrology, meteorology, downy mildew, forecasting models, measurement uncertainty, EPI

3.1. Introduction

Plasmopara viticola (Berk et Curt.) Berlese et De Toni is the causal agent of downy mildew, one of the most important disease of grapevine (*Vitis vinifera* L.) and its development is closely related by rain, temperature, and humidity (Lafon and Clerjeau, 1988).

The oospores present on the leaf litter break their winter dormancy and in spring the oospores germination can occur at a minimum temperature of 10 °C, up to a maximum of 32 °C, with an optimum of 23-24 °C. Blaeser (1978) has in fact observed that at 30 °C arise a rapid loss of germination ability. The value of 10 °C, according to Vercesi (1994), should be referred to the average temperature and not to the minimum. Further, to occur sporulation of *P. Viticola,* the temperature must be at least 13 °C and the relative humidity at 98%, during at least four hours of darkness (Vercesi, 1994). The incubation period, between onset of symptoms and the formation of conidiophores, is influenced by the daily average values of temperature and relative humidity, with optimal 21-24 °C and 90%, respectively (Müeller and Sleumer, 1934).

The disease is potentially destructive and is currently controlled by a massive use of fungicides, which has considerable economic costs (Friesland and Orlandini, 2011), negative effects on environment, human health and wine quality (Perazzolli, *et al.,* 2008). Some of these treatments are usually unnecessary given the sporadic occurrence of the infection. In order to identify high-risk and fungicide treatment periods, forecasting models have been proposed in France (Stryzik, 1983; Tran Manh Sung *et al.*, 1990; Magnien *et al.*, 1991), Germany (Hill, 1990), Switzerland (Blaise *et al.,* 1999; Viret and Bloesch, 2002), Italy (Rosa *et al.*, 1993; Rossi *et al*, 2005; 2008), Australia (Magarey *et al.*, 1991) and the USA (Park *et al*., 1997).

From the first forecasting models based on simple rule of thumb of the "3-10" proposed by Baldacci (1947) or Goidànich model (1964) which predicts the latent period, without considering the hours of leaf wetness and the meteorological trend, is reached to date at the modern mechanistic models. These latter take into account quantitative aspects of both sexual and asexual stages, the definition of primary inoculum season, the seasonal oospore dose, and its division into many coeval cohorts. This model represents a remarkable improvement since it achieved a higher level of confidence on the production of infections by oospores with probabilities ranging from 99.4% to 99.9% (Rossi *et al.*, 2008).

These models have improved the quality of the output data, but none of them considered the quality of the input data in terms of evaluation of measurement uncertainty and traceability of the sensors of the weather conditions measuring system.

As Guide to the expression of Uncertainty in Measurement (GUM) asserts, the uncertainty is a *Parameter, associated with the result of a*

*measurement, that characterizes the dispersion of the values that could reasonably be attributed to the measurand (*GUM 1995). The GUM, regularly published by BIPM (Bureau International des Poids et Mesures), also reported that the word "uncertainty" means doubt, and thus in its broadest sense "uncertainty of measurement" means doubt about the validity of the result of a measurement. Therefore, we cannot take as valid the value measured by an instrument if it is not associated with this parameter.

In situ calibrations of weather stations are usually performed by positioning standard instruments, such as hygrometers, thermometers, etc., close to the station under calibration. Reference sensors are left for a short period and the calibration is performed by comparison (Rana *et al.*, 2004). This procedure was metrologically evaluated and showed relevant weak points. Reference sensors are not always made to operate in open air; it is not possible to cover the whole range for the quantities, thus it is not possible to evaluate linearity and uncertainties for several sensors over the whole range and the evaluation of the mutual influences between parameters is not achievable. There is a need in agrometeorological studies for testing various types of sensors, their calibration, discontinuity in observations, avoid waiting for sensor imports results and loss of data (Rao *et al.*, 2009).

Furthermore, with the Directive on the Sustainable Use of Pesticides 2009/128/EC, art. 3, the European Commission establishing minimum rules for the use of pesticides in European Community so as to reduce risks to human health and the environment. In Italy, this Directive has been transposed by Legislative Decree n. 150 of August 14, 2012. One important rule is the implementation of Integrate Pest Management (IPM),

which focus on pest, disease and weed management, and will become mandatory in 2014.

The proposed research aims at achieving a first example at European level of metrological approach applied to agrometeorological studies. It goes to implement of traceability in weather and climate measurements, allowing production of the whole range of possible values of temperature and humidity observed in agricultural sites, disseminating by international researchers of calibration methods and procedures to agriculture operators and improve the reliability of forecasting models.

3.2. Materials and methods

3.2.1. *Vineyard*

Data analysis on the epidemic of *P. viticola* were carried out during 2011-12 in vineyard selected to be representative of vine-growing area, for cultivar, position, slope, soil type, solar exposure and proximity of trees. Vineyard is placed in locality Vezzolano (fraction of Albugnano, province of Asti) and it is supposed to had a representative dose of overwintering oospore populations, since a regular fungicide schedule was applied the previous season to control downy mildew.

The two vine variety assayed are Arneis and Sauvignon, with identical vine rootstock, S04 ISV-VCR6 and S04 CL.102 respectively, and two clones for each: VCR1 and CVT CN 19 for Arneis; ISV-F5 and R3 for Sauvignon, susceptibility to infection of downy mildew as reported in the National Register of Grapevine Varieties (Registro Nazionale delle Varietà di Vite, 2011). The vine variety were distributed in three rows for vine clone with alternating every two rows in order to have a homogeneous system.

3.2.2. *Forecasting models*

Forecasting models are tools that transform the relations between culture, adversity and the surrounding environment into mathematical equations. In general, are able to provide information about the onset and evolution of a disease or indicate a period of time in which it is improbable that the disease appears starting by meteorological data.

In this study we have evaluated the feasible improvement of EPI model – (État Potentiel of Infection), for the potential state of grapevine infection proposed by Strizyk (1983). This model was chosen considering that is still most widely used, it has been the subject of comparative studies (Cossu *et al.*, 2004), it is an application tool validated (Caffi *et al.*, 2006) and with long experience of investigation in different wine-growing areas of Italy (Vercesi 1990; Fronteddu and Cossu, 2002; Fremiot, 2008).

The assessments of mechanistic models are still under our evaluation.

EPI is a model of epidemic behaviour. The model follows the entire life cycle of the pathogen, giving priority to the rainfall in autumn and winter affecting the potential of germination of wintering oospores. The model assumes that the pathogen will adapts to the average climatic conditions of a given area, which are favourable to disease development in the current season, to the accumulated values from an historical database, therefore, deviations from these conditions limit the potential development of the epidemic. The EPI index value depends on the sum of a component called "potential energy" ***Ep*** and another called "kinetic energy" ***Ec*** and is defined as Equation 1.1:

$$EPI(t_i) = \sum_{i=1}^{n-1} Ep(t_i) + \sum_{i=n}^{m} Ec(t_i) \qquad \text{(Eq. 1.1)}$$

where:

EPI(t_i) express the value of the EPI at the range of discrete time ***t_i***;

Ep(t_i) is calculated for the period October 1 (i=1) March 31, (i=n-1), every ten days, and expresses the elementary contribution of the potential energy;

Ec(t_i) is calculated daily during the period April 1 (i=n) August 31 (i=m) and expresses the elementary contribution of the kinetic energy of the pathogen.

The potential phase is used to delay the onset of fungicide spray programs. Fungicides treatments are also avoided when disease development predicted by kinetic phase is below the average.

The EPI model was calibrated respect the weather and climatological conditions of the site under study (data are obtained from the Phytosanity Service of the Piedmont Region, in which are calculated the individual contributions of ***Ep(t_i)*** and ***Ec(t_i):***

Potential energy phase *Ep(t_i)*

The potential energy of the oospores is estimated on the deviations from the averages of the climatological values of air temperature and rainfall. The formula for calculating the contribution per unit of potential energy in a generic time interval, between October 1 and March 31, is as follows Equation 1.2:

$$Ep = 2ct\left(\sqrt{ht} - \sqrt{Hm} * 0.95\right) + \left(0.2\left(\sqrt{ht} * \sqrt{t} - \left(\sqrt{Hm} * 0.95\right) * \sqrt{Tc}\right) - \left(NPGm * \frac{1.5}{18} * \log_{10}\frac{h}{npg}\right)\right) \qquad (Eq.\ 1.2)$$

where:

Ep = contribution of potential energy relative to the processing time interval considered (10 days);

ct = pondering factor for the processing period, with values of: 1.2 for October-November, 1 for December, 0.8 for January, February, March;

ht = monthly rainfall (mm);

Hm = climatological monthly rainfall (mm);

t = average monthly air temperature (°C)

Tc = climate monthly air temperature value (°C);

NGPm = average number of rainy days per month;

h = rainfall per decade (mm);

ngp = number of rainy days per decade.

Kinetic energy phase *Ec(t_i)*

Ec(t_i) was calculated daily during the period April 1 - August 31 and expresses the contribution of the kinetic energy of the pathogen. In this phase, the processing was performed daily according to the following equation 1.3:

$$Ec = 0.012\left(\frac{\left(\left(\frac{5Ucn + 3Ud^2}{8}\right)\sqrt{T}\right)}{100} - \frac{Uc^2\sqrt{Tc}}{100}\right) \quad \text{(Eq. 1.3)}$$

where:

Ec = index of kinetic energy calculated for each interval (day) processing;

Ucn = value of climatological monthly night-time humidity (%) from 7 pm to 9 am;

Ud = average daytime humidity (%) from 10 am to 6 pm;

T = average daily temperature (°C);

Tc = climate monthly air temperature value (°C);

All climate data refer to the period to which belongs the time interval considered.

A risk situation is marked when two conditions arise: the values of EPI must be greater than -10 and they must occur progressive increases in the value of EPI for three days following that in which it is registered EPI > -10 (e.g. - 9, -7, -5).

3.2.3. *Automatic Weather Stations*

An Automatic Weather Stations (AWS), was selected among the commercially available models in terms of measured quantities, resolution, measurement accuracy, specific for agricultural purposes, and conform to WMO recommendations (WMO, 2008). The AWS suitable for detect, acquire, process, store and transmit data is of the type Off line AWS, correlated to a data logger, modem GPRS and a photovoltaic panel, composed as described in Tab. 1.

The air temperature sensor was calibrated using a prototype facility developed under the ENV07 MeteoMet project (Merlone *et al.*, 2012). This facility is the transportable climatic chamber "EDIE 1– Earth Dynamics Investigation Experiment" developed at INRiM laboratories (Lopardo *et al*., 2015). The sensing element that detects the air temperature, a Platinum Resistance (Pt 100), was placed inside the chamber together with the reference sensor, a Platinum Resistance Thermometers (PRT 100 Ω) calibrated at the ITS-90 fixed points. The reading in resistance of the sensor was carried out by means of a nanovoltmeter Agilent A34420A with uncertainty in the final temperature of 0.01 C.

The reference temperature was the result of 20 repeated measures read from the nanovoltmeter every 30 s. The temperature of the sensor to characterize was stable in the recording period.

Tab 1: Automatic weather station installed in Vezzolano (AT), sensors, description of quantities, measurement principle, and resolution**.**

Variables	Unit	Sensing element	Measurement principle	Resolution
Air temperature	*t* (°C)	Platinum Resistance (Pt 100)	Resistance variation	0.1 °C
Air relative humidity	*U* (%)	Hygroscopic polymer	Capacitive variation	0.1 % RH
Solar radiation - PAR	µV/(µmol/ $m^{-2}s^{-1}$)	Silicon photo diode	Electro-optical (photoelectric) Transducer	1µV/(µmol /$m^{-2}s^{-1}$)
Wind speed	m/s	Three cups (Robinson's anemometer)	Incremental rotary encoder	0.1 m/s
Wind direction	° (degree)	Gonio-anemometer	Optical encoder (Gray code)	± 0,08°
Soil moisture*	m^3/m^3 (%)	Two-prong probe	dielectric constant	0.001 m^3/m^3 VWC
Soil temperature	*t* (°C)	Platinum Resistance (Pt 100)	Resistance variation	0.1 °C
Precipitation	mm	Tipping bucket rain gauge	**	0.2 mm

* $\theta v = V_{water}/V_{sample}$; θv, is The volumetric water content of a soil sample, V_{water} is the volume of water in the soil sample and V_{sample}, the ratio is usually expressed in per cent.
**When approximately 15 ml of water collected (equivalent to 0.2 mm of rainfall), the bucket tips and empties, bringing the other bucket under the funnel, and in the process activates a reed switch. Each tip is counted by the data logger, and this is converted to an accumulated rainfall amount over the desired measurement period.

The calculated calibration curve is of the type $t=(t_{AWS})$ obtained by means of a polynomial fit on the differences between the value read from the

datalogger linked to air temperature sensor in calibration (t_{AWS}) and reference sensor (t_C).

In the calculation of the uncertainty were taken into account the contributions of resolution of sensor in calibration, the uncertainty related to the position and the uncertainty of t_C (Tab. 2).

Tab. 2: Uncertainty contributions for air temperature sensor calibration.

Resolution of sensor in calibration	0.028 °C
Uncertainty related to the position	0.03 °C
Uncertainty t_C	0.01 °C

All these contributions were added in quadrature and multiplied by the covering factor $k = 2$, to obtain the final calibration uncertainty ($\mathbf{U_t}$) with a confidence level of 95%.

Tab. 3: Calibration results for air temperature sensor uncertainty evaluation. t_C = air temperature of reference sensor; Dev st t_C = standard deviation of t_C; t_{AWS} = air temperature of sensor in calibration; Δt = difference obtained by subtracting t_{AWS} from t_C; t_{calc} = value obtained by calibration curve inclusion; Residues = difference in temperature obtained by subtracting t_{calc} from t_C.

t_C	t_{AWS}	Δt	t_{calc}	Residues
44.085 °C	44.7 °C	-0.615 °C	44.067 °C	0.018 °C
25.338 °C	25.8 °C	-0.462 °C	25.375 °C	-0.037 °C
11.068 °C	11.3 °C	-0.232 °C	11.083 °C	-0.015 °C
0.983 °C	1 °C	-0.017 °C	0.955 °C	0.028 °C
-8.918 °C	-9.1 °C	0.182 °C	-8.955 °C	0.037 °C
-19.953 °C	-20.3 °C	0.347 °C	-19.922 °C	-0.031 °C

The statistical contribution $\boldsymbol{U_t}$ was given by the equation 1.4:

$$\boldsymbol{U_t} = \sqrt{\frac{\sum(\boldsymbol{t_{calc}} - \boldsymbol{t_C})^2}{\boldsymbol{d}}} \qquad \textbf{(}\text{Eq. 1.4)}$$

Where:

($\boldsymbol{t_{calc}}$-$\boldsymbol{t_C}$) is a residue, **d** is the number of degrees of freedom (6 measures less than 2 degree of the polynomial fit = 4 in this case).

It was obtained the following calibration curve:

$t_{\mathbf{calc}} = t_{AWS} + \mathbf{a}\ t_{AWS}^2 + \mathbf{b}\ (t_{AWS}) + \mathbf{c}$

a=0.000098 °C^{-}

b=-0.017950

c=-0.026809 °C

$\mathbf{U}_t$= 0.11 °C

The calibration of the relative air humidity sensor was performed at INRiM laboratories, where the measurand is the relative humidity percentage measured by the sensor in calibration. The sensor was placed in the test chamber. The calibration was done using the direct method by comparing the relative humidity reference produced by a generator of air humidity, secondary measurement standard, with the reading of the sensor in calibration in accordance with INRiM procedure T/07/06 REV00. For the evaluation of the uncertainty, the values read both temperature AWS sensor (t_{AWS}) and temperature reference sensor (t_C) were also considered.

The calibration uncertainty was obtained taking in account the follow contributions:

- The uncertainty in the determination of the conditions applied (RH_C);
- Resolution of the sensor in calibration;
- Measurement repeatability of the sensor in calibration;
- Hysteresis (evaluated on the return point) of the sensor in calibration;

The standard measurement uncertainty associated to hysteresis was within 1.0 % *RH*.

The expanded measurement uncertainty of calibration U_{RH} is expressed as standard measurement uncertainty multiplied by the coverage factor $k = 2$ which for a normal distribution of probability corresponds to a confidence level of 95 %.

Tab. 4 - Calibration results for relative humidity sensor uncertainty (**U_{RH}**). **RH_C** = relative humidity of reference sensor; **RH_{AWS}** = relative humidity of the sensor in calibration;

t_C (°C)	t_{AWS} (°C)	RH_C (%)	RH_{AWS} (%)	$RH_{AWS} - RH_C$ (%)	U_{RH} (%)
23,05	23,5	29,9	31	+1,1	0,88
23,05	23,4	59,8	62	+2,2	1,44
23,06	23,5	89,6	91	+1,4	2,05
23,06	23,5	59,8	62	+2,2	1,44

3.3. Results and discussion

Sites where meteorological data series are collected are equipped with instruments that rarely have well-defined traceability and usually the data are collected without an uncertainty evaluation, only an assessment of the quality of output data is generally done.

Meteorological data required for preliminary simulations were collected hourly from 2011 to 2013, from the AWS installed in Vezzolano, in the same site where the vineyard is located, through the agrometeorological service of Piedmont Region. The sensors of this AWS were not calibrated since 2002, before installation has occurred; in situ calibration is not

achievable. The instrumental drift is ± 0.01 °C per year for air temperature sensor, and ± 1% per year for air relative humidity, as the technical data sheet was reported (instrumental drift for precipitation and leaf wetness sensors are not specified).

During all period of research, it was evaluated the potential improvement of forecasting model by inclusion of traceable data and uncertainties in the model input values. Contemporary pathogens growth observation, meteorology data recording (air temperature, air relative humidity, leaf wetness, rainfall), and evaluation of measurement uncertainty. Diagnosis through observation of symptoms in field, supported by humid chambers and subsequent observations by light microscopy and analysis of the measurement results and reporting were also performed.

Going backward from the date of primary infection symptoms (DPIS) onset, the most probable period of infection (PPI) was calculated according to Giosuè et al. (2002). The DPIS was deducted through observation of symptoms in field to be between May 9 and 10.

The length of incubation period was calculated as a function of air temperature, using two regression equations accounting for both low and high level of relative humidity, adapted to the evaluation table of the incubation period of Goidànich (1957), as shown in Fig. 1. Starting from DPIS, was calculated, for each previous day, the progress of incubation, as the reciprocal of the duration of incubation in correspondence of the average daily temperature. The incubation period was deemed to have ended the day on which the sum of these daily rates of advancement was equal to or greater than one (Caffi et al., 2011).

Taking into account the precipitation event that started the germination process and leaded to infection, the most predicted day on which sporangia

are formed is between April 30 and May 1, and the beginning of germination between April 6 and 7 (Tables 5 and 6).

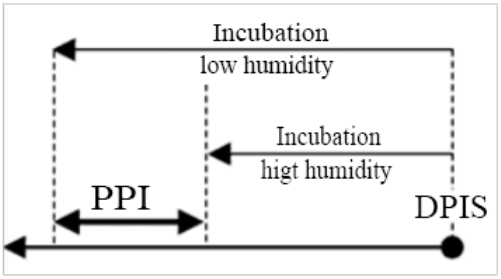

Fig. 1 - Most probable period of infection (PPI) accounting for both low and high level of RH, going backward from the date of primary infection symptoms (DPIS) onset (from Giosuè, 2002 modified).

The evaluation of the improvement of the forecasting model was performed through the forecasting simulations of infection, achieved by including uncertainties in the EPI model input values.

Tab. 5 – Event that started the germination process and leaded to infection, onset data of germination, sporangia formed, infection and symptoms of primary infection.

Event that lead to infection	**Beginning of germination**	**Sporangia formed**	**Day of infection**	**Symptoms**
Precipitation: 04/04: 18.6 mm	06 April 12	30 April 12	1 May 12	9 May 2012
precipitation 05/04: 16.4 mm	06 April 12	01 May 12	1 May 12	9 May 2012
precipitation 06/04: 0.8 mm	07 April 12	1 May 2012	1 May 12	10 May 2012
precipitation 07/04: 2.2 mm	08 April 12	1 May 2012	1 May 12	10 May 2012

Tab. 6 – mm of precipitation essential for primary infection onset.

Day	3 Apr	4 Apr	5 Apr	6 Apr	7 Apr	8 Apr	28 Apr
Precipitation (mm)	1.2	18.6	16.4	0.8	2.2	0.8	0.0
Day	29 Apr	30 Apr	1 May	2 May	3 May	4 May	5 May
Precipitation (mm)	3.2	19.6	43.0	7.8	0.2	0.0	8.0

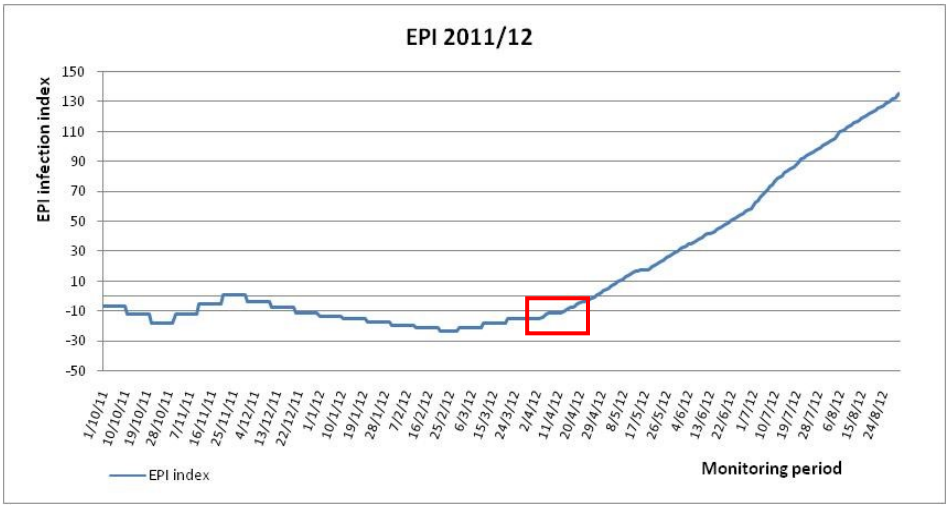

Fig. 2 - EPI index value depends on the sum of ***Ep*** and ***Ec*** using data without measurement uncertainty. ☐ Period in which is highly recommended make an anti-downy mildew treatment.

3.3.1. *Simulations on EPI forecasting model*

In Fig. 2 is represented the EPI index value depends on the sum of ***Ep*** (from October 1to March 31) and ***Ec*** (from April 1 to August 31), without inclusion of uncertainties in input values. The period in which is highly recommended make a treatment starts by 13 April as indicated in red box.

In Tab. 7 and in Fig. 4 and 5, are shown the EPI values in seven different simulations. The first simulation was performed without inclusion of

uncertainties in the input values (powder blue trend line – EPI no-unc); the second with inclusion of the upper limits of the confidence interval for the measurement uncertainty of temperature (blue trend line – EPI T-up). The third simulation with inclusion of the lower limits for the measurement uncertainty of temperature (red trend line – EPI T-down), the fourth simulation with inclusion of the upper limits of relative humidity (green trend line – EPI RH-up), the fifth simulation with inclusion of the lower limits of the measurement uncertainty of relative humidity (purple trend line – EPI RH-down), the sixth simulation with inclusion of the upper limits of the measurement uncertainties of temperature and relative humidity (cyan trend line – EPI T_RH-up), the seventh with inclusion of the lower limits in the confidence interval for the measurement uncertainties of temperature and relative humidity (orange trend line – EPI T_RH-down).

EPI no-unc simulation shows that the potentially infection starts on April 13, in the same day predicted by EPI RH-up scenario. In simulation EPI T-up, the predicted potential epidemic risk also starts on April 13, but the second condition (increase in the recorded values on following days) occurs only by April 17. A similar situation occurs in simulations EPI RH-down and EPI T_RH-up, where the potential epidemic risk begins by April 6 and 7, respectively, and the progressive increasing values starting since April 12 and 13, respectively. In simulations EPI T-down and EPI T_RH-down the epidemic risk begins by April 18 and 14, respectively, and the two conditions are complied, in which there is an increase in the recorded values in the following days.

Tab. 7 - EPI index value of ***Ec***, focused on period in which is highly recommended make a treatment, data used are without uncertainty (column 2) and with uncertainty in input values (columns 3-4-5-6-7-8). Green boxes indicate the day in which EPI index reached value 10, yellow boxes the days in which EPI values occur progressive increases.

DATA	EPI no-unc	EPI T-up	EPI T-down	EPI RH-up	EPI RH down	EPI T_RH_ up	EPI T_RH_ down
06-apr	-12	-12	-15	-12	-10	-10	-13
07-apr	-11	-11	-14	-11	-9	-10	-12
08-apr	-11	-11	-14	-11	-9	-9	-12
09-apr	-11	-11	-14	-11	-9	-8	-12
10-apr	-11	-11	-14	-11	-9	-7	-12
11-apr	-11	-11	-14	-11	-9	-7	-12
12-apr	-11	-11	-14	-11	-9	-7	-12
13-apr	-10	-10	-13	-10	-8	-6	-11
14-apr	-9	-10	-13	-9	-7	-6	-10
15-apr	-8	-9	-12	-8	-6	-6	-9
16-apr	-7	-8	-11	-7	-5	-5	-8
17-apr	-7	-7	-11	-7	-4	-5	-7
18-apr	-6	-7	-10	-6	-3	-5	-6
19-apr	-5	-6	-9	-5	-2	-4	-5
20-apr	-4	-5	-8	-4	-1	-3	-4
21-apr	-3	-4	-7	-3	0	-2	-3
22-apr	-3	-4	-7	-3	1	-2	-2

The following Fig. 3 shows the correlation among EPI index values (from April 1 to July 31 period) and meteorological conditions; in Fig. 4 are represented the trend lines of EPI index focused on *Ec* phase. The boxes explain, for each simulation, the day in which EPI index reach the value -10, day in which is highly recommended start the treatment in the vineyard. In the trend lines, the rhombus markers are positioned in the relative day.

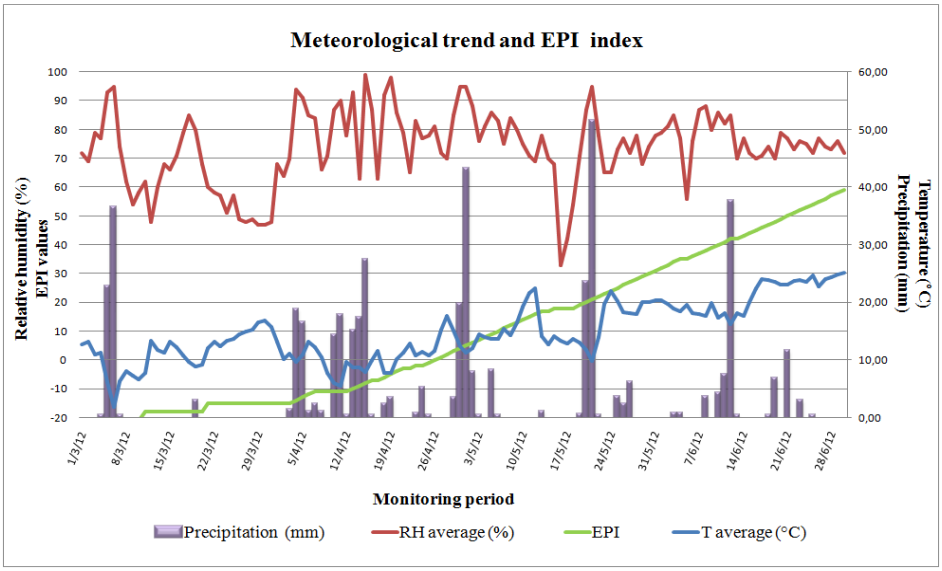

Fig. 3 - Meteorological trend (temperature, humidity and precipitation) compared to EPI index values focus on ***Ec*** period.

The precipitations from April 29 to May 2, the temperature over 13 °C and the relative humidity of around 95% at the same period allow the oospores sporulation that lead to the infection and the symptoms onset on May 9-10. Trends of air temperature, air relative humidity and precipitation, the infection evolution expressed in number of cohorts of oospores that begin germination (started on April 6, highlighted by a red circle), and cohorts of oospores that leading to the symptoms onset (days of onset highlighted by a red rectangle) are shown in Fig. 5.

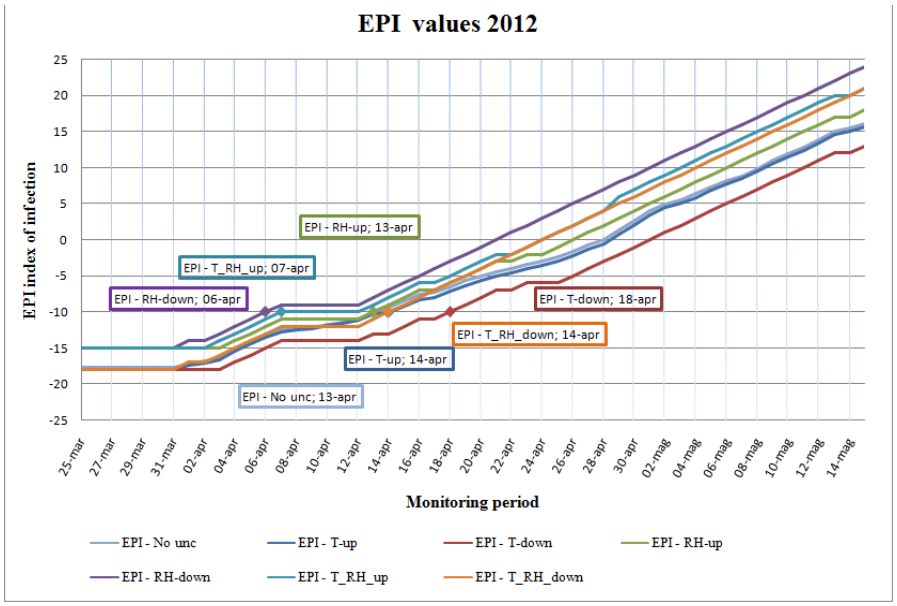

Fig. 4 - EPI index value kinetic energy (***Ec***). For each simulation the boxes explained the day in which EPI value reach the value -10, and the rhombus marked highlighted the day in which is highly recommended starts the treatment.

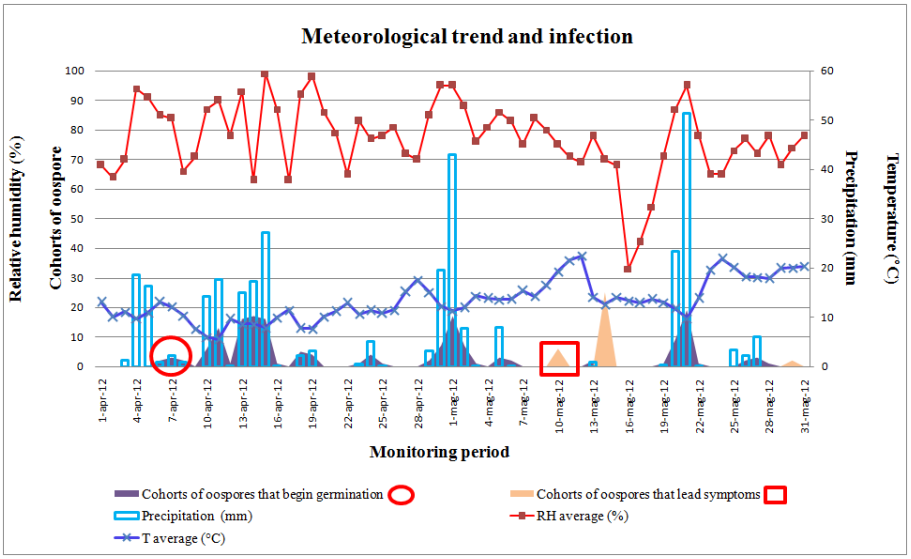

Fig. 5 - Trend of temperature (line with X, in °C), relative humidity (line with ■, in %), precipitation (empty rectangles, in mm), and infection evolution expressed in number of cohorts of oospores that begin germination (dark grey area, starting day highlighted by a circle), and cohorts of oospores that leading to the symptoms onset after germination and sporulation (light gray area, days of onset highlighted by a rectangle).

The results show that simulation without uncertainties, with uncertainty in T-up, in T-down, RH-up and T-RH-down predict the beginning of the epidemic risk with a deviation from the real situation of infectious of 7, 7, 12, 8 days, respectively. The oospores begin the germination on April 6, the same day on which the R-up simulation predicts the beginning of the epidemic risk, as well as in the simulation T_RH-up with only one day of deviation (April, 7).

3.4. Conclusions

Relying on the prediction of the simulation without uncertainties, pesticide treatments would been carried out from April 13, when oospores germination had already beginning at least by a week, and taking into account the potentially washout rains of following days (precipitations April 13: 15 mm; April 14: 17.2 mm; April 15: 27.2 mm), the fungicide sprays would have been useless, with significant costs in terms of loss of the fungicide, human labour and the final product. The scenario would be different if we had taken into consideration the simulations with inclusion of measurement uncertainty for the air temperature and relative humidity, where, moreover, the washout rains in the days following the situation of epidemic risk were absent or mild.

Therefore, in light of the elucidated considerations, it is considered that forecasting models should include measurement uncertainties in the input values, and provide traceability of the reference sensors to the AWSs sensors in order to have more accurate meteorological data and better models output data. Moreover, further studies are needed to better understand the metrological phenomenon and improve these powerful tools which are the epidemiological forecasting models.

3.5. Acknowledgment

The author thanks the Servizio Fitosanitario of Piedmont region for useful data needed in preliminary simulations and epidemiological data; the technicians of Azienda Agricola Sperimentale IMAMOTER-CNR of Vezzolano (AT) for support during AWS installation.

This study is funded by the EMRP participating countries within EURAMET and the European Union, in the framework of ENV07-REG4 MeteoMet European project.

3.6. References

Baldacci E., 1947. Epifitie di *Plasmopara viticola* (1941–46) nell'Oltrepò Pavese ed adozione del calendario di incubazione come strumento di lotta. Atti Istituto Botanico, Laboratorio Crittogamico, 8: 45–85

Blaeser M., Weltzien H.C., 1978. Die Bedeutung von Sporangienbildung, -ausbreitung und-keimung für die Epidemiebildung von *Plasmopara viticola*. Zeitschrift für Pflanzenkrankheiten und Pflanzenschutz, 85: 155-161

Blaise P., Dietrich R., Gessler C., 1999. Vinemild: an application oriented model of *Plasmopara viticola* epidemics on *Vitis vinifera*. Acta Hortic, 499: 187–192

Caffi T., Rossi V., Bugiani R., Spanna F., Flamini L., Cossu A., Nigro C., 2006. Validation of a simulation model for *Plasmopara viticola* primary infections in different vine-growing areas across Italy. International Workshop on Grapevine Downy and Powdery Mildew. San Michele all'Adige, 18-23 June 2006

Caffi T., Rossi V., Carisse O., 2011. Evaluation of a dynamic model for primary infections caused by *Plasmopara viticola* on grapevine in Quebec. Online. Plant Health Progress doi:10.1094/PHP-2011-0126-01-RS

Cossu A., Dalla Marta A., Orlandini S., 2004. Studio comparativo di due modelli per la previsione della peronospora della vite (*Plasmopara viticola*). Atti III Giornate di Studio "Metodi Numerici, Matematici e Statistici nella Difesa delle Colture Agrarie e delle Foreste: Ricerca e Applicazioni". – Firenze 2004

Decreto Legislativo 14 agosto 2012, n. 150. Attuazione della direttiva 2009/128/CE che istituisce un quadro per l'azione comunitaria ai fini

dell'utilizzo sostenibile dei pesticidi. (12G0171) G.U. n. 202 del 30-8-2012 - Suppl. Ordinario n. 177. Serie generale 202: 44-63

Egger E., Marinelli E., D'Arcangelo M., 1996. Influenza di diversi metodi per la stima della bagnatura fogliare sulla previsione degli attacchi di peronospora e muffa grigia sulla vite. Informatore Fitopatologico, 3: 61–67

European Commission 2009. Directive 2009/128/EC of the European Parliament and of the Council of 21 October 2009 establishing a framework for Community action to achieve the sustainable use of pesticides. Official Journal of the European Union, L 309/71-309/86

Friesland H., Orlandini S., 2011. Simulation models of plant pests and diseases. Meteorol. Appl. for Agriculture - Final report. COST Action, 718: 1-19

Fremiot P., Parisi N., Pinzetta M., Tonni M., Salvetti M., Strizyk S., Vercesi A. 2008. Andamento delle epidemie di *Plasmopara viticola* e valutazione del modello EPI nei vigneti lombardi. In: Giornate fitopatologiche: protezione delle piante, qualità, ambiente: atti Cervia (Ra), 12-14 marzo 2008, CLUEB 237-244

Fronteddu F., Cossu A., 2002. Indagine sull'affidabilità del modello EPI Plasmopara nei vigneti della Sardegna Orientale. Atti II Giornate di Studio "Metodi numerici, statistici ed informatici nella difesa delle colture agrarie e delle foreste". Pisa 22-23 maggio 2002

Giosué S., Girometta, B., Rossi V., Bugiani R., 2002. Analisi geostatistica delle infezioni primarie di *Plasmopara viticola* in Emilia Romagna. Atti II Giornate di studio "Metodi numerici, statistici e informatici nella difesa delle colture agrarie e delle foreste: Ricerca e applicazioni", Pisa, Italy, 2002, 1: 229 -237

Goidànich G., 1964. Le *Peronosporales*. In: Manuale di Patologia Vegetale, Vol. II. Edizione agricole, Bologna, Italy, 315–346

Goidànich G., Casarini B., Foschi S., 1957 - Lotta antiperonosporica e calendario di incubazione. Giornale di Agricoltura, 13 gennaio: 11-14

GUM, 1995. Evaluation of measurement data - Guide to the expression of uncertainty in measurement. JCGM 100:2008, pp. 134

Hill G.K., 1990. Plasmopara Risk Oppenheim – a deterministic computer model for the viticultural extension service. Notiziario sulle Malattie delle Piante, 111: 231–323

Lafon R., Clerjeau M., 1988. Downy mildew. In: Pearson, R.C., Goheen, A.C. (Eds.), Compendium of Grape Diseases. APS Press, St. Paul, Minnesota, USA: 11–13

Lopardo G, Bellagarda S, Bertiglia F, Merlone A, Roggero G, Jandric N, 2015. A calibration facility for automatic weather stations. Meteorol. Appl. 22: 842-846.doi: 10.1002/met.1514

Magarey P.A., Wachtel M.F., Weir P.C., Seem R.C., 1991. A computer-based simulator for rationale management of grapevine downy mildew *Plasmopara viticola*. Aust. Plant Protect. Quart, 6: 29–33

Magnien C., Jacquin D., Muckensturm N., Guillemard P., 1991. MILVIT: a descriptive quantitative model for the asexual phase of grapevine downy mildew. IOBC/WPRS Bulletin, 21: 451-459

Merlone A. Lopardo G., Bell S., *et al.*, 2012. A new challenge for meteorological measurements: the "MeteoMet" project – metrology for meteorology, proceedings of the WMO-CIMO TECO Conference, Brussels 16-18 October.

Müller K., Sleumer H., 1934. Biologische Untersuchungen über die Peronosporakrankheit des Weinstockes. Landwirtschaftliche Jahrbucher, 79: 509–576

Park E.W., Seem R.C., Gadoury D.M., Pearson R.C. 1997. DMCAST: a prediction model for grape downy mildew development. Viticult. Enol. Sci. 52: 182–189

Perazzolli M., Dagostin S., Ferrari A., Elad Y., Pertot I. 2008. Induction of systemic resistance against *Plasmopara viticola* in grapevine by *Trichoderma harzianum* T3 9 and benzothiadiazole. Biol. Control, 47: 228-234

Rana G., Rinaldi M., Introna M., 2004. Methods and algorithms for evaluating the data quality at hourly and daily time scales for an agrometeorological network: application to the regional net of Basilicata (Italy) Rivista Italiana di Agrometeorologia, 1: 14-23

Rao V., Rao G., Rao A., Tripathi M.K., 2009. Synergizing Agrometeorology for managing future agriculture in India. 4th National Seminar on "Agrometeorology-needs, Approaches and Linkage for Rural Development" held at CCS HAU, Hisar 26-27 November, Proceedings of National Seminar of Agrometeorology "Journal of Agrometeorology, 11: 11-17

Registro Nazionale delle Varietà di Vite, 2011. D.P.R. 24.12.1969 n.1164, implement by Decreto 22 aprile 2011 Modificazioni al registro nazionale delle varietà di vite, Gazzetta Ufficiale n. 170 del 23 luglio 2011

Rosa M., Genesio R., Gozzini B., Maracchi G., Orlandini S., 1993. Plasmo: a computer program for grapevine downy mildew development forecast. Comput. Electron. Agricult., 9: 205–215

Rossi V., Caffi T., Giosuè S., Bugiani R., Girometta B., Spanna F., Dellavalle D., Brunelli A., Collina M., 2005. Elaboration and validation of a dynamic model for primary infections of *Plasmopara viticola* in north Italy Rivista Italiana di Agrometeorologia, 3: 7-13

Rossi V., Caffi T., Giosuè, S., Bugiani R., 2008. A mechanist model simulating primary infections of downy mildew in grapevine. Ecol. Modelling, 212: 480-491

Stryzik S., 1983. Modèle d'État Potentiel d'Infection: application a *Plasmopara viticola*. Association de Coordination Technique Agricole, Maison Nationale des Eleveurs: 1–46

Tran Manh Sung C., Strizyk C., Clerjeau M., 1990. Simulation of the date of maturity of *Plasmopara viticola* oospores to predict the severity of primary infections in grapevine. Plant Disease, 74: 120-124

Vercesi A., Cortesi P., Zerbetto F., Bisiach M. (1990) - Valutazione del modello EPI in Oltrepo Pavese e nel Veronese: rapporto di attività. Not. Mal. Piante, 111: 203-236

Vercesi A., 1994. Strumenti innovativi per la gestione della difesa contro la peronospora della vite – Informatore patologico, 5

Viret O., Bloesch B., 2002. Observation on germination of oospores and primary infection of *Plasmopara viticola* under field conditions in Switzerland. In: Proceedings of the 4th International Workshop on Powdery & Downy Mildew in Grapevine, Napa, 30th September–4th October: 10–11

WMO – CIMO. 2008. Guide to Meteorological Instruments and Methods of Observation, WMO-No. 8 2008 edition, Updated in 2010, Geneva, pp. 716

4. Vineyard diseases detection: a case study on the influence of weather instruments calibration and positioning

Francesca Sanna[a,c,1], Angela Calvo[a,b], Roberto Deboli[b], Andrea Merlone[c]

[a] *DiSAFA Dipartimento di Scienze Agrarie, Forestali e Alimentari, Università degli Studi di Torino, Largo Paolo Braccini, 2, 10095 Grugliasco (TO), Italy*

[b] *IMAMOTER-CNR – Istituto per le Macchine Agricole e Movimento Terra – Consiglio Nazionale Ricerche, Strada delle Cacce, 73, 10135, Torino, Italy*

[c] *INRiM – Istituto Nazionale di Ricerca Metrologica, Strada delle Cacce 91, 10135, Torino, Italy*

[1] *Corresponding author: francesca.sanna@unito.it*

Published in Meteorological Applications 2018, 25(2) 228-235 DOI: 10.1002/met.1685

Abstract

Weather monitoring instruments installed on hill and mountain agricultural sites are often forced into non-ideal positioning due to slopes, tree proximity and other obstacles such as rivers and rocks that primarily affect relative humidity, temperature, and solar radiation. Moreover, data from these weather stations do not take into account the measurement uncertainties related to these influences. The aim of this study is to investigate weather instruments' calibration and positioning in a vineyard located in the Monferrato region in north-western Italy.

Meteorological data from two weather stations were analysed metrologically, in terms of evaluation of calibration uncertainty and traceability to the International System of Units, and using a statistical test, with the purpose of evaluating primarily the effect of the sensors'

calibration and positioning on sloping hills. To better understand these influences, and in order to improve vineyard disease predictions reducing the use of chemicals in agriculture, the data recorded from the weather stations were included with the calibration uncertainties and used as input values of an epidemiological forecasting model. The inclusion of the calibration uncertainties and positioning contribution affected disease prediction up to five days; this can be explained by the effect of the tree canopy's spatial arrangement, which tends to alter the vineyard's microclimate.

Keywords Weather station; positioning; agriculture; calibration; uncertainty; metrology for meteorology

4.1. Introduction

Vineyards and other agricultural sites are often positioned on slopes and close to forests where the canopy influences weather conditions in the vicinity. This enforces a non-ideal position for installing weather instruments and the resulting data do not take into account the effect of slope, the proximity of trees or intensity of solar radiation (Matese *et al.*, 2014). The contribution of measurement uncertainty arising from these conditions is not generally considered; in addition, there is a lack of sensor calibrations.

The calibrations of weather stations are generally performed by comparison, positioning the reference sensors for a short period close to the station under calibration (Rana *et al.*, 2004). This procedure has shown relevant weak points (Sanna *et al.*, 2013). Reference sensors are not always made to operate in open air and it is not possible to cover the entire range

for the quantities, thus, evaluating the mutual influences among parameters is not achievable.

In 2010, the World Meteorological Organization (WMO) signed the Mutual Recognition Arrangement (MRA) of the International Committee for Weights and Measures (*Comité International des Poids et Mesures* - CIPM) during a workshop with the Bureau of Weights and Measures (*Bureau International des Poids et Mesures* - BIPM) (WMO-BIPM, 2010). The signing of the MRA by WMO lead to closer liaising and cooperation with the metrology community, encouraging the National Metrology Institute to face new perspectives, needs, projects and activities related to traceability, quality assurance, calibration procedures and definitions for those quantities involved in climate studies and meteorological observations.

In relation to agriculture, metrology can be usefully applied in the measurement of meteorological quantities for sustaining *Decisions Support Systems*. A case in point is the epidemiological forecasting model for vineyard diseases detection, such as grapevine downy mildew, one of the most important infections affecting viticulture (Lafon and Clerjeau, 1988). This disease strictly depends on temperature, humidity, rain and solar radiation. Indeed, the fungus *Plasmopara viticola*, causing the infection, releases the zoospores in a minimum temperature of 10 °C and up to a maximum of 32 °C, with an optimum of 23 °C - 24 °C, (Blaeser and Weltzien, 1978). Further, needs at least four hours of darkness, during which the temperature must be at least 13 °C and the relative humidity at 92 %rh, in order to sporulate (Vercesi, 1994).

With the purpose of relating meteorological quantities to the biological cycle of this pathogen, several forecasting models have been developed

that provide information on the progress and evolution of infection. The forecasting models proposed –both empirical types (Stryzik, 1983; Hill, 1990; Magarey *et al.*, 1991; Rosa *et al.*, 1993; Blaise *et al.*, 1999) and dynamic types – (Rossi *et al.*, 2008), use as input values meteorological data collected from sensors not calibrated, or calibrated without traceability and without inclusion of measurement uncertainties. In general, these models do not consider the quality of input data (Sanna *et al.,* 2014). Indeed, considering the quality of input data and the calibration of sensors used in meteorological application are important aspects for ensuring the reliability of the measurements performed over time (Begeš *et al.* 2015).

The aims of this study are to investigate weather instruments' calibration and positioning, to achieve a metrological approach applied to agrometeorological studies and to implement the traceability of weather measurements. Specifically, this work investigated metrological processes' effect on meteorological measurements as a result of automatic weather stations' (AWS) positioning in a vineyard located on a hilly agricultural site for downy mildew detection, in order to improve vineyard disease predictions and reduce the use of chemicals in agriculture.

4.2. Material and methods

4.2.1. *Field site*

The vineyard locality is Vezzolano (Monferrato, north-western Italy) at an altitude between 416 m and 437 m, at an average slope of 28 % (maximum 35 %). It is surrounded by lawn to the east, from the copse to the west and south, and by other vineyards in the north. The vineyard selected is representative of vine-growing area, cultivar, position, slope, solar exposure and proximity of trees.

The two vine variety assayed were Arneis and Sauvignon and two clones for each vine, susceptibility to infection of downy mildew; these were distributed in three rows for vine clone with alternating every two rows in order to have a homogeneous system.

Meteorological data and surveys on the evolution of the *P. viticola* were carried out from 1 October 2013 to 30 June 2014. Data from the Regione Piemonte - Servizio fitosanitario database, gathering from an AWS placed in sun-exposed place, installed at about 500 m distance from the vineyard under study (called V-SP), were also used in order to calculate the climate trend and for the model's simulation.

4.2.2. *Instrumentation*

Two AWSs, (provided by MTX S.r.l, Italy), were installed in the vineyard, both composed by sensors for measuring air temperature, relative humidity, photosynthetically active radiation (PAR) and a tipping bucket rain gauge for precipitation. The first AWS, called VA, was placed in sun-exposed place, in conformity to WMO recommendations and class 4 of the Siting classification of surface observing stations (WMO – ET-AWS, 2008). The second, called VB, was installed in proximity of trees (approx. 8 and 17 m), where the tree canopy influenced weather measurements.

The air temperature and relative humidity sensors were calibrated using the "EDIE – Earth Dynamics Investigation Experiment" facility (Lopardo *et al.*, 2015), developed under the European ENV07 MeteoMet project (Merlone *et al.*, 2015).

The chamber (Fig. 1 a-c) is equipped with the reference sensor Platinum Resistance Thermometers 100Ω (Pt100), where the measurand (W) consists by the ratio between the electrical resistance of the thermometer measured at the fixed points temperatures (t_{90}) of the International

Temperature Scale (ITS-90) (Preston-Tomas, 1990), with respect to the electrical resistance measured at triple point of water (TPW) (Equation 1):

$$W = R(t_{90})/R(TPW) \qquad \text{(Eq. 1)}$$

The fixed points involved in the calibration are: mercury, water, gallium and indium.

Fig. 1 Transportable calibration chamber EDIE. a) project drawing, b) external and c) internal configuration

The nominal ranges of the chamber are: absolute pressure from 50 kPa to 110 kPa, and temperature from -25 °C to 50 °C. The expanded uncertainty (k = 2) of pressure and temperature reading inside the chamber are 10 Pa and 0.076 °C, respectively. This apparatus was also designed to allow the humidity control to complete the characterization of the whole AWS pressure-temperature-humidity modulus. The independent control of the

three quantities allows AWS calibration in a large atmospheric variability range and the study of the mutual influence effects on sensors response.

4.2.2.1. Air temperature

The calibration of the air temperature sensors was performed by positioning the sensor into the calibration chamber equipped with the Pt100 used as reference sensor.

The calculated calibration curve t_{calc} was obtained through a polynomial fit on the differences between the readings of the sensors in calibration (t_{AWS}) and the reference sensor (t_c).

Concerning both the temperature sensors, the contribution of the calibration uncertainty included also: the resolution of t_{AWS} (0.028 °C), the vertical uniformity (0.021 °C); the axial uniformity (0.028 °C) and the stability (0.01 °C) of the chamber, the calibration of t_C (0.011 °C), and the nanovoltmeter readings (0.004 °C) (Lopardo *et al.* 2015).

The statistical expanded uncertainty ($\boldsymbol{U_t}$) for the final temperature calibration was different for the two sensors and was given by Equation 2.

$$\boldsymbol{U_t} = \sqrt{\frac{\sum(\boldsymbol{t_{calc}} - \boldsymbol{t_C})^2}{\boldsymbol{d}}} \qquad \text{(Eq. 2)}$$

Where: (t_{calc}-t_C) is the residue, and d the degrees of freedom.

4.2.2.2. Air relative humidity

A similar procedure (T/07/06 REV00, INRiM internal procedure) was applied to the air relative humidity sensors. The sensors were placed in the calibration chamber and the calibration was done using the direct method by comparing the relative humidity reference sensor (RH_c), where the physical quantity is produced by a generator of air humidity secondary calibration reference standard, with the reading of the sensors in calibration (RH_{AWS}). For each points of calibration was calculated: the

mean of the standard hygrometer's measures, the mean of the standard thermometer's measures, the RH mean and the standard deviation readings of the instrument being calibrated. In order to evaluate the calibration uncertainty budget, stability (0.06 %) and uniformity (0.02 %) of the climatic chamber, resolution (0.05 %) and sensibility (0.05 %) of the instrument being calibrated, and repeatability (0.08 %) are needed. The expanded uncertainty U is expressed as the standard uncertainty multiplied by the coverage factor $k = 2$, corresponding to a confidence level of ~ 95.45 % (GUM, 1995). In evaluating the standard uncertainty is considered the long-term stability of the instrument being calibrated.

4.2.3. *Forecasting model*

The selection of the forecasting model used in this research falls into EPI - Plasmopara (*État Potentiel d'Infection*) model, proposed by Stryzik (1983), modified by Vercesi (1997).

The model follows the entire life cycle of the pathogen; the index of risk infection is the sum of a component called "potential energy" (P_e), which requires climate data during the October-March period and a second component, "kinetic energy" (K_e), which uses weather data during the March-August period, and provides estimates for the risk of a severe epidemic by accumulating favourable conditions for primary and secondary infections.

The EPI model was validated with respect to the climate and weather conditions of the site under study. The $P_e(t_i)$ *and* $K_e(t_i)$ contributions, as described in Sanna *et al.* (2014), were calculated according to deviations from the means of the climate values of air temperature and rainfall, and the equations refer to the contribution per unit of potential energy in a generic time interval.

4.2.3.1. The EPI value

The EPI(t_i) value is therefore given by Equation 3.

$$EPI(t_i) = P_e(t_i) + K_e(t_i) \quad \text{(Eq. 3)}$$

The risk situation was marked when the value of EPI was greater than -10 (threshold) and when a progressive increase in the value occurred for the following three days. Following the alert, a preventive fungicide intervention was recommended. In order to detect the EPI value, the most likely period of infection was calculated using a linear regression both temperature and relative humidity dependent, as per Giosuè *et al.* (2002) and modified as in Caffi *et al.* (2011), working backward from the date of the emergence of the first onset of downy mildew symptoms.

4.2.4. *Experimental design*

Simulations were carried out using the EPI forecasting model with data from the two automatic weather stations VA and VB. Four different conditions were simulated: (i) VA without inclusion of calibration uncertainties in the input values for temperature and relative humidity (VA-NC); (ii) VA with inclusion of the calibration uncertainty (VA-C); (iii) VB without inclusion of calibration uncertainties (VB-NC); (iv) VB with inclusion of the calibration uncertainty (VB-C).

4.2.5. *Data analysis*

Mean data of temperature, solar radiation and relative humidity from the same AWS (calibrated/not calibrated) and between the two AWS (VA/VB) were analysed using the statistic Kruskal-Wallis non parametric test in order to compare the mean daily meteorological value for temperature and relative humidity, using the statistical software package SPSS (IBM, release 22.0.0). Meteorological data, focused on the potential

risk period, were collected hourly. The ANOVA was not used because the variance homogeneity was not verified.

4.3. Results and discussion

4.3.1. *Statistic evaluation*

From a statistic point of view, given the considerable amount of information and slightly hourly differences among the registered data in comparison to the daily variation, the mean daily temperature and relative humidity were always statistically different (Kruskal-Wallis non parametric test) both inside each AWS (calibrated and not calibrated) and between the two AWS (VA/VB).

Data representation was more useful for appreciating the environmental influences on the positioned sensors (temperature, humidity and solar radiation), as the VA sensor was placed in a sunny area, whereas the VB was installed in the proximity of tree canopies.

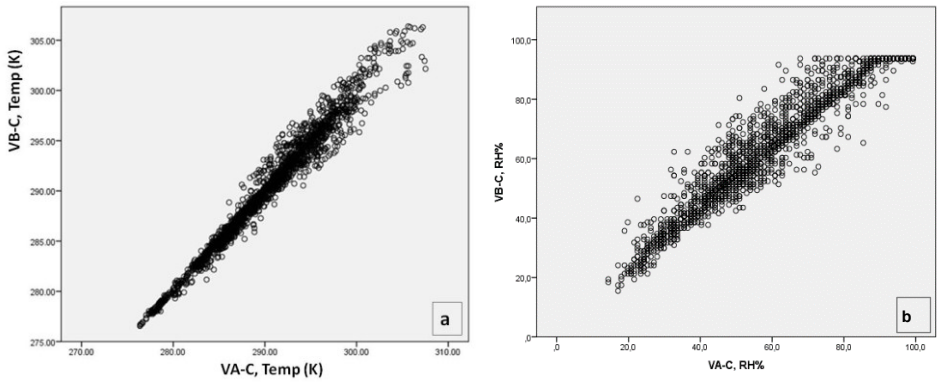

Fig. 2 a) Temperature (in K) and (b) relative humidity (in %) comparison between VA-C and VB-C

A slight difference was evident in the information recorded by the two AWS positioned in the different areas (both calibrated and not calibrated couples) with regard to both temperature and the humidity (Fig. 2a and Fig. 2b), relationship among the calibrated AWS). The difference was also confirmed by the high coefficient of variance in their ratios, measured

hourly. The relative humidity registered in VB-C was greater than in VA-C, thus confirming the influence of sensor positioning.

4.3.2. *Air temperature sensors calibration*

The reference temperature was the result of 20 repeated measures taken from the nanovoltmeter, (Agilent A34420A), one every 30 s for each of the six points from -20 °C to 45 °C. The calculated calibration curve t_{calc} was obtained through a polynomial fit on the differences between the readings of the sensors in calibration (t_{AWS}) and the reference sensor (t_c) (Fig. 3a and Fig. 3b). The statistical expanded calibration uncertainty ($\boldsymbol{U_t}$) was different for the two sensors.

The Equation (4) reports the temperature calibration curve.

$$t_{calc} = a\, t_{AWS}{}^2 + t_{AWS}(1 + b) + c \qquad \text{(Eq. 4)}$$

Where: a, b and c are the coefficients of the polynomial fitted.

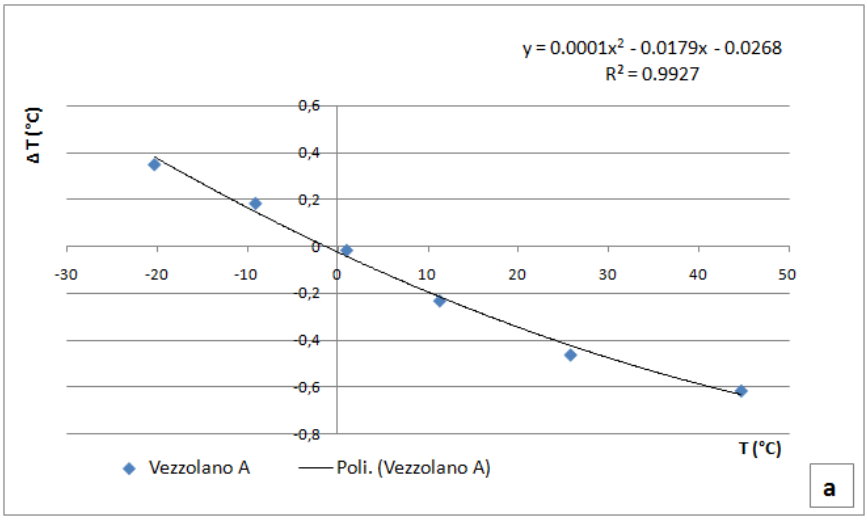

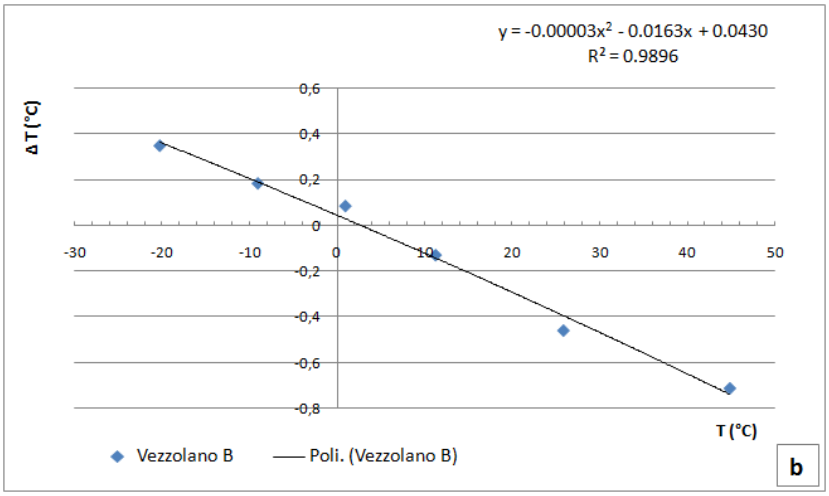

Fig. 3 Calibration curve obtained by the polynomial fitted equation for temperature sensors in (a) VA and (b) VB

The sensor installed in VA had an expanded calibration uncertainty of 0.11 °C, similar to the uncertainty of the sensor installed in VB, which had a value of 0.13 °C, both inclusive of residues with coverage factor $k = 2$. These values are to be considered components of the measurement uncertainty. Considering the mean daily temperature during the interval of time considered in this study, the measurement uncertainty had a minimum of 0.13 °C and a maximum of 0.53 °C for VA, and a minimum of 0.14 °C and a maximum of 0.57 °C for VB.

4.3.3. *Relative air humidity sensors calibration*

The reference relative humidity was the result of four repeated measures from 30 %rh to 90 %rh and a return point at 60 %rh to evaluate hysteresis. The standard measurement uncertainty associated with hysteresis was within 1.0 %. The relative humidity calibration uncertainty ($\boldsymbol{U}_{\mathbf{RH}}$) was obtained by taking into consideration the resolution, measurement repeatability, hysteresis and the uncertainty in the determination of the conditions applied to the sensor under calibration RH_{AWS}. The

corresponding relative humidity calibration curves were obtained (Fig. 4a and 4b).

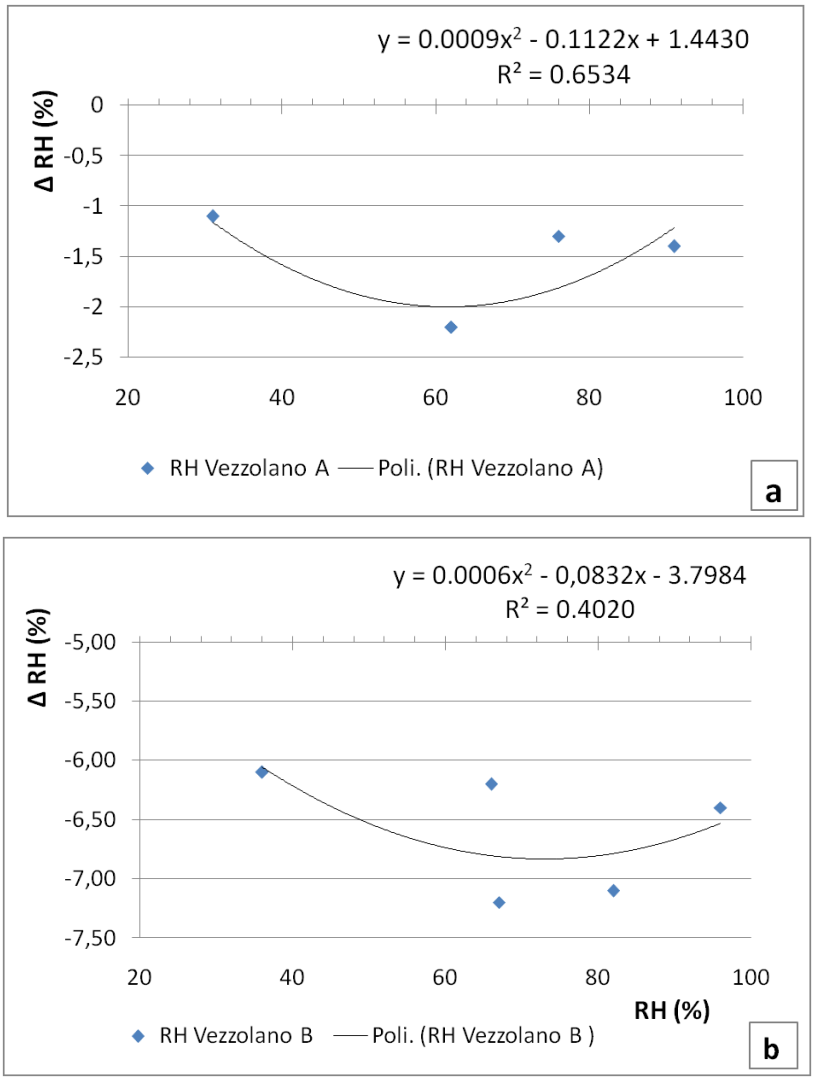

Fig. 4 Calibration curve obtained by the polynomial fitted equation for the relative humidity sensors in (a) VA and (b) VB

The calibration of the relative humidity sensors returns dissimilar results: the uncertainty of the sensor in VA had a minimum value of 0.9 %, a maximum of 2.1 % and a calibration curve with R^2 of 0.6534 (Fig. 4a), while for the sensor in VB, the minimum value was 1.0 %, the maximum

2.1 % and a calibration curve with R^2 of 0.4020 (Fig. 4b). In this last case, the standard calibration uncertainty associated with hysteresis was within 1.0 %, evaluated at the point of return. As a result, the difference range of relative humidity calibration uncertainty reached up to 6.7 % for VB.

The analysis carried out in this work showed that sensors of the same type, purchased from the same supplier and with the same resolution and accuracy, guaranteed by certificates released by the manufacturers produced dissimilar values if they were not properly calibrated.

4.3.4. *Forecasting model*

In this study, the date of emergence of the first symptoms was observed between 10 and 11 May and the most probable period of infection was calculated to be around 28 and 29 April, as previously explained in paragraph 2.3.1. During these days, the AWS registered seven rain events (a total of 38.9 mm of rainfall) as necessary for triggering the infection.

The five simulations of pathogen infection delivered different results. The forecast for VA-C and VB-C overlapped at the estimate period of infection, on 29 April and between 28 and 29 April, respectively. The prediction of VA-NC anticipated the estimate period of infection four days in advance, on 25 April, while V-SP simulation postponing the estimate period to 4 May, due the position of the AWS. The simulation on VB-NC amplifying the prediction up to roughly five days, on 24 April, overestimating the risk of primary infection (Fig. 5).

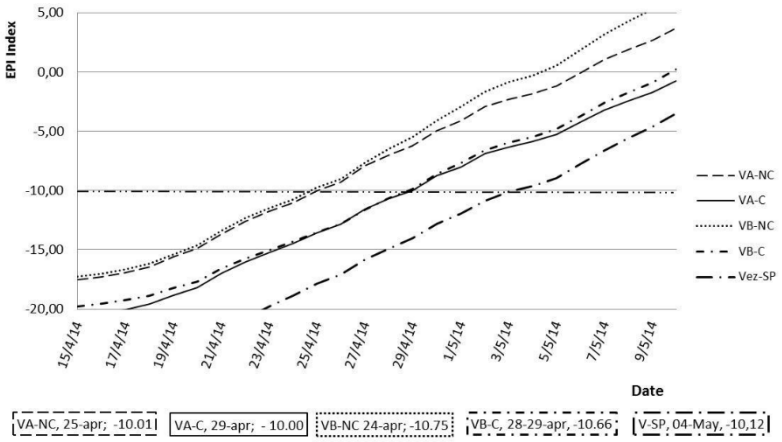

Fig. 5. EPI index focused on period in which is highly recommended to make a treatment. The boxes explained the day in which EPI value reached the critical value -10 (threshold — · · — · · –)

The EPI model proposed by Stryzik (1983) was widely modified during the last decades, due to its difficulty to reach an exhaustive definition of the rules concerning the system plant-pathogen-environment. Nevertheless, EPI is still one of the most used and validated forecasting model.

The model modified by Vercesi (1997) is accurate in predicting the level of risk during the primary infection but less accurate in predicting the level of secondary infection cycle. In studies related the efficiency, Fronteddu and Cossu (2002), argue that in general terms EPI showed the typical gaps of an empirical model and the inaccuracies of the simulations are due, at least in part, to a limited database of climate parameters. Fremiot *et al*. (2008) state that EPI model returns promising results, but remark the importance to used more reliable data to obtain better and robust simulations. The need for more reliable data was also observed in studies in hillside vineyards. The simulation provided by EPI has shown a tendency to overestimate the risk, especially for secondary infection,

compared to studies conducted on ground level and allowed to develop more rational intervention strategies (Vercesi *et al.*, 2012).

In this study, it could be noticed that using as input values of the model the data from calibrated sensors this overestimation was reduced (Fig. 6). As a result of infectious rains of 13 to 17 June, in which the mean daily relative humidity has reached and exceeded 90 % (data not shown), it has created the ideal conditions for secondary infection which has led to the emergence of slight symptoms observed around 19-20 June. In the same days the EPI index produces a value of about 46 and 37 in VB-NC and VA-NC, respectively, compared to the lower values obtained with the data from calibrated sensors of 28 and 33 in VA-C and VB-C, respectively.

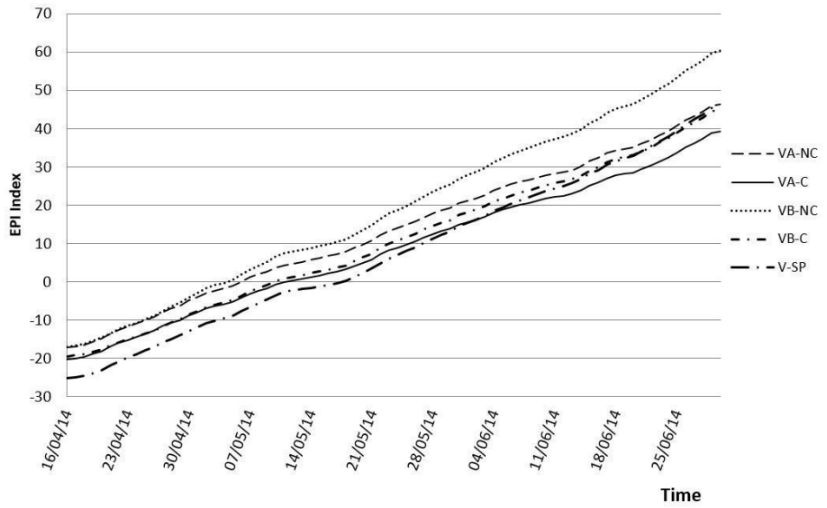

Fig. 6 EPI index focused on the first period of K_e phase, in which gives estimates of risk for the primary and secondary infections

4.3.5. *Effects of the calibration and position on output data*

In order to improve the understanding of the influences of the temperature and the relative humidity on pathogen growth, comparisons among the

four scenarios were carried out, focused around the period in which the EPI model marks a potential infection onset and evolution.

Comparing the four scenarios (VA-NC, VA-C, VB-NC and VB-C), as expected, the differences (Δ_t) between the data with inclusion of uncertainties are lower than the data without inclusion. As well as the data recorded in VB are lower than the data collected from the AWS in VA. This difference is more marked for the recorded relative humidity values with respect to the temperature values. In the specific, as showed in Figure 7, VA-NC always records higher temperatures, while VB-NC always lower, with a Δ_t up to 1.07 °C. Generally, Δ_t values over 0.50 °C are recorded in particular when the temperature is over 16 °C (mean daily temperature).

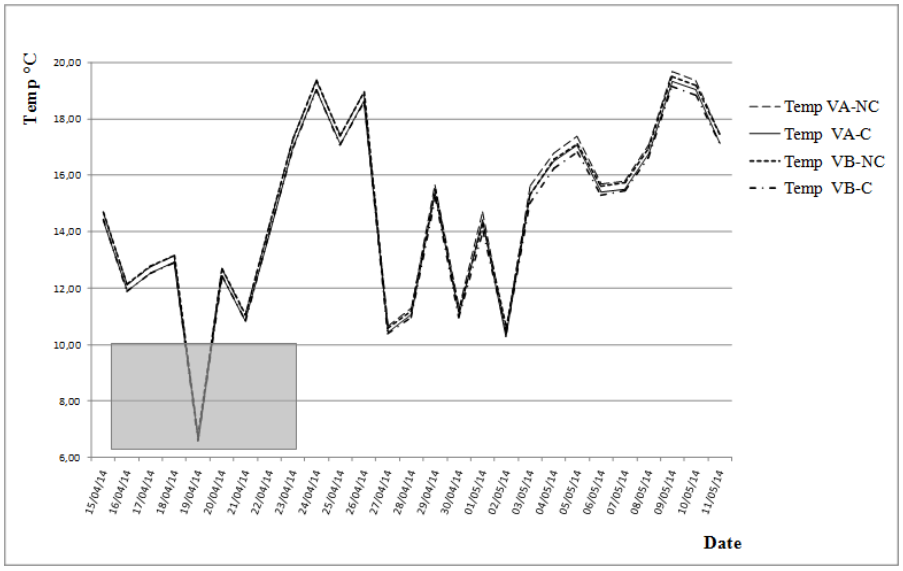

Fig. 7 Comparison among the four scenarios of air temperature measurements, focus on the period in which the EPI model marked a potential infection onset (mean daily data). Grey box shows the range of values of temperature where treatments of plants are not efficient.

Comparing VA-NC and VB-C, the lower values of the latter, are recorded in 97 days of the considered period, with a Δ_t ranging up to 1.12 °C. In the

third comparison carried out, the days in which the recorded data of VB-C are lower than VA-C is reduced at 53 with a maximum Δ_t of 0.74 °C. In the comparison between VA-NC and VB-NC the number of days in which VB-NC is lower is 45 with a maximum Δ_t of 0.74 °C, but in 27 days the two mean values are equal, while comparing VB-NC with VA-C, in contrast to the others results, the values of the latter are lower in 89 days with a Δ_t that reach up to 1.07 °C.

The result comparisons of the four scenarios for the relative humidity measurement are shown in Figure 8. In this case, unlike the temperature comparisons, the differences (Δ_{RH}) between the data with inclusion of uncertainties are lower than the data without inclusion and the value of the data recorded in VB are higher than the value recorded in VA.

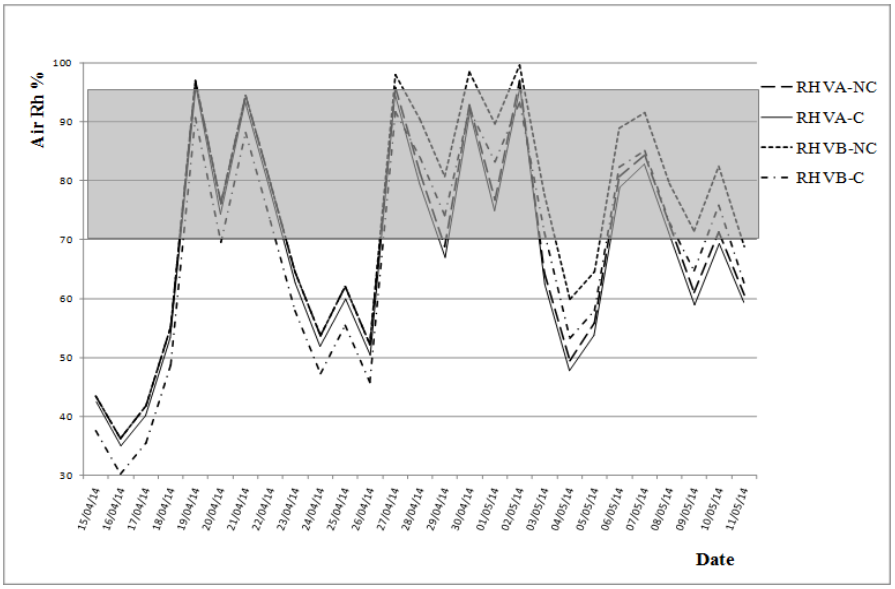

Fig. 8 Comparison among the four scenarios of air relative humidity measurements, focus on the period in which the EPI model marks a potential infection onset (mean daily data). Grey box shows the range of values of relative humidity where treatments of plants are efficient.

In particular, VB-NC always records higher values of humidity, with a Δ_{RH} from 3.0 % up to 14.0 % as respect VA-NC and from 4.0 % to 16.0 % as respect VA-C. Generally, Δ_{RH} over 10.0 % is recorded when the relative humidity is under 70 % (mean daily).

Comparing VA-C and VB-C, the higher values of the latter, are recorded in 93 days of the considered period, with a Δ_{RH} ranging up to 9.5 %, indeed, in the remaining 9 days the Δ_{RH} ranged from 0.1 % to 2.3 %. In the fourth comparison carried out, the days in which the recorded data of VB-C are lower than VA-NC is reduced at 88 with a maximum Δ_{RH} of 7.5 %; in 14 days VA-NC values are higher, with Δ_{RH} from 0.5 % to 3.4 % but this values are usually recorded when the relative humidity is over 90 %.

As far as the siting is concerned, VB-C, VB-NC and V-SP simulations including intrinsically the position contribution, since for VB-C and VB-NC the tree canopy's spatial arrangement tended to alter the vineyard's microclimate, while for V-SP, the distance from the vineyards is the predominant factor that tamper with the estimate period of infection. VB-C simulation estimated the period of infection one day in advance, although VB-NC and V-SP forecasts amplifying the prediction up to five days. Considering that calibration contribution affects the prediction up to four days we could suppose that the position contribution is about of one day. In terms of temperature and relative humidity, the contribution is up to 0.33 °C and 6.5 %rh, respectively.

It is worth considering the scenario that will arise if the choice of fungicide spray programme falls within the simulation carried out where no data were calibrated. The risk of a failed treatment will be high in the case of no zoospores having been released or during washout rainy days, with the implication of soil poisoning (hypertrophication), costs of labour man and

products as a consequence. These encouraging results lead to the conclusion that further studies are needed using traceable data, both on vineyards with the same characteristics, as well as those that differ from one another. Such a *Decision Support System* must also take into consideration support of the environment.

4.4. Conclusions

In this study, the forecasts provided by the epidemiologic model with data inclusive of uncertainty overlapped around the estimate period of infection, confirming that the inclusion of calibration uncertainties produces data closer to the real value of the measurand. Moreover, the inclusion of the instrument positioning contribution affected disease prediction up to five days. This can be explained by the effect of the distance and the vine canopy's spatial arrangement, which tended to alter the vineyard's microclimate. Therefore, calibration procedures and instrument positioning are important factors in agrometeorology, although further in-depth studies are needed in this field focus in particular to define a *reference grade sensor,* within regional baseline observing networks, for agricultural sector. Measurements should be based on fully documented traceability and forecasting models should include measurement uncertainties in their input values to improve output data accuracy.

4.5. Acknowledgement

The authors would like to thanks the researcher and technician staff of INRiM and IMAMOTER-CNR for their collaboration and support to this research. This study is funded by the EMRP participating countries within European Association of National Metrology Institutes (EURAMET) and the European Union, in the framework of ENV07 MeteoMet project.

4.6. References

Begeš G, Drnovšek J, Bojkovski J. Knez J, Groselj D, Černač B, Hudoklin D. 2015. Automatic weather stations and the quality function deployment method. *Meteorol. Appl*. **22**: 861–866

Blaeser M and Weltzien HC (1978). The importance of sporulation, dispersal, and germination of sporangia in the epidemiology of Plasmopara viticola.) *Zeitschrift fur Pflanzenkrankheiten und Pflanzenschutz*. **85**: 155–161.

Blaise P, Dietrich R, Gessler C, 1999. Vinemild: an application oriented model of *Plasmopara viticola* epidemics on *Vitis vinifera*. *Acta Hortic*. **499**: 187–192.

Caffi T, Rossi V, Carisse O, 2011. Evaluation of a dynamic model for primary infections caused by *Plasmopara viticola* on grapevine in Quebec. Online. Plant Health Progress

Fremiot P, Parisi N, Pinzetta M, Tonni M, Salvetti M, Strizyk S, Vercesi A. 2008 *Plasmopara viticola* epidemics and evaluation of EPI model in the Lombardy vineyards. *Giornate Fitopatologiche 2008*, Cervia (RA), 12-14 marzo 2008, Volume **2**: 237-244

Fronteddu F, Cossu A, 2002. Studies on EPI plasmopara model efficiency on eastern Sardinian grapevines. *Atti II Giornate di Studio* "Metodi numerici, statistici ed informatici nella difesa delle colture agrarie e delle foreste". Pisa 22-23 maggio.

Giosué S, Girometta, B, Rossi V, Bugiani R, 2002. Analisi geostatistica delle infezioni primarie di *Plasmopara viticola* in Emilia Romagna. *Atti II Giornate di studio* Pisa. *Notiziario sulla Protezione delle Piante*, **1**: 229 -237.

GUM, 1995. Evaluation of measurement data - Guide to the expression of uncertainty in measurement. *JCGM 100:2008*, 134 pp.

Hill, GK. 1990. Plasmopara Risk Oppenheim – a deterministic computer model for the viticultural extension service. *Notiziario sulle Malattie delle Piante* **111**: 231–323.

Lafon R, Clerjeau M, 1988. Downy mildew. In: Pearson, R.C., Goheen, A.C. *Compendium of Grape Diseases*. APS Press, St. Paul, Minnesota, USA: 11–13.

Lopardo G, Bellagarda S, Bertiglia F, Merlone A, Roggero G, Jandric N, 2015. A calibration facility for automatic weather stations. *Meteo. Appl*. **22**: 842-846

Magarey PA, Wachtel MF, Weir PC, Seem RC, 1991. A computer-based simulator for rationale management of grapevine downy mildew *Plasmopara viticola*. *Aust. Plant Protect*. Quart. **6:** 29–33.

Matese A, Crisci A, Di Gennaro SF, Primicerio J, Tomasi D, Marcuzzo P, Guidoni S. 2014. Spatial variability of meteorological conditions at different scales in viticulture. *Agricultural and Forest Meteorology*,**189:** 159-167.

Merlone A, Lopardo G, Sanna F, *et al.* (2015). The MeteoMet project–metrology for meteorology: challenges and results. *Meteorol. Appl*. **22**: 820-829.

Preston-Tomas H, 1990. The International Temperature Scale of 1990 (ITS-90), *Metrologia*. **27**: 3-10

Rana G, Rinaldi M, Introna M, 2004. Methods and algorithms for evaluating the data quality at hourly and daily time scales for an agrometeorological network: application to the regional net of Basilicata (Italy). *Rivista Italiana di Agrometeorologia*, **1**: 14-23.

Rosa M, Genesio R, Gozzini B, Maracchi G, Orlandini S, 1993. Plasmo: a computer program for grapevine downy mildew development forecast. *Comput. Electron. Agricult*. **9:** 205–215

Rossi V, Caffi T, Giosuè S, Bugiani R, 2008. A mechanist model simulating primary infections of downy mildew in grapevine. *Ecol. Modelling*, **212**: 480-491

Sanna F, Cossu QA, Bellagarda S, Roggero G, Merlone A, 2014. Evaluation of EPI forecasting model for grapevine infection with inclusion of uncertainty in input value and traceable calibration. *Ital. Jour of Agrometeo.* **19**:, 33-44

Sanna F, Roggero G, Deboli R, Merlone A, 2013. Metrology for Meteorology in Agricultural Sites. *Italian Journal of Agrometeorology.* **11:** 31-32

Stryzik S, 1983. Modèle d'état potentiel d'infection: application a *Plasmopara viticola*. Association de Coordination Technique *Agricole, Maison Nationale des Eleveurs*: 1–46

Vercesi A. 1994. Strumenti innovativi per la gestione della difesa contro la peronospora della vite. *Informatore patologico* **5**/1995

Vercesi A. 1997. Possible use of epidemic models in grapevine downy mildew management. Petria 7: 183-192

Vercesi A, Toffolatti SL, Sordi D, Pedrazzini A, Parisi N, Venturini G. 2012. Verso una gestione razionale della difesa antiperonosporica in vigneto *Quaderni della ricerca*, **145**: 4-20

WMO-BIPM 2010. Workshop on "Measurements Challenges for Global Observation Systems for Climate Change Monitoring" 30 Mar. Geneva

WMO – ET-AWS-5, 2008. Expert Team on requirements for data from Automatic Weather Stations-fifth session, *Final Report, Annex8*, Mar 2008 Geneva, 44-52

5. Variability of tomato cultivar in protected cultivation in response to meteorological parameters

Francesca Sanna[1,3], Roberto Deboli [2], Angela Calvo[1]

[1]*Dipartimento di Scienze Agrarie, Forestali e Alimentari (DiSAFA) Università degli Studi di Torino, Turin, Italy*

[2]*Istituto Macchine Agricole e Movimento Terra - Consiglio Nazionale Ricerche (IMAMOTER-CNR), Turin, Italy*

[3]*Istituto Nazionale di Ricerca Metrologica (INRiM), Turin, Italy*

Corresponding author*: francesca.sanna@unito.it*

Published in Plant, Soil and Environment 2018 ().

Abstract

Solar radiation is an important parameter for plants since it provides the energy for photosynthesis and it modulates growth and development in response to environmental conditions. The amount and the spectral distribution of solar radiation, when operating in protected environment, undergo to modifications that depend on the type of cover used. Currently, measurements of meteorological parameters in protected cultivation lack of measurement uncertainties that could affect the characteristics of the product.

An experimental site for the measurement of meteorological parameters in protected environment and the evaluation of the variability of a table tomato cultivar is presented in this paper. The site was equipped with cultivation structures (tunnel type) and calibrated sensors traceable to the International System of Units. The microclimate conditions were monitored by sensors for: solar radiation, operating in the spectral range

from 290 nm to 2800 nm; air temperature in the range between -10 °C and 40 °C; relative air humidity from 10 %rh to 98 %rh; inside and outside the tunnel with different covering materials. The instruments followed calibration procedures defined *ad hoc*. The following aspects were evaluated: (i) microclimate and solar radiation within the different cultivation environments, using calibrated instrumentation and traceable measurements; (ii) phenological and morphological observations of the crops in response to the type of plastic film adopted and the different microclimate environments; (iii) monitoring of the optical and radiometric properties of the films used as covering material.

High temperatures recorded (over 40 °C) changed the transmissive feature of the films and consequently affected the growth, anthesis, leaf area index and fruit setting of tomatoes. Statistical analysis was carried out as regard the morphological parameters compared to UV-B measurements, relative humidity and temperature values calibrated and non-calibrated. Results were statistically significant ($p < 0.001$).

Keywords:

Metrology, protected cultivation, calibration, uncertainty, tomato, meteorological parameters

5.1. Introduction

Light is a factor of paramount importance for plants since, in addition to providing the radiant energy for photosynthesis, it modulates growth and development in response to the environmental conditions. Plants have the ability to monitor intensity, spectral distribution, direction and daily duration of the direct and incident light (Li and Yang, 2015).

When operating in protected cultivation (greenhouse or tunnel) the amount and the spectral distribution of solar radiation inside the cultivation undergo modifications that depend on the type of the cover used. The productivity of a protected crop is highly correlated to the amount of electromagnetic radiation received, which in turn depends on the amount of UV, PAR and IR radiation transmitted through the cover material of these structures (Krizek, 2004).

Studies aimed at quantifying the effects of UV radiation on crop quality have led to unclear results. Indeed, data take into account some aspects of the problem separately, such as physiological, production or quality (Bacci *et al.* 1999; Ribeiro *et al.,* 2012; Castagna *et al.,* 2013). Particularly the increase in UV-B radiation (280-315 nm) is a potential risk to the physiology and the plants growth, as it can damage DNA, proteins, cell membranes, and affect the physiologic function (Fedina and Velitchkova, 2009). However, subsequent research showed that comparatively low doses of radiation in plants induce a metabolic response to stress plant resistance, which leads to an increase of molecules with high antioxidant capacity (Schreiner and Huyskens-Keil, 2006).

Physiological parameters, such as seed dormancy, gases produced during the germination and in the period immediately after the harvest (abscisic acid, ethylene, ethane, carbon dioxide) are affected by meteorological parameters i.e. temperature, solar radiation and precipitation that in turn, affect the variability of crop productivity (Fišerová *et al.,* 2015).

On the other hand, instruments that measure solar radiation need constant maintenance and calibration, to obtain UV measurements of required quality (Hülsen and Gröbner, 2007). The calibration value was underestimated or neglected for a long time. It has been shown that the

introduction of the measurement uncertainty for *ground based* spectroradiometric measurements increases significantly the reliability of measured data (Schaepman, 1998).

Moreover, the calibration of the weather stations' sensors installed in agriculture sites are usually not performed, or in some cases are carried out for comparison before installation. This procedure was metrologically evaluated and showed relevant weak points. Reference sensors are not always made to operate in open air; therefore, it is not possible to cover the whole range for the quantities for the specific site, thus the mutual influences evaluation among parameters is not achievable (Sanna *et al.,* 2017).

This paper presents a new experimental site for the measurement of meteorological parameters in protected cultivation and the assessment of product variability of a tomato cultivar in an experimental site located in Northern Italy.

5.2. Objectives

On the basis of the experience acquired in metrology for agro-meteorology (Sanna *et al.,* 2014; 2017; Merlone *et al.,* 2017), an experimental site equipped with cultivation structures (tunnel type) and calibrated sensors for the measurements of meteorological parameters was assembled. The research activities concerned the quality of table tomatoes (*Solanum lycopersicum* L*,* var. *Saint Pierre*) grown in protected environment. The following aspects were evaluated:

- Microclimate conditions (air temperature in the range from -10 °C to 40 °C, relative humidity from 10 %rh to 98 %rh with a target uncertainty of 0.3 °C and 5 %rh, respectively in accordance to Guidance on Instrumentation for Calibration Laboratories

(Groselj/WMO, 2010) and Guide to Meteorological Instruments and Methods of Observation (WMO-CIMO, 2010); solar radiation measurement in the spectral distribution from 290 nm to 2800 nm) using calibrated instrumentations and traceable data, within the different cultivate environments;

- Phenological and morphological observations of the crops in response to the type of plastic film adopted in the different microclimate environments.
- Change of the ageing and radiometric properties of the films used as covering material due to their exposure to the solar radiation and their deterioration.

5.3. Materials and methods

5.3.1. *Experimental site set up*

An experimental measurement site was selected at the Research Area of CNR, Turin. The following structure and instruments were installed (Figure 1):

- 2 adjacent high-tunnels (called INside-Clear and INside-Block, – IN-C and IN-B) of equal size with different covering material having opposite filtering properties with respect to UV-B solar radiation. The first was transmissive type (Clear, 8.50x7x200 μm), the second being diffusive and filtering the UV-B radiation (Diff, 9.20x7x200 μm);
- 2 Automatic Weather Stations (AWS), one per tunnel, including sensors for the detection of: air temperature and relative air humidity (FAR019AA, MTX Srl, Italy), solar radiation for UV-B (DH-Si 45503, MTX Srl, Italy) and solar photosynthetically active radiation (PAR, PCTRA070, MTX Srl, Italy);

- 1 AWS outside the tunnels (called OUT - outside), including sensors for the detection of: air temperature and relative air humidity, solar radiation for UV-B, global radiation (pyranometer, PCTRA060, MTX Srl, Italy).

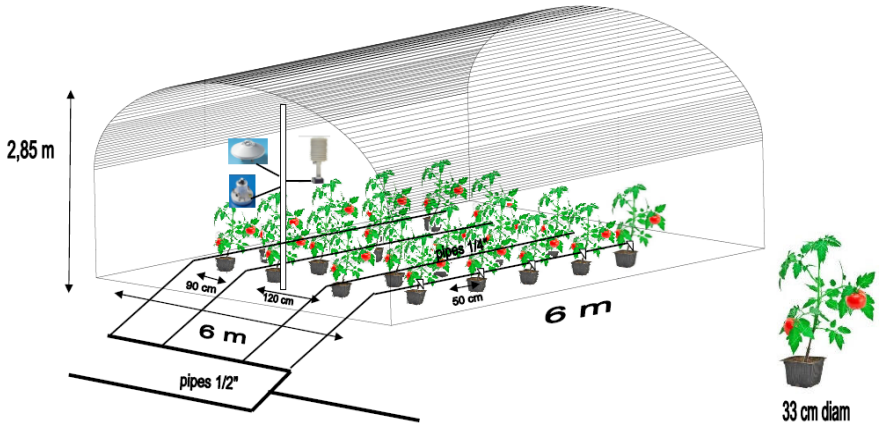

Figure 1 Scheme of hight tunnel, instrumentes set up, irrigation sistem and planting layout

1.1. Cultivar

On 20 May 2016, 46 seedlings of Saint Pierre tomato cultivar, previously sowed in a microclimate-controlled greenhouse at IPSP-CNR (*Istituto per la Protezione Sostenibile delle Piante – Consiglio Nazionale delle Ricerche*) and pricked out in planting trays' pots, were selected, transplanted in individual pots and moved into the site (20 per tunnel and 6 outside). Fungicidal treatments were performed once a month for the control of downy mildew. A drip irrigation system was installed to control the amount of water and fertilizer supplied (Biswas *et al.*, 2015).

During the growing period of the plants, phenological and morphological aspects were recorded: plant growth, leaf area index (LAI), anthesis and

fruit set. The plant growth was calculated by measuring the stem from the collar to the apical meristem. For the estimation of LAI, the software PocketLAI was used. This is an implementation of a simplified model of light transmittance based on the assumption of a random spatial distribution of infinitely small leaves (Confalonieri *et al.*, 2013). The result of each measurement of LAI was in turn the result of the mean of three measurements performed on the same plant, one every 10 seconds. Anthesis is defined here as the appearance of a flower for each flowering, counted up to five, for a total of 100 flowers for each tunnel, and 30 flowers outside. Fruit set on each flowering means the onset of the first fruits for each flowering for a maximum of three fruits, for a total of 300 fruits for each tunnel and 90 fruits outside.

5.3.2. *Meteorological instrumentations*

The meteorological instrumentations were calibrated by means of procedures defined *ad hoc*. The air temperature and relative humidity sensors were calibrated using the "EDIE – Earth Dynamics Investigation Experiment" facility (Lopardo *et al.,* 2015), developed under the European ENV07 MeteoMet project (Merlone *et al*., 2015), equipped with a Pt100 Platinum Resistance Thermometers (PRT, model 5615-6 - Fluke) used as reference sensor. In PRT calibration, the measurand consists by the ratio between the electrical resistance of the thermometer measured at the fixed points temperatures of the International Temperature Scale (ITS-90) (Preston-Tomas, 1990), with respect to the electrical resistance measured at triple point of water.

In order to cover the whole range for atmospheric measurements, the selected set points were: −20 °C, −10 °C, 0 °C, 10 °C, 25 °C, and 45 °C for T sensors; 30 %rh, 60 %rh, 75 %rh and 90 %rh for RH sensors, plus a

second point at 60 %rh for the evaluation of the hysteresis, in accordance with INRiM internal procedure T/07/06 REV00.

The temperature data were recorded by a thermometry bridge (Super thermometer 1594A – Fluke) having a resolution of 8-1/2 digits corresponding to 0.000015 °C. The sampling recording time was every 10 s. The repeatability is assumed to be the standard deviation of the readings along 5 min.

The resulting plots show the calibration curves for T and RH sensors (Figures 2 and 3, respectively) installed in IN-C, IN-B and OUT.

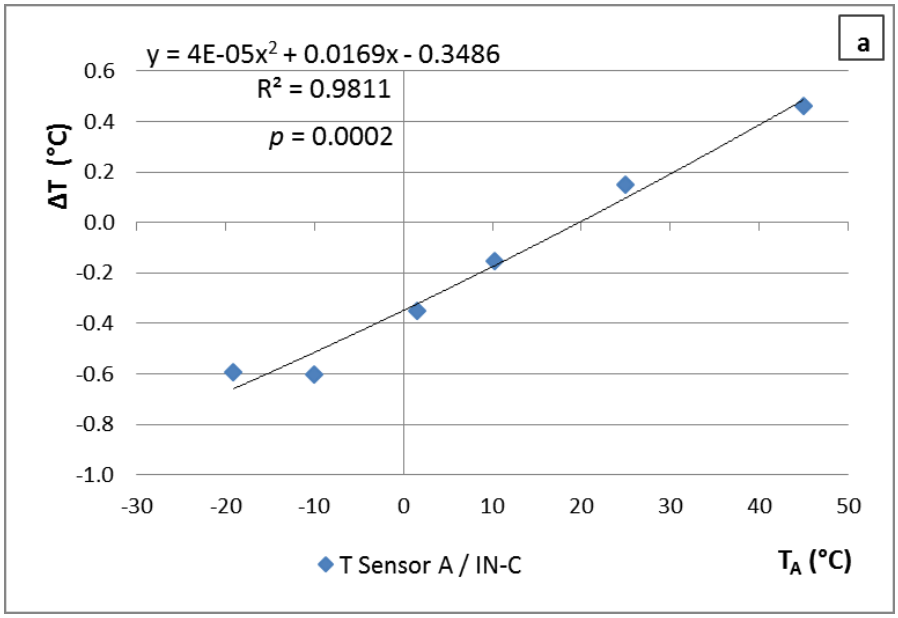

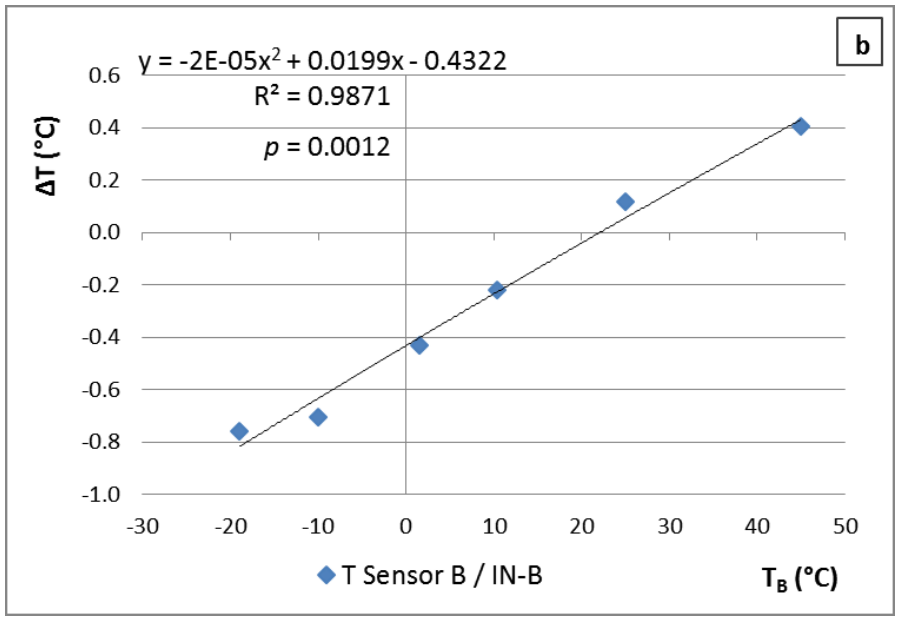

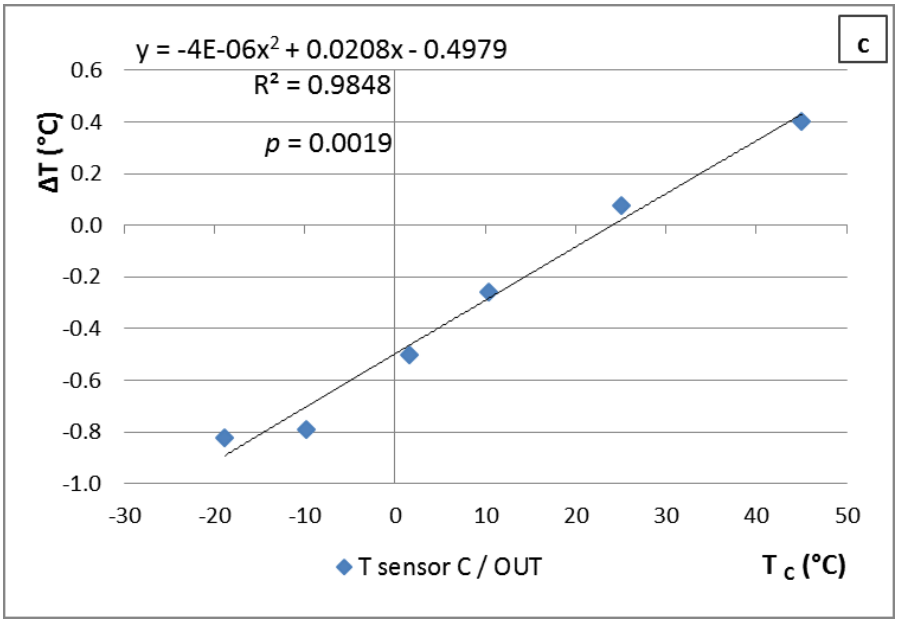

Figure 2. Temperature (a, b, c) calibration curves obtained by the polynomial fitted equations between the sensors under calibration (A, B and C), installed in IN-C, in IN-B and in OUT, and the reference sensor, for the selected six points

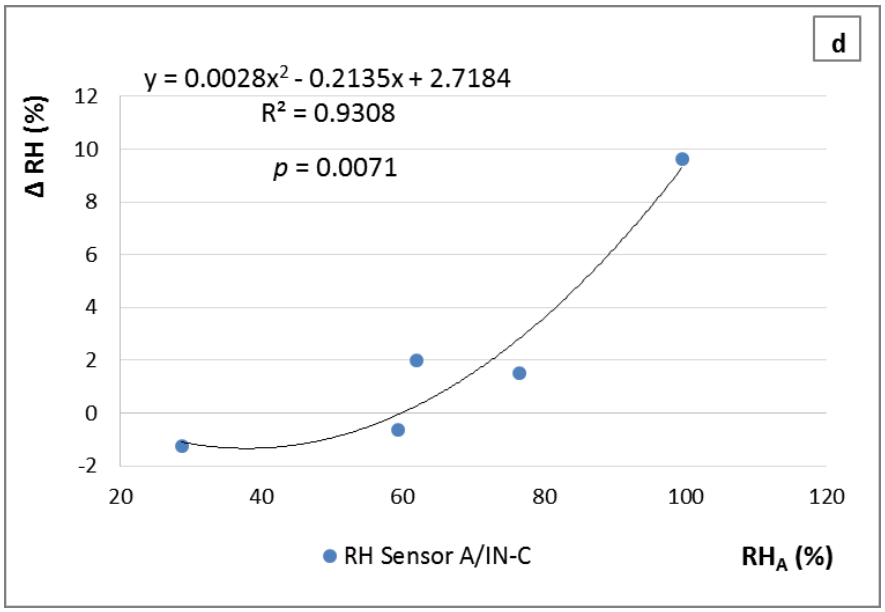
d
y = 0.0028x² - 0.2135x + 2.7184
R² = 0.9308
p = 0.0071
Δ RH (%)
12
10
8
6
4
2
0
-2
20
40
60
80
100
120
RH Sensor A/IN-C
RH_A (%)

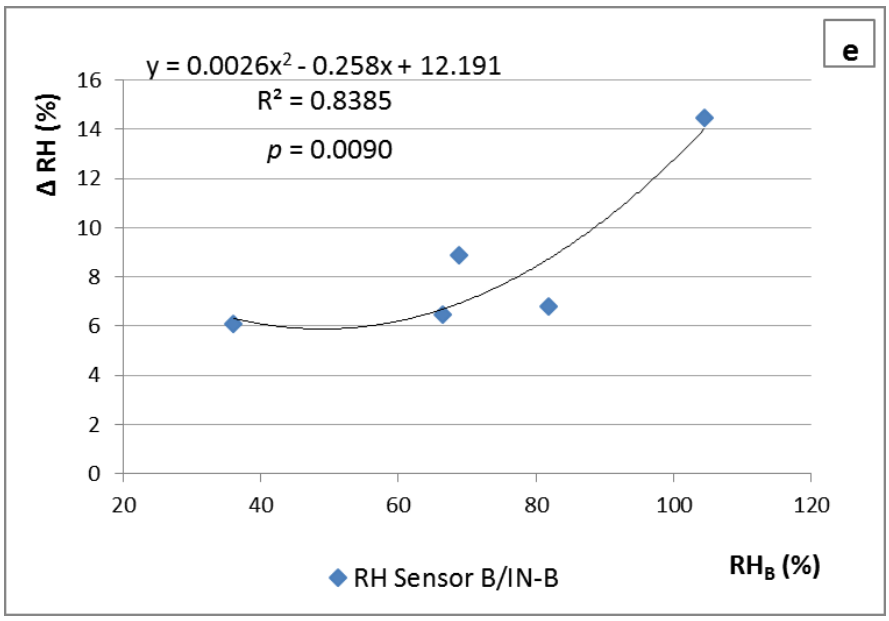
e
y = 0.0026x² - 0.258x + 12.191
R² = 0.8385
p = 0.0090
Δ RH (%)
16
14
12
10
8
6
4
2
0
20
40
60
80
100
120
RH Sensor B/IN-B
RH_B (%)

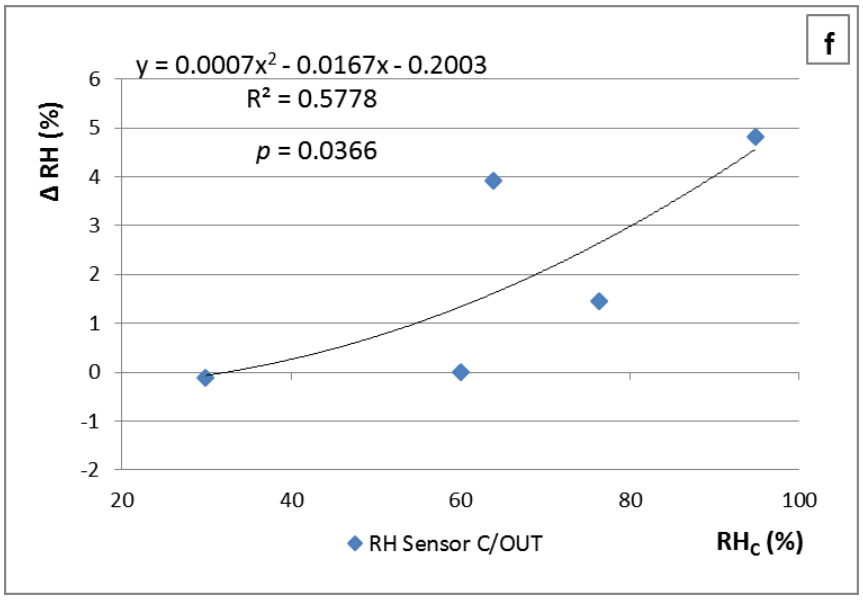

Figure 3. Relative humidity (d, e, f) calibration curves obtained by the polynomial fitted equations between the sensors under calibration (A, B and C), installed in IN-C, in IN-B and in OUT, and the reference sensor, for the selected five points and second point at 60 %rh for the evaluation of the hysteresis

The meteorological parameters were acquired with an interval of 15 minutes, and hourly and daily averages were calculated.

5.3.3. *Covering materials*

The optical properties of the polymers are correlated to the structure of the polymer itself and its degree of crystallinity. The index of refraction *n* of a material is an optical feature, dimensionless number, which describes how light propagates through that medium. It is defined as the equation 1:

$$n = \frac{c}{\upsilon} \qquad \text{(Eq. 1)}$$

where *c* is the speed of light in vacuum and *v* is the phase velocity of light in the medium.

The refractive index determines how much light is bent, or refracted, when entering a material, as described by Snell's law (equation 2):

$$n = \frac{\sin \theta i}{\sin \theta r} = \frac{v_1}{v_2} = \frac{n_2}{n_1} \qquad \text{(Eq. 2)}$$

where: θi is the angle of incidence and θr *is the* angle of refraction.

The index of refraction depends on the density of the material, the temperature and the wavelength of the incident light. If incidence angle is different from zero, increasing angle of incidence increases refraction *r*.

Temperature and humidity are components that can cause a variation on the film's transmissivity (Michel *et al.*, 1986; Priyadarshi *et al.*, 2006). According to Priyadarshi and colleagues, the change of thermo-optic coefficient suggests that the change of refractive index may have a relationship with density. Moreover, according to Lorenz–Lorentz law (Born and Wolf, 1999), refractive index is related to density by the following equation 3:

$$\frac{n^2-1}{n^2+2} = \frac{\rho RD}{M} \qquad \text{(Eq. 3)}$$

where ρ is the density of material *RD* is the molar refraction and *M* is the molecular weight. Molar refraction and molecular weight remain nearly constant with changes of temperature. As the temperature changes, the refractive index of polymeric films changes. Indeed, the refractive index is of the type (equation 4):

$$\frac{\delta n}{\delta \mathrm{T}} = \left(\frac{\delta \mathrm{n}}{\delta \rho}\right)_T \left(\frac{\delta \rho}{\delta \mathrm{T}}\right) + \left(\frac{\delta \mathrm{n}}{\delta \mathrm{T}}\right)_\rho = -\left(\frac{\rho \delta \mathrm{n}}{\delta \rho}\right)_T \alpha + \left(\frac{\delta \mathrm{n}}{\delta \mathrm{T}}\right)_\rho \qquad \text{(Eq. 4)}$$

where δn/δT: temperature-caused index change, α: volume coefficient of a polymer thermal expansion, $(\delta n/\delta T)\rho$: index change under constant

density, $(\rho\delta n/\delta\rho)T$: constant for a given polymer based on the Lorenz–Lorentz law (Zhang *et al.*, 2006).

5.3.4. *Statistical analysis*

The R packages 'Rcmdr' and 'stats' (RStudio Team, 2015), were used to performed statistical analysis by means of: Pearson's correlation coefficient (r); Spearman's rank correlation (ρ) (alternative two sided); General Linear Model (GLM) including Standard Error (SE), Residual of SE (RSE), coefficient of determination (R^2). The GLM was used in order to compare the growth, the anthesis, the fruit setting and the LAI values respect to RH and T values calibrated and non-calibrated, and UV-B. A second statistical analysis was performed comparing the morphological values in combination with UV-B values respect to RH and T values calibrated and non-calibrated. Daily mean of T, RH and UVB measurements in IN-C, for Pearson and Spearman methods were used.

5.4. Results and discussion

5.4.1. *Morphological observations*

In the three weeks after transplanting, the tomato plants cultivated in IN-B featured a higher mean growth with respect to the plants cultivated in IN-C (mean difference of about 1 cm). They then had a turnaround on 17 June, with a gap up to 6 cm on 6 July (Figure 4). A basal leaves damage was observed in the last week of June attributed to a mite infection (*Aculops lycopersici* - tomato russet mite). A greater damage was noticed (largest number of affected leaves) in plants grown under diffusive coverage and blocking UV-B (IN-B).

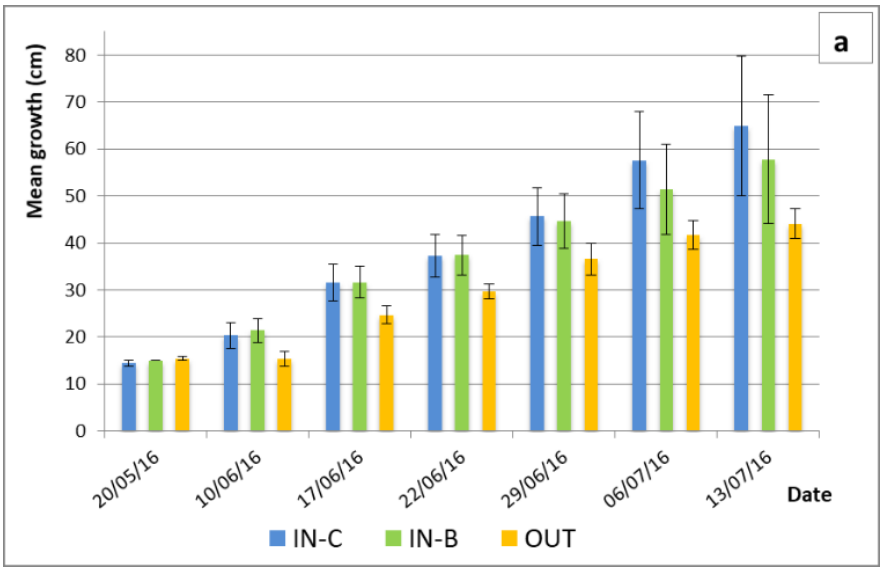

Figure 4. IN-C: Mean growth of tomato plants cultivated under transmissive UV-B coverage; **IN-B:** Mean growth of plants cultivated under diffusive coverage, filtering UV-B; **OUT:** Mean growth of plants cultivated outdoors, without coverage

Plants grown in OUT showed a lower growth and underwent a lower infectious damage than IN-C and IN-B. The lower growth might be due to excessive irrigation resulting in radical waterlogging, with slower growth rate as a consequence.

The blooming of the first flower was observed on 17 June in OUT, on 22 June in IN-C and on 24 June in IN-B. In IN-C, anthesis gradually increased for the first three weeks of onset, then slowed down around 85% between 1 and 7 July and reached 100% after 6 days. In percentage terms, anthesis in IN-B proceeded slowly compared to IN-C and OUT but with constant percentage increase until 6 July, whit a settling around 90%, then reached 100% in 4 days (figure 5).

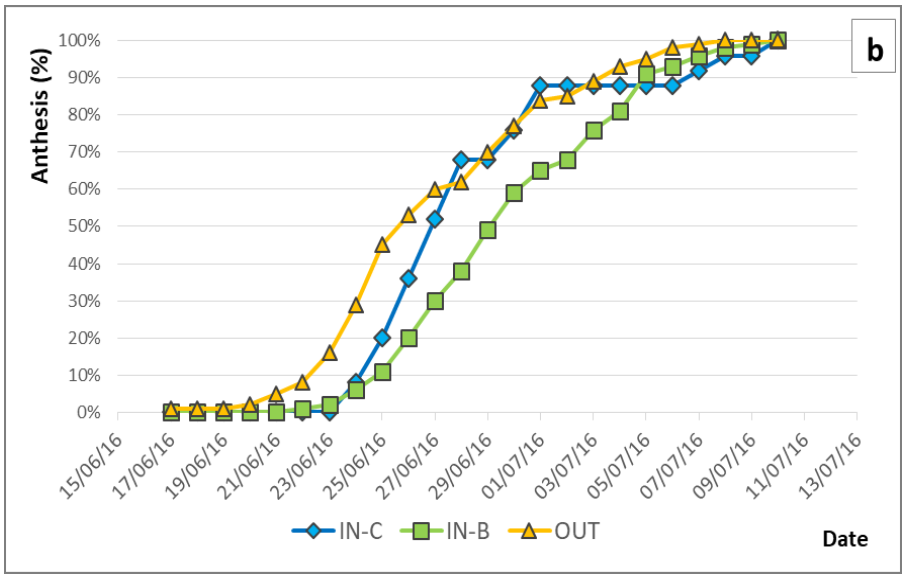

Figure 5. Anthesis of tomato plants cultivated under transmissive UV-B coverage (IN-C); under diffusive coverage filtering UV-B (IN-B); and plants cultivated outdoors, without coverage (OUT)

The fruit setting was observed primary in OUT on 26 June, followed by IN-B on 28 June and IN-C on 2 July. In the first ten days, in percentage terms, in OUT the occurrence of new fruits took place in a gradual and progressive trend, then slowed down around 16 July. The trend of IN-B followed the one in IN-C. However, the trend of IN-C was more uniform but lower than IN-B and out. Around 20 July, a reversal trend was observed between IN-C and IN-B (Figure 6).

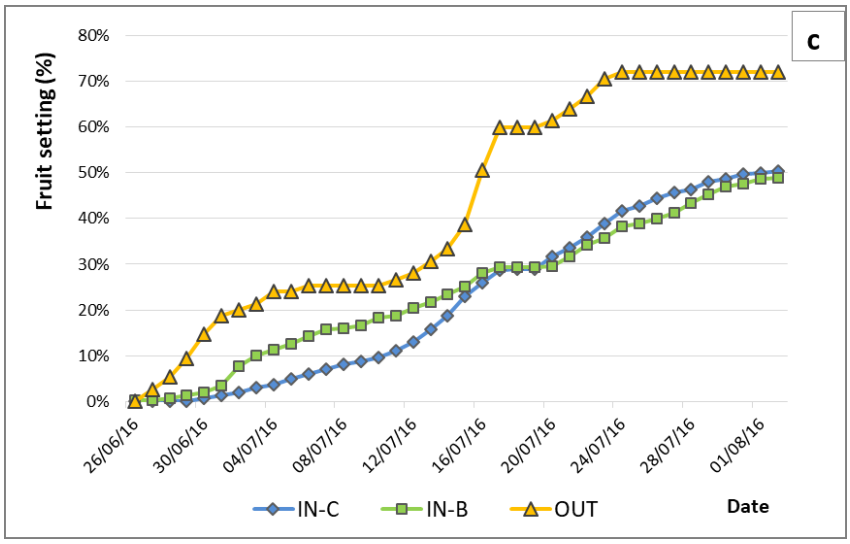

Figure 6. Fruit setting of tomato plants cultivated under transmissive UV-B coverage (IN-C); under diffusive coverage filtering UV-B (IN-B); and plants cultivated outdoors, without coverage (OUT)

Considerations are similar regarding the LAI, as shown in Figure 7. Indeed, in the first three weeks of cultivation a higher mean LAI for plants grown in IN-B compared to those in IN-C was observed, with a maximum difference of 0.37 m^2m^{-2} on 10 June. A turnaround on 20 June was followed. Likewise, for the plant growth, the reversal of tendency might be due to higher pathogen infection. The mean LAI of plants cultivated in OUT seemed to follow the trend of the plants in IN-B.

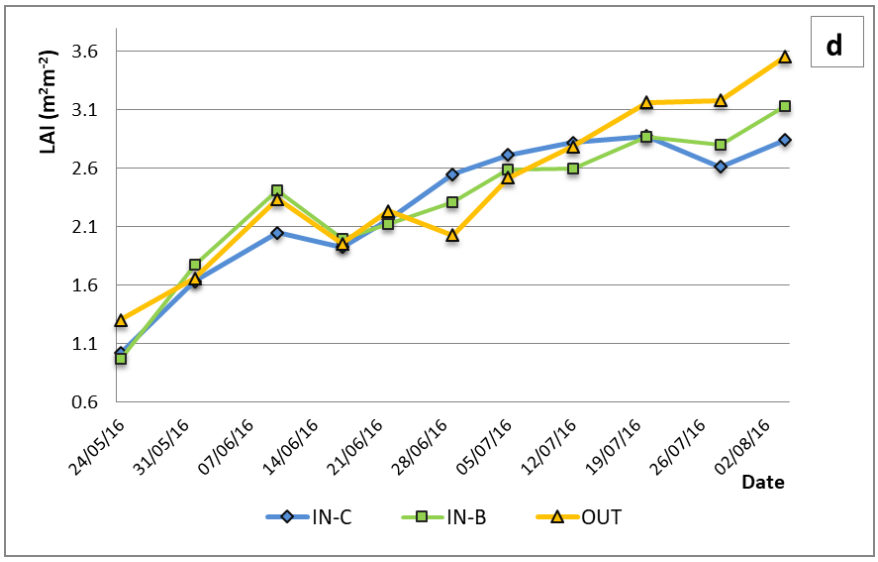

Figure 7. IN-C: Mean LAI of tomato plants cultivated under transmissive UV-B coverage; **IN-B:** Mean of LAI of plants cultivated under diffusive coverage, filtering UV-B; **OUT:** Mean of LAI of plants cultivated outside, without coverage

5.4.2. *Sensors calibration*

As far as the T and RH sensors' calibration are concern, the expanded calibration uncertainty is expressed as standard uncertainty multiplied by the coverage factor $k = 2$ which for a normal distribution corresponds to a confidence level of 95.45 % (BIPM, 2012).

In the calculation of the expanded uncertainty were taken into account the contributions of the sources of uncertainty for temperature measurements: thermometry bridge resolution, thermostat bath stability and homogeneity, EDIE stability and homogeneity, resolution and sensibility of sensors in calibration, uncertainty of reference sensor, sum of residues in quadrature. The values of their calibration uncertainty were 0.264 °C; 0.259 °C and 0.267 °C for T and 2.648 %; 3.242 % and 3.232 % for RH in sensors A/IN-C, B/IN-B, C/OUT respectively (Tables 1 and 2), meeting the target of calibration uncertainty proposed.

Table 1. Summary of the sources of uncertainty for all the temperature measurements. The standard uncertainty is the root squared of the quadratic sum of all uncertainty contributions and expanded uncertainties is the standard uncertainty multiplied for the coverage factor k =2.

Source	**Value (°C)**	**Probability distribution**	**Contribution to uncertainty (°C)**
Thermometry bridge	0.000015	Rectangular	1.299E-05
Thermostat bath homogeneity	0.045	Rectangular	0.025981
Thermostat bath stability	0.022	Normal	0.011000
EDIE stability	0.005	Rectangular	0.002887
EDIE homogeneity	0.198	Rectangular	0.114315
Uncertainty of T reference sensor	0.00366	Normal	0.001829
Resolution of sensor in calibration	0.01	Rectangular	0.008660
Sensibility of sensor in calibration	0.02	Rectangular	0.011547
Standard uncertainty contributions			*0.19*
	Sensor A/IN-C (°C)	**Sensor B/IN-B (°C)**	**Sensor C/OUT (°C)**
Uncertainty of T sensor in calibration	0.001593	0.001684	0.001990
Sum of residuals in quadrature	0.058283	0.052228	0.060709
Standard uncertainty U_T	*0.132*	*0.130*	*0.133*
Expanded uncertainty $\boldsymbol{U_T}$ (k = *2*)	**0.264**	**0.259**	**0.267**

Table 2. Summary of the sources of uncertainty for all the relative humidity measurements.

Source	**Value (%)**	**Probability distribution**	**Contribution to uncertainty (%)**
Climatic chamber homogeneity	0.21	Rectangular	0.121244
Climatic chamber stability	0.25	Rectangular	0.144338
Climatic chamber uncertainty	.30	Normal	0.150000
Uncertainty of RH reference sensor	0.637	Normal	0.318464
Sensor in calibration resolution	0.1	Rectangular	0.086602
Sensor in calibration sensibility	0.5	Rectangular	0.288675
Standard uncertainty contributions			*1.573*
	Sensor A/IN-C (%)	**Sensor B/IN-B (%)**	**Sensor C/OUT (%)**
Uncertainty of RH sensor in calibration	0.441086	0.638941	0.441086
Sum of residues in quadrature	1.143929	1.403216	1.471869
Standard uncertainty U_{RH}	*1.324*	*1.621*	*1.616*
Expanded uncertainty $\mathbf{U_{RH}}$ (k = 2)	**2.648**	**3.242**	**3.232**

The calibration uncertainties of the relative humidity sensors were obtained taking in account the contributions of the uncertainty in the determination of the conditions applied: the resolution; the measurement

repeatability and the hysteresis (evaluated on the return point) of the sensors in calibration. The standard measurement uncertainty associated to hysteresis was within 1.0 % RH.

For UV-B solar radiation and pyranometer sensors, the calibration aims to obtain the sensor transduction curve (calibration curve) and to determine the value of the solar-coefficient (K) at the variation of the height of sun (h):

$$\mathrm{K}(h) = \frac{V}{G} \qquad \text{(Eq.5)}$$

where K(h) is the solar-coefficient defined as the proportionality coefficient between the voltage V generated by the photocell or by the thermopile, and the incident radiation G.

One of the largest cause for measurement uncertainty of these instruments is that when the sun position changes with respect to the instrument, the solar coefficient K(h) remains constant only for angles greater than about 35 °, while varying (decreasing or increasing, depending on the type of sensor), for lower angles (Arca *et al.*, 2003).

Pyranometers can be calibrated by comparison in field with a reference pyranometer or using a pyrheliometer for direct radiation measurement (I) and measuring global and diffused (D) radiation with the pyranometer to be calibrated. Among these three parameters there is the relationship:

$$G = D + I \cdot \sin h \qquad \text{(Eq. 6)}$$

The sensors under study were calibrated with a reference pyranometer Ph. Schenk 8101, ISO 9060 First Class. In table 3 are listed the calibration results for the UV-B and pyranometer sensors.

Table 3. Calibration values for solar radiation measurements. UV-B solar radiation sensors installed in IN-C; IN-B, and OUT and pyranometer installed in OUT. K factor is a constant calculated after the calibration test.

	UV-B Sensors			**Pyranometer**
	IN-C	**IN-B**	**OUT**	**OUT**
Reference value [mW/m^2]	24.8	25.1	23.9	1022 W/m^2
Measured value [mV]	28	28	28	2598 mV (1039 W/m^2)
Calibration factor [$V/(W/m^2)$]	1.13	1.11	1.17	1.017
K factor [W/m^2 per mV]	0.886	0.896	0.853	0.984

5.4.3. *Meteorological parameters*

Data from all the thermo-hygrometers sensors, calibrated and non-calibrated, were compared. Figures 8a and 8c show the daily mean of T and RH. Differences among the recorded measurements can be appreciated, as well as the dispersion of the T and RH values from the hourly mean in the day mean (Figure 8b and 8d for non-calibrated data).

In general, the T values obtained from the data to which the calibration curves were applied and associated with the calibration uncertainty, were higher than the values obtained from data without application of the curve and the uncertainty, vice versa for RH values.

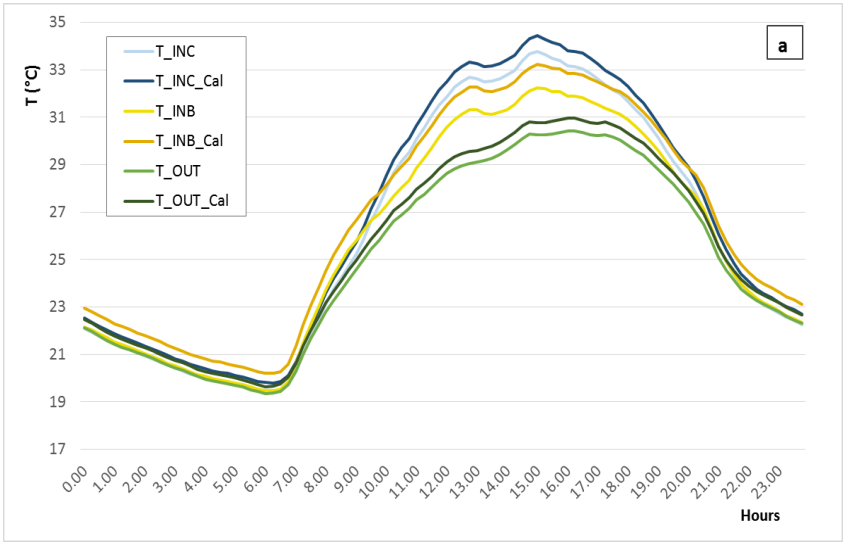
a
T_INC
T_INC_Cal
T_INB
T_INB_Cal
T_OUT
T_OUT_Cal
T (°C)
35
33
31
29
27
25
23
21
19
17
0.00
1.00
2.00
3.00
4.00
5.00
6.00
7.00
8.00
9.00
10.00
11.00
12.00
13.00
14.00
15.00
16.00
17.00
18.00
19.00
20.00
21.00
22.00
23.00
Hours

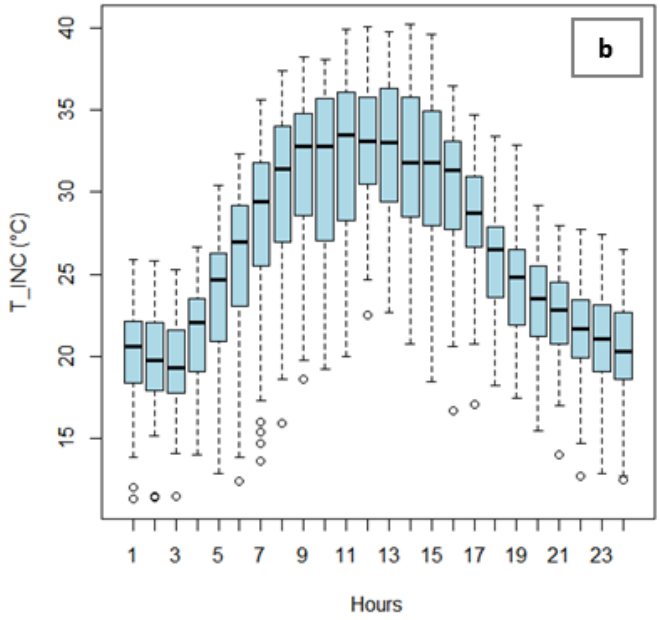
b
T_INC (°C)
40
35
30
25
20
15
1
3
5
7
9
11
13
15
17
19
21
23
Hours

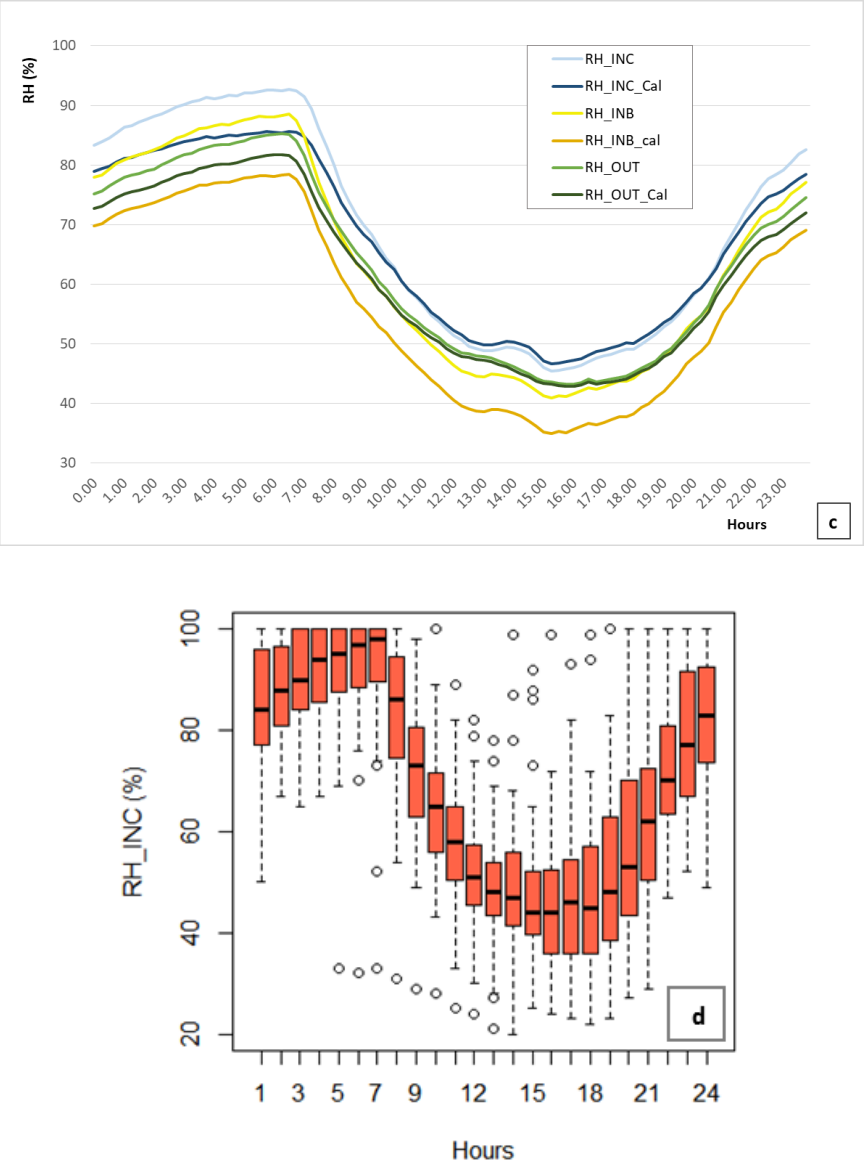

Figure 8 Comparison of daily mean for air T (a) and R sensors (c) in IN-B, IN-C and OUT, calibrated and non-calibrated during the tomatoes' growing season. Dispersion from the hourly mean of the T (b) and RH (d) values non-calibrated in IN-C in the day.

In Figure 9, the daily mean of the total amount of solar radiation (global, UV-B and PAR) is shown. The covering film in IN-B is a diffusive type, which explains the higher value of PAR inside this tunnel. The covering

film in IN-C is trasmissive to the UV-B radiation and explains the higher temperature inside this tunnel respect to IN-B and OUT.

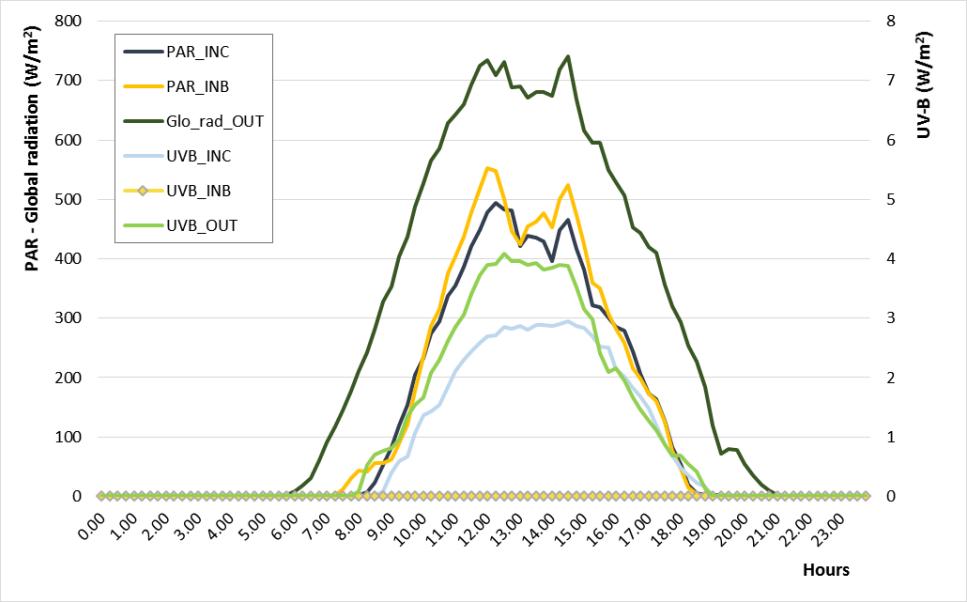

Figure 9 Amount of global radiation, UV-B in IN-C and PAR in IN-B and IN-C. Daily mean of the tomatoes' growing season.

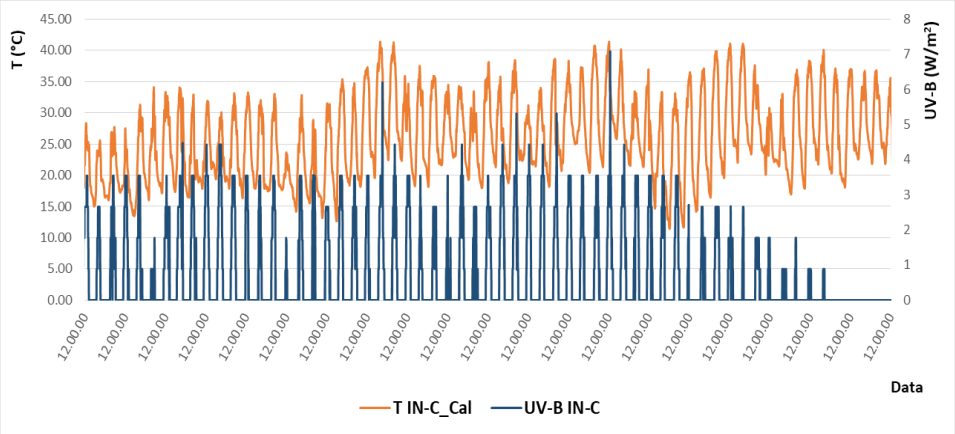

Figure 10. Temperature (calibrated values) and UV-B measurement comparison in IN-C; daily values.

The ageing and radiometric properties of the films used as covering material due to their exposure to the sun and their deterioration was

evaluated. The diffusive type covering material, filtering the UV-B solar radiation, was installed in IN-B. The transmissive type respect to UV-B solar radiation, was installed in IN-C. For all the period under study, the UV-B values recorded in IN-B were 0 W/m^2. In IN-C the values recorded at the beginning of June were in the range from 0 W/m^2 to 4.42 W/m^2, in the last ten-days of June from 0 W/m^2 to 6.2 W/m^2, to reach values of 7.08 W/m^2 the 10th of July, and with a trend reversal, to get 0 W/m^2 after few weeks (figure 10).

A temperature comparison was performed in order to evaluate potential damage of the covering material. As previous explain (section 5.3.3), the thermo-optic coefficient for polymers is temperature and humidity-dependent and, as the temperature changes, the refractive index of polymeric films changes (Priyadarshi *et al.*, 2006). Further studies are necessary to better evaluate whether the high temperature recorded, over 40 °C in the last ten-days of June and first ten-days of July (Figure 10), has changed the transmissive feature of the covering material installed in IN-C in accord to Michel (1986) and Priyadarshi (2006), whether the morphological characteristics of tomatoes have changed their growth, anthesis, LAI and fruit setting trends.

5.4.4. *Statistical analysis results*

Statistical analysis was carried out as regard the parameters recorded in IN-C. In particular, UV-B measurement compared to RH and T values calibrated and non-calibrated using Pearson's correlation coefficient (r) and Spearman's rank correlation (ρ) (Table 4). The correlation results were: -0.779 and -0.838 for RH and 0.815 and 0.845 for T, respectively, with a p-value < 0.001.

Table 4. Pearson's correlation coefficient (r) and Spearman's rank correlation (ρ) for UV-B measurement in IN-C compared to RH and T values calibrated and non-calibrated

UVB_INC ~	**Pearson correlation coefficient**			**Spearman's rank**
	t-value	***p*-value**	***r***	***ρ***
RH_INC	-11.784	< 2.2e-16	-0.772221	-0.838249
RH_INC_Cal	-12.071	< 2.2e-16	-0.779661	-0.838249
T_INC	13.626	< 2.2e-16	0.814794	0.843739
T_INC_Cal	13.628	< 2.2e-16	0.814830	0.843739

As far the morphological values in IN-C are concern, the GLM was used, comparing the growth, the anthesis, the fruit setting and the LAI values respect to RH and T values calibrated and not-calibrated, and UV-B. The analysis also included SE, RSE and R^2. As listed in table 5, all the results were statistically significant (p-values: $p < 0.001$ = ***; $p < 0.01$ = **; $p < 0.05$ = *) except for fruits set in combination with UV-B values.

A second statistical analysis was performed comparing the morphological values respect to RH, T and UV-B values. All GLM results were statistically significant (p-values in brackets, < 0.001). Specifically, R2 for growth were: 0.8393 (0.00374); 0.8390 (0.00375); 0.9872 (6.26e-06); 0.9872 (6.26e-06) and not assigned (NA) for the comparison with RH measured in IN-C not calibrated, RH in IN-C calibrated; T in IN-C not calibrated; T in IN-C calibrated and UV-B measured in IN-C, respectively. For anthesis R2 results were: 0.9898 (< 2.2e-16) for RH in IN-C not calibrated; 0.9895 (< 2.2e-16) for RH in IN-C calibrated; 0.9217 (1.184e-13) for T in IN-C not calibrated and calibrated, NA for UV-B in IN-C. For

fruit set, R2 results were: 0.1894 (0.0063); 0.1953 (0.0055); 0.1628 (0.0120); 0.1629 (0.0120) and 0.1451 (0.0183) for the comparison with RH in IN-C not calibrated, RH in IN-C calibrated; T in IN-C not calibrated; T in IN-C calibrated and UV-B in IN-C, respectively.

Table 5. -- General Linear Model including Standard Error (SE), Residual of SE (RSE) and coefficient of determination (R^2), for morphological parameters compared to RH and T values calibrated and non-calibrated, and UV-B in IN-C. *p*-values: '***' = 0.001 '**' = 0.01 '*' = 0.05; NA = Not Assigned.

GLM	SE	RSE	Multiple R^2	p-value
Growth + UVB_INC ~				
RH IN-C Cal	11.94	8.166	0.839	0.003753 **
RH IN-C	10.67	8.159	0.8393	0.003739 **
T IN-C Cal	2.867	2.298	0.9872	6.264e-06 ***
T IN-C	2.867	2.298	0.9872	6.262e-06 ***
Anthesis + UVB_INC ~				
RH IN-C Cal	NA	4.174	0.9895	< 2.2e-16 ***
RH IN-C	NA	4.113	0.9898	< 2.2e-16 ***
T IN-C Cal	NA	11.42	0.9217	1.186e-13 ***
T IN-C	NA	11.42	0.9217	1.184e-13 ***
Fruit set + UVB_INC ~				
RH IN-C Cal	93.551	51.06	0.2141	0.0400
RH IN-C	89.729	51.16	0.2110	0.0426
T IN-C Cal	223.96	51.65	0.1957	0.0573
T IN-C	228.17	51.65	0.1957	0.0573
LAI + UVB_INC ~				
RH IN-C Cal	0.2536	0.4742	0.4871	0.01694 *
RH IN-C	0.2259	0.4751	0.4852	0.01725 *
T IN-C Cal	0.2027	0.298	0.7974	0.00021 ***
T IN-C	0.2065	0.298	0.7974	0.00021 ***

As far as LAI is concern, R2 results were: 0.4852 (0.0172) for RH in IN-C not calibrated; 0.4871 (0.0169) for RH in IN-C calibrated; 0.7974 (0.0002) for T in IN-C not calibrated and calibrated and NA for UV-B in IN-C.

5.5. Conclusion

A new experimental site for the measurement of meteorological parameters in protected cultivation and for the assessment of a tomato cultivar variability has been presented in this paper. The site is equipped with cultivation structures and calibrated sensors monitoring the microclimate conditions, the optical and radiometric properties of the films used as covering material.

The absence of UV-B radiation (IN-B) affects growth and LAI but, at the same time, it might have influenced the susceptibility of plants to mite infections. The presence of UV-B radiation, on the other hand, affects T and RH. Even though, the temperature values gathered from calibrated sensors were higher than the ones gathered from non-calibrated sensors, vice versa for relative humidity values. Moreover, the high temperature recorded, over 40 °C, might have changed the transmissive feature of the covering material installed in IN-C and, as a consequence, the morphological characteristics of tomatoes in turn changed. Indeed, the growth, the anthesis, the LAI and the fruit setting of the crop cultivated in IN-C underwent to a reversal trends respect the crop cultivated in IN-B. Statistical analysis shown significant results ($p < 0.001$).

Further studies are necessary to evaluate the measurement uncertainties of meteorological parameters that can be translated in percentage uncertainties on the productivity of the agricultural product and to assess

the quality through chemical characterization of the crop with *health promoting compounds*.

5.6. Acknowledgments

The authors would like to thanks Donatella Duraccio from IMAMOTER-CNR for her contribution on the analysis of the covering materials and the IPSP-CNR researchers for the plants advice.

5.7. References

Arca A., Battista P., Ventura A. (2003): Analysis of spectral sensitivity of photocell solarimeters. Journal of Agricultural Engineering. 2003(3): 33-39

Bacci L., Grifoni D., Sabatini F. and Zipoli G. (1999): UV-B radiation causes early ripening and reduction in size of fruits in two lines of tomato (*Lycopersicon esculentum* Mill.). Global Change Biology, 5: 635–646. doi:10.1046/j.1365-2486.1999.00258.x

BIPM, (2012): The international vocabulary of metrology—basic and general concepts and associated terms (VIM), 3rd edn. Paris, JCGM 200:2012.

Biswas S.K., Akanda A.R., Rahman M.S., Hossain M.A. (2015): Effect of drip irrigation and mulching on yield, water-use efficiency and economics of tomato. Plant, Soil and Environment, 61(3): 97–102 doi: 10.17221/804/2014-PSE

Born M., Wolf E., (1999): Principles of Optics: Electromagnetic Theory of Propagation, Interference and Diffraction of Light, section 2.3.3; 7th Edition, Cambridge University Press, UK

Castagna A., Chiavaro, E., Dall'Asta C., Rinaldi, M., Galaverna G., & Ranieri A. (2013): Effect of postharvest UV-B irradiation on nutraceutical quality and physical properties of tomato fruits. Food chemistry, 137(1): 151-158.

Confalonieri R., Foi M., Casa R., Aquaro S. *et al.* (2013): Development of an app for estimating leaf area index using a smartphone. Trueness and precision determination and comparison with other indirect methods. Computers and Electronics in Agriculture, 96: 67-74

Fedina I.S., Velitchkova M.Y. (2009): Physiological Responses of Higher Plants to UV-B Radiation 2009. In Climate Change and Crops, Environmental Science and Engineering, Springer-Verlag Berlin Heidelberg.

Fišerová H., Hartman I., Prokeš J. (2015): The effect of weather and the term of malting on malt quality. Plant, Soil and Environment, 61(9): 393–398

Groselj D., (2010): Guidance on Instrumentation for Calibration Laboratories, including Regional Instrument Centres. Instruments and Observing Methods Report No. 101, WMO /TD- No. 1543

Hülsen G., Gröbner J. (2007): Characterization and calibration of ultraviolet broadband radiometers measuring erythemally weighted irradiance. Applied Optics, 46(23): 5877-5886

Krizek D.T. (2004): Influence of PAR and UV-A in determining plant sensitivity and photomorphogenic responses to UV-B radiation. Photochemistry and Photobiology, 81: 1026–1037

Li T., Yang Q. (2015): Advantages of diffuse light for horticultural production and perspectives for further research. Frontiers in Plant Science, 6:704. doi: 10.3389/fpls.2015.00704

Lopardo G., Bellagarda S., Bertiglia F., Merlone A., Roggero G., Jandric N. (2015): A calibration facility for automatic weather stations. Meteorological Applications, 22(S1); 842-846

Merlone A., Lopardo G., Sanna F., et al. (2015): The MeteoMet project – Metrology for Meteorology: challenges and results. Meteorological Applications, 22 (S1): 820-829. DOI: 10.1002/met.1528

Merlone A., Sanna F., Bell S., Beges G., et al., (2017): The MeteoMet2 Project–Highlights and Results. Measurement Science and Technologies (*in press*)

Michel P., Dugas J., Cariou J.M., Martin L. (1986): Thermal variations of refractive index of PMMA, polystyrene, and poly (4-methyl-1 -pentene). Journal of Macromolecular Science, Part B, 25(4): 379-394

Preston-Tomas H. (1990). The International Temperature Scale of 1990 (ITS-90). Metrologia, 27: 3-10

Priyadarshi A., Shimin L., Wong E.H., Rajoo R., Mhaisalkar S.G., Kripesh V. (2005): Refractive Indices Variation with Temperature and Humidity of Optical. Adhesive Journal of Electronic Materials, 34(11): 1378-1384

Ribeiro C., o Canada J., Alvarenga B. (2012): Prospects of UV radiation for application in postharvest technology. Emirates Journal of Food and Agriculture, 24(6): 586-597

RStudio Team (2015): RStudio: Integrated Development for R. RStudio, Inc., Boston, MA URL http://www.rstudio.com/

Sanna F., Cossu Q.A., Bellagarda S., Roggero G., Merlone A. (2014): Evaluation of EPI forecasting model with inclusion of uncertainty in input value and traceable calibration. Italian Journal of Agrometeorology, 3: 33-42

Sanna F., Calvo A., Deboli R., Merlone A. (2017): Vineyard diseases detection: a case study on the influence of weather instruments calibration and positioning. Meteorological Applications, 24(4): doi:10.1002/met.1685

Schaepman, M.E. (1998): Calibration and Characterization of a Non-Imaging Field Spectroradiometer Supporting Imaging Spectrometer Validation and Hyperspectral Sensor Modelling. PhD dissertation in Natural Science. Faculty of Mathematics and Natural Sciences Faculty of the University of Zurich.

Schreiner M., Huyskens-Keil S., (2006): Phytochemicals in Fruit and Vegetables: Health Promotion and Postharvest Elicitors. Critical Reviews in Plant Sciences, 25:267–278

WMO-CIMO, Guide to Meteorological Instruments and Methods of Observation, WMO-No. 8, 2008 edition, update 2010

Zhang Z., Zhao P., Lin P., Sun F., (2006): Thermo-optic coefficients of polymers for optical waveguide applications. Polymer Communication. Polymer, 47(14): 4893-4896

6. The Meteomet2 Project – Highlights and Results

A. Merlone[1], F. Sanna*[1], G. Beges[2], S. Bell[3], G. Beltramino[1], J. Bojkovski[2], M. Brunet[4], D. del Campo[5], A. Castrillo[6], N. Chiodo[7], M. Colli[8], G. Coppa[1], R. Cuccaro[1], M. Dobre[9], J. Drnovsek[2], V. Ebert[10], V. Fernicola[1], A. Garcia-Benadí[11], C. Garcia-Izquierdo[5], T. Gardiner[3], E. Georgin[12], A. Gonzalez[5], D. Groselj[13], M. Heinonen[14], S. Hernandez[5], R.Högström[14], D. Hudoklin[2], M. Kalemci[15], A. Kowal[16], L. Lanza[8], P. Miao[2], C. Musacchio[1], J. Nielsen[17], M. Nogueras-Cervera[11], P. Pavlasek[18], M. de Podesta[2], S. Oguz Aytekin[15], M. K. Rasmussen[17], J. del-Río-Fernández[11], L. Rosso[1], H. Sairanen[14], J. Salminen[14], D. Sestan[19], L. Šindelářová[20], F. D. Smorgon[1], Sparasci[6], R. Strnad[20], M. Voldan[20], R. Underwood[2], A. Uytun[15]

* *corresponding author:* Francesca Sanna *f.sanna@inrim.it*

1 INRiM Istituto Nazionale di Ricerca Metrologica, Turin, Italy
2 NPL National Physical Laboratory, Hampton Road, Teddington, Middlesex, UK
3 UL-FE/LMK Univerza v Ljubjani, Ljubljana, Slovenia
4 C3 Centre for Climate Change, Dep. of Geography, University Rovira i Virgili, Tarragona, Spain
5 CEM Centro Español de Metrología, Tres Cantos, Madrid, Spain
6 Università degli Studi della Campania "Luigi Vanvitelli" Dipartimento di Matematica e Fisica, Caserta, Italy
7 LNE-Cnam Conservatoire national des arts et métiers, La Plaine Saint-Denis, France
8 University of Genova, Dept. of Civil, Chemical and Environmental Engineering, Italy
9 SMD Federale Overheidsdienst Economie, KMO, Middenstand en Energie, Brussels, Belgium
10 PTB Physikalisch-Technische Bundesanstalt, Braunschweig, Germany
11 UPC Universitat Politècnica de Catalunya Vilanova i la Geltrú, Spain
12 LNE-CETIAT Centre Technique des Industries Aérauliques et Thermiques, Villeurbanne Cedex, France
13 ARSO - Agencija Republike Slovenije za okolje, Ljubljana, Slovenia
14 VTT MIKES Mittatekniikan Keskus, Espoo, Finland
15 TUBITAK Ulusal Metroloji Enstitusu, Kocaeli, Turkey
16 INTiBS Instytut Niskich Temperatur i Badań Strukturalnych, Wroclaw, Poland
17 DTI Teknologisk Institut, Gregersensvej, Taastrup, Denmark
18 SMU Slovenský Metrologický Ustav, Bratislava, Slovakia
19 HMI/FSB-LPM Faculty of Mechanical Engineering Zagreb, Croatia
20 CMI Cesky Metrologicky Institut, Brno, Czech Republic

Published in Measurement Science and Technologies. 29 025802 pp. 17. (2018) DOI: 10.1088/1361-6501/aa99fc

Abstract

Launched in 2011 within the European Metrology Research Programme (EMRP) of EURAMET, the joint research project "MeteoMet" – Metrology for Meteorology – is the largest EMRP consortium: National Metrology Institutes, Universities, meteorological and climate agencies, Research Institutes, collaborators and manufacturers are working together, developing new metrological techniques, as well as improving already existing ones, for meteorological observations and climate records. The project focuses on: humidity in the upper and surface atmosphere, air temperature, surface and deep-sea temperatures, soil moisture, salinity, permafrost temperature, precipitation and snow albedo effect on air temperature. All tasks are performed under rigorous metrological approach and include design and study of new sensors, new calibration facilities, investigation of sensors characteristics, improved techniques for measurements of Essential Climate Variables with uncertainty evaluation, traceability, laboratory proficiency and inclusion of field influencing parameters, long-lasting measurements, and campaigns in remote and extreme areas.

MeteoMet vision is to make a further step towards establishing full data comparability, coherency, consistency and long-term continuity, through a comprehensive evaluation of the measurement uncertainties for the quantities involved in the global climate observing systems and the derived observations. The improvement of quality of Essential Climate Variables

records, through the inclusion of measurement uncertainty budgets, will also highlight possible strategies for the reduction of the uncertainty.
This contribution presents selected highlights of the MeteoMet project and reviews the main ongoing activities, tasks and deliverables, with a view to its possible future evolution and extended impact.

Keywords:
Metrology for meteorology and climatology; atmospheric air temperature, humidity and pressure measurements; sea temperature and salinity measurements; albedo, soil moisture and permafrost; weather station; interlaboratory comparison.

Glossary:

BEV/PTP	Physikalisch-Technischer Pruefdienst des Bundesamt fuer Eich- und Vermessungswesen, Austria
BIPM	*Bureau International des Poids et Mesures*
CCT	Comité Consultatif de Thermométrie
CEM	Centro Espanol de Metrologia, Spain
CETIAT	Centre Technique des Industries Aerauliques et Thermiques, France
CIMO	Commission for Instruments and Methods of Observations
CMCs	Calibration Measurement Capabilities
CMI	Cesky Metrologicky Institut Brno, Czech Republic
CNAM	Conservatoire National des Arts et Metiers, France
CSIC	Agencia Estatal Consejo Superior de Investigaciones Cientificas, Spain
CTD	Conductivity, Temperature and Depth
DTI	Teknologisk Institut Denmark, Denmark
ECVs	Essential Climate Variables
EDIE	Earth Dynamics Investigation Experiment
EMRP	European Metrology Research Programme
EURAMET	European Association of National Institutes of Metrology
FBGs	Fiber Bragg Gratings
GCOS	Global Climate Observing System
GRUAN	GCOS Reference Upper-Air Network
GUM/MG	Ministerstwo Gospodarki, Poland

INRiM	Istituto Nazionale di Ricerca Metrologica, Italy
INTiBS	Institut Niskich Temperatur i Badan Strukturalnych, Poland
KCDB	Key Comparison Database
KNMI	Royal Netherlands Meteorological Institute
LMD	Laboratoire de Météorologie Dynamique
NIOZ	Royal Netherlands Institute for Sea Research
NMHS	National Meteorological and Hydrological Services
NMI	National Measurement Institutes
NPL	National Physical Laboratory, United Kingdom
OBSEA	Submarine observatory at of Vilanova i la Geltrú, Spain
ppmv	parts per million by volume
PRT	Platinum Resistance Thermometer
PTB	Physikalisch-Technische Bundesanstalt, Germany
RA	Regional Associations
SHOM	Service hydrographique et océanographique de la Marine, France
SI	International System of Units
SMD	Federale Overheidsdienst Economie, KMO, Middenstand en Energie, Belgium
sccm	standard cubic centimeters
T&RH	Temperature and Relative Humidity
TBRGs	Tipping-Bucket Rain Gauges
TDLAS	Tunable Diode Laser Absorption Spectroscopy
TUBITAK	Türkiye Bilimsel ve Teknolojik Araştirma Kurumu, Turkey
UL	Univerza v Ljubljani, Slovenia
UniGe	Università degli Studi di Genova
UPC	Universitat Politècnica de Catalunya
VSL	Van Swinden Laboratorium B.V., Netherlands
VTT MIKES	Teknologian tutkimuskeskus / Mittatekniikan Keskus, Finland
WMO	World Meteorological Organization
WOCE	World Ocean Circulation Experiment

6.1. Introduction

6.1.1. *Background*

Measurements are at the core of meteorology and climatology, but typically, instruments and methods of observation in these fields have evolved – quite understandably – with extreme conservatism. Thus, great

value was placed on the continuity of measurement series made using the same technique, despite questions being raised over the continued appropriateness of the measurement technique, and the availability of new techniques. Viewed from a metrological perspective, we can view this tension between conservatism and innovation as arising from a combination of two weaknesses in traditional meteorological practice.

Firstly, traditional meteorological techniques can fail to adequately characterise the measurand and thus, for example, a measurement of humidity using a wet-bulb thermometer can be strongly influenced by wind speed at the measurement station. Changing instruments or methods can result in the measurement with quite different susceptibility to other quantities, and thus introduce different error characteristics – known as an inhomogeneity – into a measurement series.

Secondly, there is often a reluctance to fully quantity the measurement uncertainty associated with a measurement. This is because the conditions of measurement are frequently so hostile that issues of conventional measurement traceability are considered of secondary importance. Additionally, measurements from around the world are rarely taken in ideal conditions with professional metrologists at hand.

Meteorologists and climatologists are well aware of these shortcomings and have developed sophisticated strategies for analysing measurement series containing inhomogeneities. Nonetheless, the situation is far from ideal. It is in this context that the two MeteoMet and MeteoMet2 pan-European projects were created with aim of improving meteorological best practice by the application of new concepts and technology applied with a metrological perspective.

As stated by the Global Climate Observing System (GCOS), “long-term, high-quality and uninterrupted observations of the atmosphere, land and

ocean are vital for all countries, as their economies and societies become increasingly affected by climate variability and change" [1]. High-quality observations are possible only if they are based on a sustained traceability to the International System of Units (SI) and with uncertainties associated to the measured ECVs.

6.1.2. *MeteoMet*

MeteoMet – Metrology for Meteorology – is a Joint Research Project (JRP) of the *European Association of National Institutes of Metrology* (EURAMET). Its first phase began in 2011 [2, 3] and focussed on the traceability of a subset of Essential Climate Variables (ECVs) to the International System of Units (SI) with specified uncertainties. In 2014, the project began its second phase, *Meteomet* 2, extending the investigations to additional variables and contributions to uncertainty in field measurements. The aim is that quality improvement of the recorded ECV data will eventually lead to strategies for the reduction of the uncertainty.

The MeteoMet 1 and 2 projects involves 18 National Measurement Institutes (NMI) and 6 Designated Institutes from 20 European countries, 14 universities, 13 research centres, 14 manufacturers and private companies, and 22 hydro-meteorological agencies. It is through this combination of organisations and perspectives that the project aims to translate ideas in practical implementation in the field. The project key data since the first phase is summarized in the table1 of annex I, with the full list of MeteoMet 1 and 2 partners (table 2).

The project is structured into three main areas of observation: Air, Sea and Land. These categorisations are really shorthand because many of the 'land' ECVs refer to measurements of the temperature and humidity of air, but specifically address measurements in meteorological stations.

In Section 2 below, we outline the challenges identified in the project considered in each domain: Air (Section 2.1), Sea (Section 2.2) and Land (Section 2.3). Within each subsection, we list the specific work packages which respond to the identified measurement challenges along with the lead institution taking part in the research. Because MeteoMet 2 is not due to finish until the end of September 2017, as we write this paper, not all projects have been finished. However, we consider it valuable to include details to convey the scope of the work being undertaken. In Section 3, we select eight work packages for further exposition, and In Section 4 we describe the anticipated impact of the project and prospects for further research.

6.2. Topics

6.2.1. *Air: humidity and temperature measurements above ground level*

Climate science could be alternatively described as the study of the dynamics and thermodynamics of water in the Earth's atmosphere. Yet measurements of water vapour in air are especially problematic. Ideal sensors would be able to cover a range of specific humidity (g H_2O per kg dry air) covering a factor of more than 10^4 and would be fast responding to quantify dynamic changes. For ground level measurement, the targets are: at 23 °C and 50 %rh = 8.79 g H_2O/kg dry air; at -20 °C and 50 %rh = 0.388 g H_2O/kg dry air; at 40 °C and 50 %rh = 23.65 g H_2O/kg dry air; and it is even lower in the upper atmosphere. However real sensors are highly non-ideal. The sensors display a significant hysteresis; they dry down considerably more slowly than they get wet; and their response time is particularly poor when the surround environment is cold. These combined shortcomings create significant measurement challenges for radiosondes, which travel from the warm, wet troposphere to cold dry stratosphere.

The MeteoMet consortium set the following scientific and technological objectives:

1. Development of metrological procedures to calibrate radiosondes under atmospheric conditions including reduced pressures and temperatures.
2. Measurement of the water vapour enhancement factors, which cause deviation from calculated specific humidity in air, compared to water vapour only calculations.
3. Development of new spectroscopic methodologies as standards for traceable humidity measurements and on-site references.
4. Development of a traceable humidity source capable to provide on-site calibration to airborne instruments.
5. Development of a reference instrument for the measurement of fast transients of temperature and humidity.
6. Development of traceable humidity sensors based on microwave resonators having short response time and small size.

In response to these identified aims, the following steps have been taken.

6.2.1.1. Calibration of radiosondes under atmospheric conditions

The development of a calibration facility for water-vapour measurements in radiosondes in the range from 0.03 µmol/mol to 1.5 µmol/mol [4] was completed at VTT MIKES. The pressure and dew-point temperature limits were decreased down to 10 hPa (abs.) and -90 °C at VTT MIKES and 200 hPa and -95 °C at INRiM, respectively, to simulate the conditions met during the ascent in the troposphere and lower stratosphere. The calibration of a radiosonde at a single temperature can be performed within 15 h. The facility shows a very good repeatability and no hysteresis. The water vapour amount fraction uncertainty is less than 2%. This task is described further in the ‘Highlights’ Section 3.1

6.2.1.2. Measurement of the enhancement factor under atmospheric conditions

The CETIAT completed a literature review to identify pros and cons of different experimental set-ups. Currently two measuring methods are generally used, a direct one, by measuring the second virial coefficient, and an indirect one, by measuring humidity, therefore, studies were carried out to identify the most synergic methods with other measurements. The indirect method was chosen and an apparatus was designed. The assembly is in progress and a measurements campaign will follow. The humidity range aimed to be comprised between -60 °C and 10 °C, and the pressure range between 400 hPa (abs.) and 1000 hPa (abs.).

6.2.1.3. On-site calibration of airborne instruments

PTB has built a portable instrument for *in situ* calibration of airborne hygrometer with uncertainty in the (1-20) parts per million by volume (ppmv) interval. A mobile, compact, and robust water vapour generator, which uses water permeation through air-purged plastic tubing was developed and manufactured. By stabilising the gas flow and the bath temperature, a well-defined mixing ratio is achieved. Performance tests are ongoing.

6.2.1.4. Measurement of fast transients of temperature and relative humidity

NPL upgraded an airborne combined acoustic thermometer and infrared hygrometer for measurement of fast transients during ascents through the atmosphere [5]. The instrument can make 30 independent readings per second with a resolution of 0.001 °C and uncertainty <0.1 °C, measurement of water vapour mixing ratios from 10000 ppmv (~10%) to $3 \cdot 10^4$ ppmv (corresponding to dew points from -42 °C to 24 °C at 10^5 1000 hPa).

6.2.1.5. Microwave hygrometry

CNAM realized a prototype of a fast airborne microwave hygrometer (volume 200 cm^3) operating from -50 °C to 10 °C (frost point temperature) and from -20 °C to 20 °C (dew point temperature). The measurement range is from few to 10^5 ppmv, and the uncertainty of measurement is approximately 5 ppmv. A comparison with a CETIAT calibrated chilled-mirror hygrometer showed that it could be an alternative standard for humidity measurements (see figure 1). However, the measurement time is about 100 seconds, considered still extensive for the purpose, primarily because a long sampling tube was used. A second generation was made and the assembly of the full system is in progress.

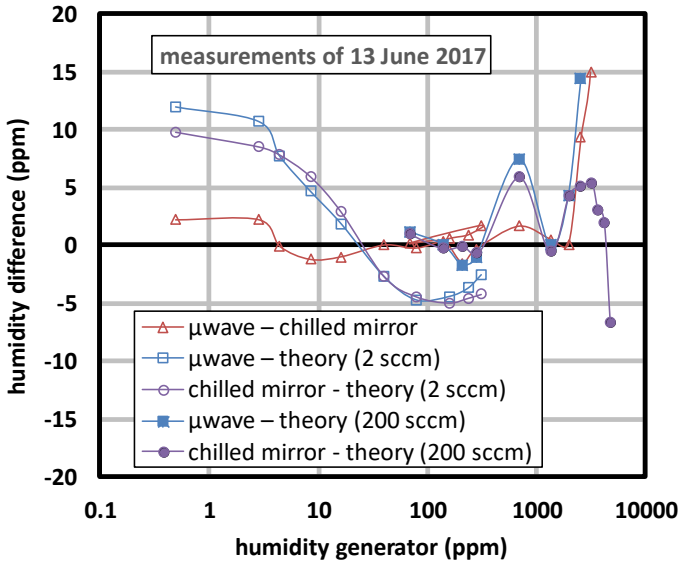

Figure 1. Comparison between the uncalibrated microwave hygrometer developed at CNAM and a calibrated chilled mirror hygrometer supplied by CETIAT (µwave – chilled mirror). sccm = standard cubic centimeters. The picture shows also comparisons of the microwave hygrometer and the chilled mirror with theoretically calculated humidity values in low flow regime (2 sccm) and high flow regime (200 sccm).

6.2.2. *Sea: temperature and salinity measurements in oceans*

Temperature and salinity are two key oceanic ECVs, for monitoring and understanding decadal changes in heat content and heat transport. A comprehensive study of the characteristics of the associated measurement instruments and the effect of the main quantities of influence on thermometers and salinometers is needed, in order to reduce measurement uncertainty.

The scientific and technological objectives at the outset of the project are:

1. Development of facilities to study the pressure dependence of deep-sea thermometers and to establish validated pressure-correction models.
2. To perform a thermodynamic calibration of deep-sea thermometers, to analyse the temperature-resistance models, to estimate the uncertainties or to propose improved models.
3. Development of distributed temperature sensors based on optical Fiber Bragg Gratings (FBGs), to improve the traceability of sea-surface and sea-profile temperature measurements, and to monitor temperature drifts of the thermometers used in underwater observatories.
4. Development of a facility for determining temperature and pressure effects on salinometers based on the measurement of seawater refraction index, and their metrological characterization.

6.2.2.1. Pressure dependence of deep-sea thermometers

VSL realised a comparison block and carried out measurements on deep-sea thermometers using a high-pressure chamber available at NIOZ (Royal Netherlands Institute for Sea Research). The pressure dependence of Sea-Bird Electronics thermistors (the biggest manufacturer and supplier of oceanographic thermometers) was measured at 500 bar (-0.30 mK /

100 bar) confirms the values observed in the sea (from -0.17 to -0.33 mK / 100 bar) and the proper operation of the facility. A pressure of 100 bar corresponds to a depth of approximately 1000 metres.

6.2.2.2. Thermodynamic calibration of deep-sea thermometers

The CNAM modified an acoustic gas thermometer and the associated calorimeter, in order to integrate and calibrate the deep ocean thermometers from -5 °C to 35 °C, within a calibration uncertainty below 0.5 mK.

Currently, the best achievable calibration uncertainties on high-grade deep ocean thermometers are close to 2 mK. They might be further reduced to meet the target overall uncertainty of 2 mK in deep ocean temperature measurements, required by the World Ocean Circulation Experiment (WOCE) Hydrographic Program[1]. Measurements are currently in progress at CNAM to evaluate the suitability of the most common high-grade deep ocean thermometers for such reduced uncertainty.

6.2.2.3. Ocean temperature sensors based on optical fiber Bragg gratings

CEM, CSIC and UPC designed and assembled FBGs sensors, used as thermometers, to measure profile and near-surface sea temperatures. The onsite experiment was designed and the FBGs sensors were tested and calibrated. These thermometers were integrated into the submarine observatory (OBSEA), connected to the coast of Vilanova i la Geltrú (Barcelona, Spain) and placed at a depth of 20 meters.

This task is described further in the 'Highlights' Section 3.3 and 3.4.

---

[1] World Climate Research Programme (WCRP), Scientific plan for the World Ocean Circulation Experiment, WMO/TD-No. 122, July 1986.
https://www.nodc.noaa.gov/woce/wdiu/wocedocs/sciplan/sciplan.pdf

6.2.2.4. Test and calibration facility for refractive-index salinometers

To make accurate *in-situ* measurements, CNAM and INTiBS created a test and calibration facility for determining temperature and pressure effects on a novel generation of salinometers allowing absolute salinity assessment. This facility is based on the refractive index of seawater and was used for investigating the impact of parameters such as temperature and pressure on the optical sensor, or temperature on the laser wavelength drift.

6.2.2.5. Land: temperature and humidity measurements in ground level measurements

Ground-based ECVs have been historically recorded for meteorological purposes and these records now form one of the primary tools for evaluating decadal and longer climate trends. New techniques are being developed to improve the data quality and the comparability between meteorological stations. A key focus in MeteoMet project has been the ability to make coherent of measurement uncertainty including the effects of the intrinsic sensor behaviour, and parameters of influence, including siting and thermometer screens.

An objective of the intrinsic and dynamic behaviour study of the air temperature sensors is to improve the ISO Guide 17714:2007 (Meteorology - Air temperature measurements - Test methods for comparing the performance of thermometer shields/screens and defining important characteristics), by defining calibration procedures and evaluating uncertainties through a better sensor characterisation. This will be achieved by means of different facilities, including the special wind tunnel with temperature and pressure control designed and developed by INRiM during the first three years of the project. CEM determined the self-heating effect and hysteresis effect of a selection of thermometers with

different designs, covering Pt100 alone, as well as Pt100 embedded in temperature and relative humidity (T&RH) sensors. The analysis of self-heating effect was also performed at several temperatures and with the thermometers surrounded by different mediums.
These tasks are described further in the 'Highlights' Section 3.5 and 3.6.

Regarding ECV's explicitly in the land rather than just above it, permafrost temperature is classified as a parameter to investigate climate changes but, today, few measurement procedures report a fully detailed uncertainty budget. Similarly, calibration and measurements standards for precipitation and soil moisture are not yet developed to cope with the differences between laboratory setups and field conditions.

In response to these challenges, the consortium set the following scientific and technological objectives:

1. Analysis of the siting influence on air temperature measurements in terms of uncertainty components.
2. Determination of the influence of rain and albedo on air temperature measurements.
3. To evaluate the intrinsic behaviour of thermometers and humidity sensors plus radiation shields to define calibration procedures and methods to evaluate the measurement and calibration uncertainties.
4. To ensure consistency and coherence of meteorological measurements carried out in different places.
5. Development of procedures for traceable dynamic calibrations and uncertainty calculation of hygrometers used to measure the humidity near the Earth surface.
6. Development of a high-bandwidth humidity generator to study the response of air-humidity sensors to fast humidity changes.

7. To identify the needs of traceability and uncertainty calculation of soil moisture measurements and to carry out initial experimental trials of the relevant procedures.
8. Indications of consistent measurement uncertainties in meteorological humidity data sheets.

6.2.2.6. Influence of obstacles on meteorological sites

The World Meteorological Organization-Commission for Instruments and Methods of Observations (WMO-CIMO) Guide n.8 [6] establishes a classification to help determine the ground based observation site's representativeness on a small scale. This classification associates a discrete uncertainty value/level to temperature measurements carried out in sites where exposure rules are not fully met. The work here described aimed to quantitatively evaluate uncertainty for some of the influences of siting parameters on temperature measurements: closeness to trees, buildings and asphalt roads. INRiM defined a protocol to study the influence of such obstacles on surface-based air temperature measurements that received positive feedback by the WMO Expert Team on In-situ Operational Technologies. Three experiments were carried on to improve the uncertainties associated to the presence of obstacles close to the stations and sensors in field. In Italy, an experiment is running to evaluate the road influence; in the Czech Republic a second one for tree influence; in Spain, for buildings influence. The experiments are based on identical setup and measurement protocols used to by quantify the temperature difference measured close to the obstacles and along seven measuring points up to 100 m of distance in open field. The overall goal is a providing WMO CIMO Expert team input for revising the values and prescriptions adopted by the CIMO guide.

6.2.2.7. Albedo radiation and rain effect on meteorological thermometers in screens

Thermometers use for meteorological measurements of air are normally housed in solar shields to avoid direct sun radiation introducing biases and errors in the measurement accuracy. Beside the direct solar radiation, other effect can introduce deviations from the measurement results and the air temperature value. While the effect due to the ageing of the solar shields and the associated decrease of the reflecting properties of the white painting was investigated in the previous phase on MeteoMet1 [7], in this project the effects of rain and albedo from a snow covered surface are quantified, to be included as uncertainty components in the air temperature measurements. About rain, the study is based on the fact that when rain fall on the screen housing the thermometers, an overcooling due to the lower rain drop temperature with respect to the air temperature can introduce errors in the temperature recorded. DTI assessed this influence by designing and assembling an experimental system able to generate rain drops at a known temperature in a volume with air temperature accurately measured.

Operators of weather stations in areas where snow occurs normally observe a raise in the temperature values during sunny days in presence of snow below the measuring area. A part of this phenomenon is the natural warming of the air due to the heat diffused by the reflected radiation, the albedo from the snow covered surface, and it is not the subject of this study, since it is part of the meteorological measurand characteristics. A further component is not dependent on natural phenomena: this is the overheating of the sensor due to the reflected radiation form the snow covered surface. This effect is strongly dependent on the geometry and characteristics of the shield and sensor and can be different up to more than

a degree Celsius on the measured temperature values. INRiM and BEV identified a mountain site to investigate this effect of albedo from a snow covered surface on temperature measurement and made it operational. Five pairs of shielded temperature sensors, with both naturally aspirated and mechanically ventilated shields, were used to ensure a representative group of devices. Tests were performed to evaluate the “zero” difference between each pair, as well as the necessary corrections and the relevant uncertainties. The measurements are in progress.

As a further study, SMD made the model of the temperature measurement conditions inside a radiation shield. The model described the temperature gradient occurring in Stevensons screens under wind and radiation conditions and heat reflected for the soil. Data is being analysed and validated thanks to 3-year in-field experiment made by KNMI with 10 different radiation shields.

6.2.2.8. Inter laboratory comparison

UL defined a protocol for the Inter-Laboratory Comparison (ILC) of temperature, humidity, and pressure internal standards of calibration laboratories of the National Meteorological and Hydrological Services (NMHS) [8]. The WMO made the protocol as an official document of its CIMO. Beyond the MeteoMet2 tasks, ILC with two loops of the ILC was organised using this protocol, with 18 National meteorological agencies participating [9] in the European Regional Associations (RA-VI). The equipment used in both loops exhibited stability and uncertainty, which enabled full evaluation of the participating laboratories capabilities. In the field of temperature, out of 270 submitted results, three laboratories had 5 results with $|En| > 1$. In the field of relative humidity, out of 117 submitted results, only one laboratory had 5 results with $|En| > 1$, [10]. In the field of pressure, out of 784 submitted results, only three laboratories had results

with |*E*n| > 1. It was strongly recommended that all the laboratories with unsatisfactory results, carefully checks their procedures for any potential systematic error, to check traceability of their references and to check their uncertainty budget to comply with used equipment and procedures as well as state of the art. The results of other participating laboratories were satisfactory. For the current state of the art in calibration of any instrument, it was advised that it is worthwhile to check BIPM KCDB (*Bureau International des Poids et Mesures*, Key Comparison Database) annex C, for the Calibration Measurement Capabilities (CMCs) of the best national metrology laboratories. Some of the uncertainties of the participating laboratories were on the level of the best national metrology laboratories. It is expected that the ILC will be extended also to other WMO regions outside Europe. First expressed interest was from RA-II and RA-V (Japan, Australia, Philippines, China) and later potentially to the African region. All the results of all potential ILCs could be linked to the results in the European region (RA-VI).

6.2.2.9. In situ calibration

Transportable facilities were studied and manufactured, during the first phase of MeteoMet project, for the calibration of weather sensors on site. This calibration chamber, called *Earth Dynamics Investigation Experiment* 1 (EDIE1), is capable of simultaneous and independent control of pressure and temperature. The facility is also designed to allow the control in humidity, therefore completing the characterization of the whole AWS pressure–temperature–humidity modulus. [11]. One of the greatest benefits of this facility is the reduced dimensions that makes it transportable for *in situ* calibration campaigns, also in remote areas [12]. Indeed, the facility was used in challenging missions and activities at high altitude in Himalaya and in the Arctic [13, 14].

6.2.2.10.Historical records

Historical temperature records for climate trend evaluations have also been a subject of the project: studies were made on the effect of change in instrumental methodologies on daily minimum and maximum recorded values, showing non-negligible and non-unique effects [15]. Direct calibration of historical sensors without interrupting the series were made on site of centennial stations [16]. This work illustrates one of the first examples of air-temperature data traceable to SI standards recorded in a historical series and indicates that the application of the calibration function to correct data influences the climatological analysis.

6.2.2.11.Agro-meteorology

Metrology applied to agro-meteorology was also developed since the first phase of the MeteoMet project, in terms of evaluating the effect of the calibration's uncertainty inclusion on the meteorological measurements used as input values on epidemiological forecasting models [17]. The EDIE facility (see 2.3.4) were used to calibrate the air temperature sensors. During the second phase of the MeteoMet project, the studies moved to the weather monitoring instruments installed on hill and mountain agricultural sites. These instruments are often forced into non-ideal positioning due to slopes, tree proximity and other obstacles that primarily affect relative humidity, temperature, and solar radiation measurements. The enclosure of the instrument positioning contribution in forecasting models affected positively the disease prediction [18].

6.2.2.12.Dynamic calibrations of hygrometers

A new water vapour generator was delivered to PTB and was integrated into a calibration facility. A climatic chamber reaching low temperatures (typically -60 °C) is operational at CETIAT. In collaboration with *Laboratoire de Météorologie Dynamique* (LMD), satisfactory response

time measurements were made with the LMD hygrometer and also with a chilled mirror instrument.

The humidity generator is capable of fast step changes in order to study the response of air humidity sensors. The facility is composed by a source of humid air generation, a source of dry air, a divider plate and a testing chamber set in a climatic chamber reaching low temperature (-60 °C). The divider plate is equipped with high-speed valves allowing switch from one humidity to another in few hundreds of milliseconds. Two hygrometers, with and without shields, were tested among chilled mirror, impedance hygrometer silicon oxide based. PTB and LNE-CETIAT are working on the interface of a measuring ring, developed at PTB, and testing chamber, developed at LNE-CETIAT, for having high accurate and high-speed reference instrument, Tunable Diode Laser Absorption Spectroscopy (TDLAS) type or spectroscopic type, close to the device under test.

This task is described further in the ‘Highlights’ Section 3.7.

6.2.2.13. Precipitation

UniGe and associated Research Excellent Grant analysed a typical calibration system for tipping-bucket rain gauges (TBRGs), using the gravimetric method, in accordance with the recommendations and requirements of both meteorology and metrology. As a result, major contributions of the type B uncertainty in the calibration of TBRGs are due to the weighing system calibration (1.68 %) and resolution (0.74 %). Dimensionally, rounding off errors in the conversion from inches to millimetres were observed. It was evaluated that an uncertainty of 1 mm in measuring the diameter of the collector results in 0.58 % of the calibration uncertainty contribution [19].

6.2.2.14.Soil moisture measurements and questionnaire

TUBITAK realized a soil moisture measurement set-up based on a gravimetric method and composed by a moisture analyser, a high precision balance, a desiccator, and an oven supplemented with a rotary pump. The online survey is left open so that more responses can be collected. The INRiM completed a literature search on soil moisture measurements and calibration methods focus on agriculture and traceability requirements. It turned out there are a number of issues with the calibration, i.e. the soil used for calibration that may not represent the characteristics of the soil to be measured by the technique being calibrated. The calibration is also affected by other factors such as soil temperature, barometric pressure, salts and air gaps in soil as well as the bulk density of the soil.

NPL collected the Met Office, the United Kingdom's national weather service, datasets of weather station hygrometer calibrations from 2012 to 2014 and added it to the initial subset of already analysed data for estimates of the drift.

Moreover, NPL performed a survey on the measurements (about 100 respondents) and the needs of calibrations. The soil moisture questionnaire was designed to address the applications of soil moisture measurements, techniques, calibration methods (classical gravimetric method and remote sensing techniques). 25 questions were prepared, 23 of which were technical and the questions were divided into five macro areas: application, measurement, calibration, classical gravimetric method and remote sensing techniques. Potential participants for the questionnaire were identified from numerous sources. The answers to the questionnaire were automatically sent to NPL and the survey results were reported separately. In conjunction with VSL, INRiM contributed in circulating the questionnaire to over 350 contacts. MIKES, involved with steering the

planning and realising the survey, is using the outcomes to improve the traceability of soil moisture sensors.

6.3. Selected highlights

6.3.1. *SI traceable humidity calibrations for radiosondes*

Radiosondes provide an economical method to measure vertical humidity profile in the troposphere and lower stratosphere, an activity, which is vital for weather forecasts and climate change monitoring.

Specific challenges include:

- insolation
- wetting of sensors
- Slow drying of sensors

To improve the quality of upper-air humidity data, the GCOS specified a challenging uncertainty requirement for humidity measurements (2 % in the water vapour mixing ratio) [20]. Traceability to the SI is an essential requirement for achieving the target uncertainty. To enable SI-traceable humidity calibrations of radiosondes at upper-air equivalent conditions, a new humidity calibration facility was developed by the Centre for Metrology MIKES at the VTT Technical Research Centre of Finland. In this facility, a humidity radiosonde probe can be calibrated at air temperature from -80 °C to 20 °C, dew/frost-point temperature from -90 °C to 10 °C and absolute air pressure from atmospheric pressure down to 10 hPa corresponding to an altitude of approximately 30 km.

One target of the system development was to reduce stabilisation time in the measurement chamber to enable feasible calibration times. This was achieved by an appropriate measurement chamber design [21] and by applying flow mixing in a two-saturator humidity control setup [4, 22] illustrated in figure 2.

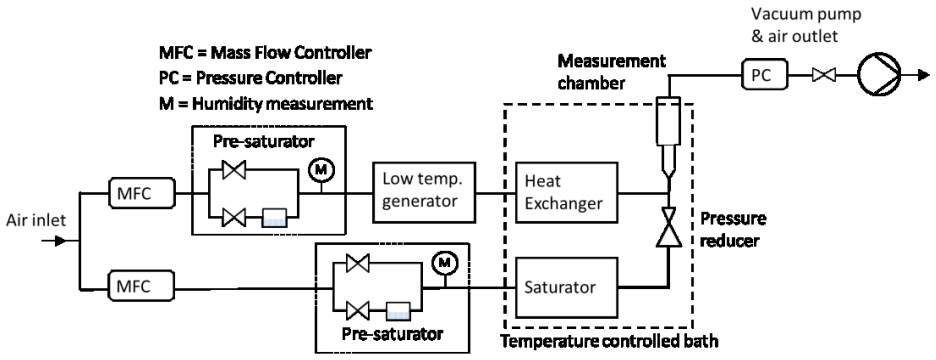

Figure 2. Schematic diagram of the facility developed by VTT MIKES for humidity calibrations of radiosondes.

The apparatus was fully characterised at surface pressure level and the uncertainty analysis showed that the target uncertainty of 2 % is achieved with this system. The characterisation will be completed with a comparison to be carried out with the recently commissioned INRiM standard frost point generator at sub-atmospheric pressure in the near future.

6.3.2. *A correction for the temperature historical series*

Daily temperature-time series, spanning over 300 years were created in particular locations and these records have allowed for the creation of climate system models of the Earth, which are used to define the long-term temperature trends and are employed for the calibration of proxies used for temperature prediction further back in time.

Prior to the 1850s, the number of continuously operated observation stations declines considerably and the creation of reliable datasets is therefore difficult. A new international temperature scale was introduced in 1927, which was truly internationally, accepted and used. The scale evolution did not stop at this point and as knowledge of thermodynamic temperature improved, a series of practical temperature scales were

introduced. However, such changes introduce a small bias in long-term temperature records, which is mostly overlooked in meteorological literature. Therefore, the determination of the scale correction from 1927 to the present day is relevant when trying to estimate historical temperature trends.

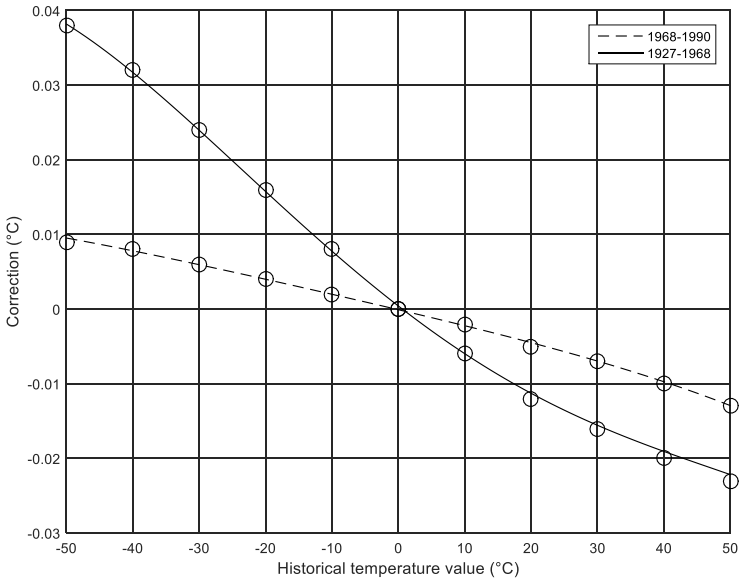

Figure 3. Corrections are necessary to adjust historical temperature data in order to be consistent with the modern temperature scale. The circles indicate the tabulated points from the BIPM documents describing the transforms from old scales to newer scales.

The difference in temperature scales that causes the problem in historical data analysis originates from the variety of interpolating instruments, scales temperature range, fixed points and mathematical equations, used to define the instruments output relation to temperature change. The net results is small, with changes in the range -20 °C to +20 °C being less than ±0.02 °C (figure 3), which is typical of the calibration uncertainty of meteorological thermometers. However, the result will show up as a bias when large numbers of thermometers

are averaged. A software tool was developed during the first phase (2011-2014) of MeteoMet [23], allows old temperature data series to be converted into ITS-90 values for a more robust comparability.

6.3.3. *Experimental sea temperature performed by fiber optics*

A new technique to perform traceable temperature measurements in seawater was studied, designed, developed and tested in field by CEM, CSIC and UPC [24, 25].

The thermometers consist of several FBGs installed at different points along the optical fibers. One fiber has 3 points of measurement and the other one has 10 points of measurement. The FBGs are written on single mode optical fiber SM-ITU652 coated with acrylate. The fiber is placed inside a ¼" x 0.35 mm wall thickness, 316L stainless steel tube, in order to protect the fiber optics from the corrosive environment of seawater, as well as to give robustness to the system. The final encapsulation is done with a layer of polypropylene/PEEK with resistance to seawater. Seawater temperature profile and the sea surface temperature were measured in the submarine observatory (www.obsea.es) (figure 4) and the devices examined for check the drift over the exposure lifetime.

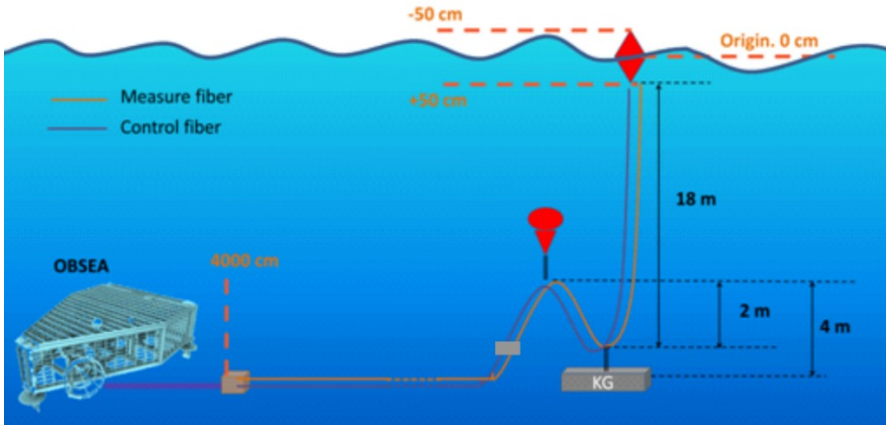

Figure 4. Design of the on-site experiment

In order to correlate the temperature with the reflected wavelength by each Bragg gratings, the fiber optics were calibrated as thermometers. The calibration results of one assembled fiber optic is shown in Figure 5.

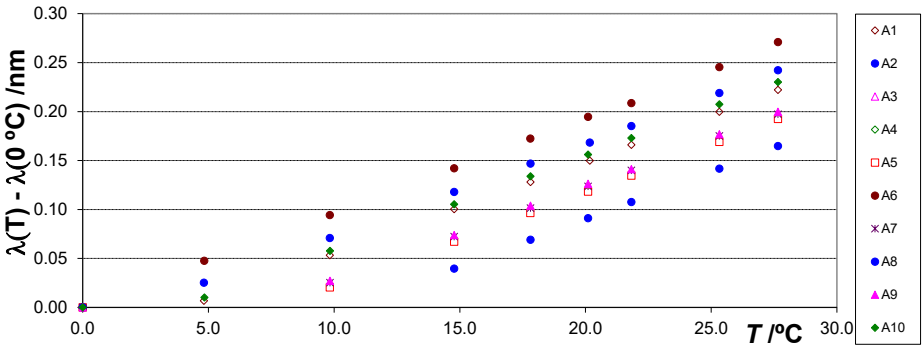

Figure 5. Calibration results of the fiber Bragg grating calibrated as a thermometer.

6.3.4. *Calibration of conductivity, temperature and depth sensors*

The temperature sensors located in submarine observatory for the measurement of salinity, temperature and depth (Conductivity, Temperature and Depth, CTDs) were calibrated at CEM. Specifically, Sea-Bird Electronics, models 16plus and 37SMP (with dimensions, 808 x 136 x 103 mm and 564 x 103 x 67 mm, respectively). These instruments are currently in use in the OBSEA submarine observatory. Due their dimensions, a large calibration bath was designed, assembled and characterized at CEM. The bath shows a stability and uniformity of 35 mK in the calibration range (0 - 30) ºC of the CTDs. A calibration procedure was developed with a complete calibration uncertainty model [26].

6.3.5. *Self-heating effect of temperature sensors*

An important issue to be considered among the uncertainty budget components of air temperature measurements is the self-heating of

resistance sensors. This influence is usually determined in calibration laboratories under fixed conditions of temperature, humidity and air speed. These conditions are highly variable when the thermometer is performing measurements on site and under real environmental conditions. In addition, the resistance thermometers sometimes are used with different measuring currents during their calibrations.

CEM evaluated the correction of the self-heating effect of some resistance thermometers used for meteorological and climate applications. The dependence of the self-heating effect with electrical current, temperature and surrounded environment was analysed.

Figure 6 shows the dependence of self-heating effect with the surrounding medium, as well as the dependence with the electrical current applied to the platinum resistor for one of the evaluated thermometer.

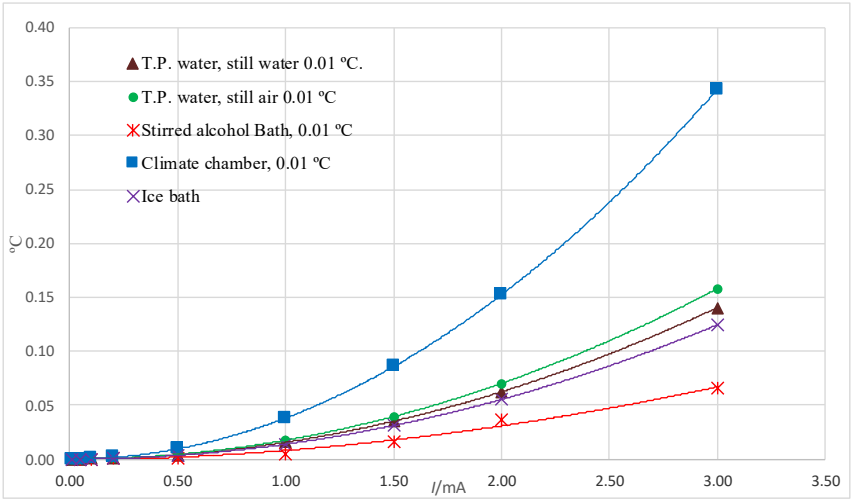

Figure 6. Dependence of the self-heating effect in a PRT with the electrical current applied to the resistance sensing element of the thermometer and dependence of the self-heating effect with the medium surrounding the thermometer

The self-heating effect depends on the design of the Platinum Resistance Thermometer (PRT), it changes with the square of the electrical current

applied to the resistance element of the thermometer and it changes strongly with the surrounding environment. [27, 28].

Moreover, CMI evaluated the self-heating effect under different wind speeds of four temperature sensors in the wind tunnel developed at INRiM laboratories (figure 7).

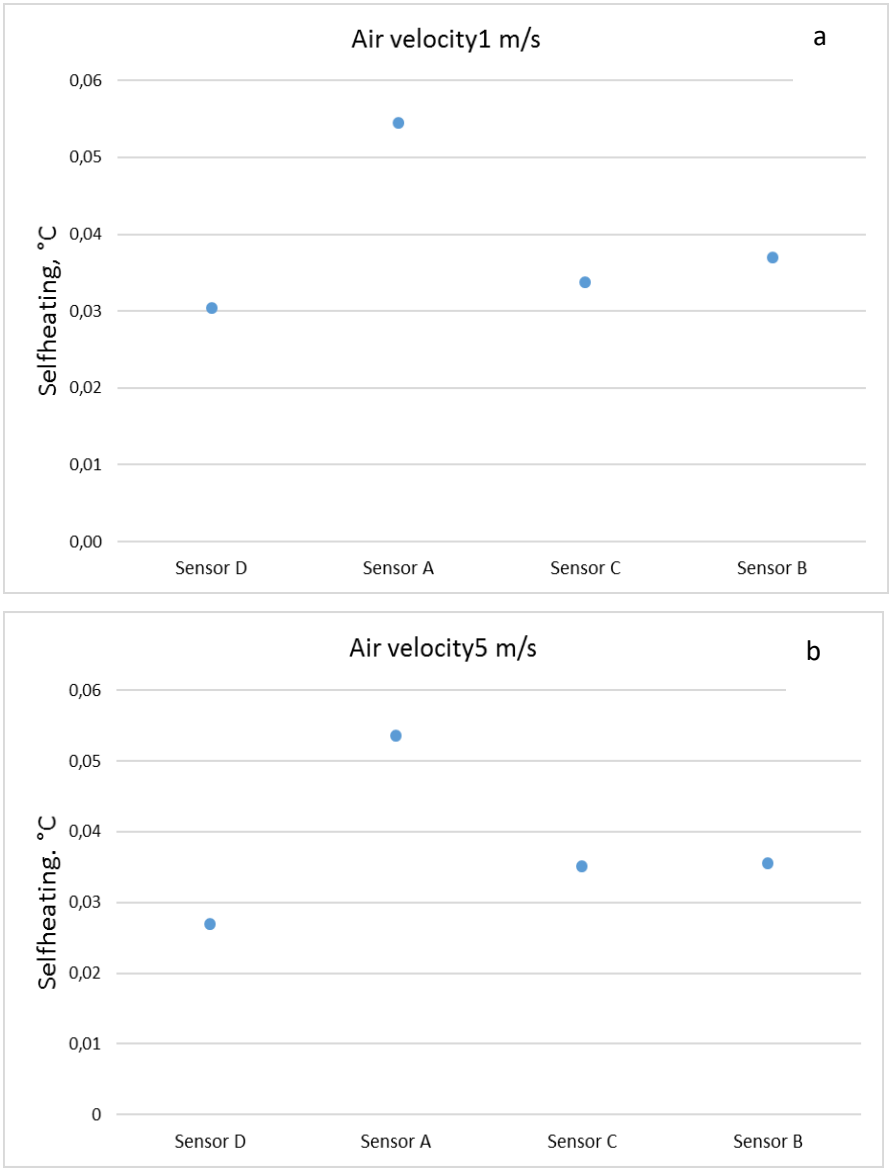

Figure 7. Self-heating effect under different wind speeds at 1 ms^{-1} (a) and 5 ms^{-1} (b)

6.3.6. *Evaluation of the hysteresis effect of some meteorological thermometers*

The hysteresis effect, the characteristic of a delayed reaction system to the applied stresses and in dependence on the previous state, was evaluated in a set of thermometers used in meteorological and climate application [29]. Two different methods were applied: in the first one the thermometers were exposed to a cycle of temperature increasing variation from 10 ºC to 50 ºC and, in a second stage, to temperature decreasing from 50 ºC to 10 ºC (Figure 8). Readings of the thermometer were taken at several intermediate points of the cycle.

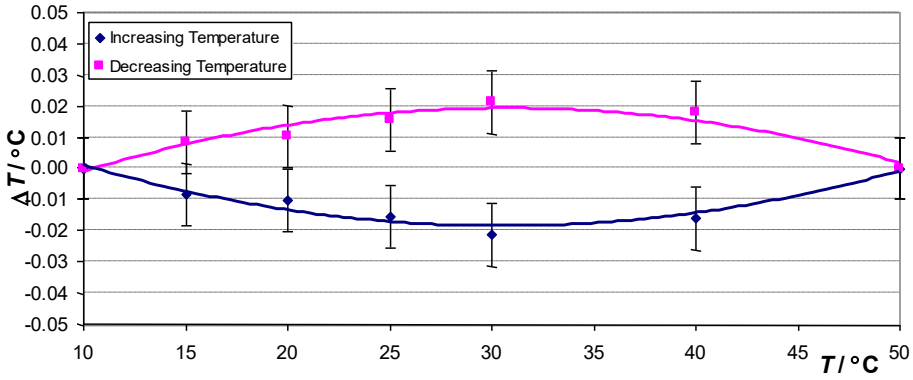

Figure 8. Hysteresis effect of a Pt100 measured in a stirred liquid bath. Complete cycle (10 ºC and 50 °C).

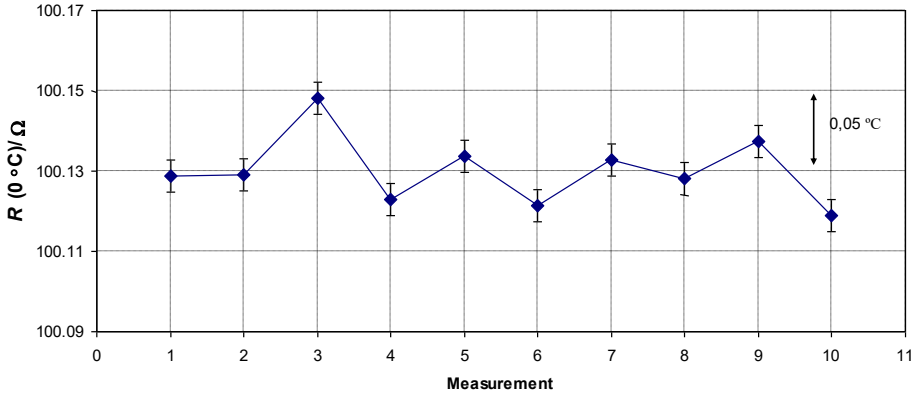

Figure 9. Hysteresis effect of a Pt100 measured in an ice bath, after exposure to extreme temperatures (-60 ºC and 50 ºC)

In the second method, the thermometers were checked at the ice melting point of water after their exposure to 10 ºC and to 50 ºC. For each extreme temperature, measurements were performed 5 times (figure 9).

From figures 8 and 9, it can be deduced that the evaluation of the hysteresis effect is similar by the two methods analysed, even though the first one was more time consuming.

6.3.7. *Response time of hygrometer*

The dynamic response of hygrometer was barely investigated in past studies. Often, manufacturers give an indication of the response time of the sensing element itself for a given temperature level. The response time at 63 %rh, or sometimes at 90 %rh, represents the length of time required, to the instrument, for reaching 63 %rh, or 90 %rh, of the final value that will be reached in steady state regime. In order to investigate response time behaviour of hygrometers, LNE-CETIAT has developed a facility composed by humid air generator associated to a divider plate and a testing chamber set in a climatic chamber (see figures 10 and 11). The divider plate is equipped with high-speed valves allowing switch from one humidity measurement to another in few hundreds of milliseconds. The climatic chamber enables to perform measurements at different temperature levels. This facility allowed to apply a humidity steps to the device under calibration, is called DUC.

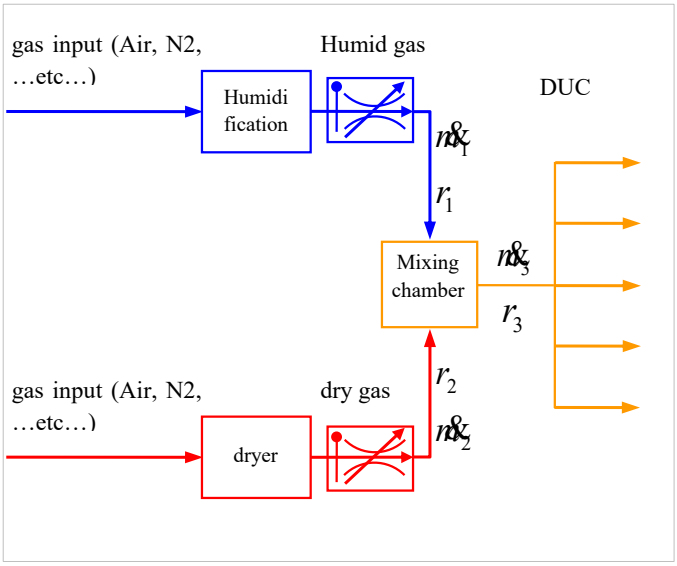

Figure 10. Schematic drawing of humid air generator based on dilution principle

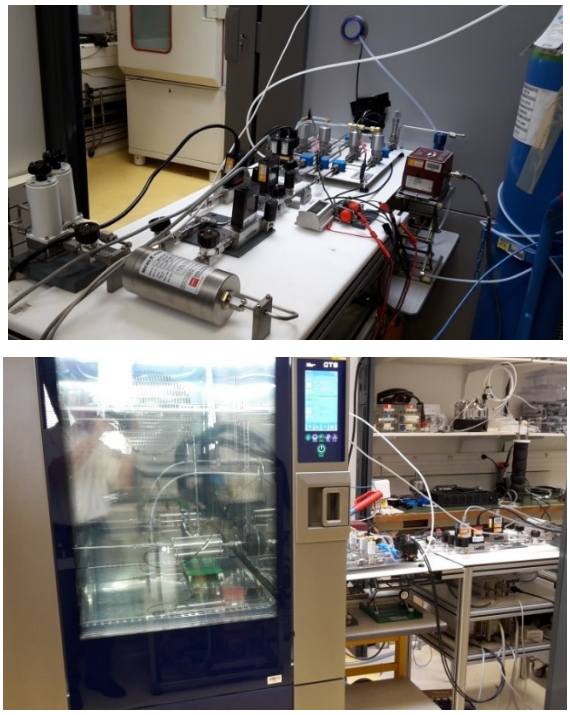

Figure 11. Overview of facility, from the left to the right, humid air generator, divider plate, climatic chamber with testing chamber

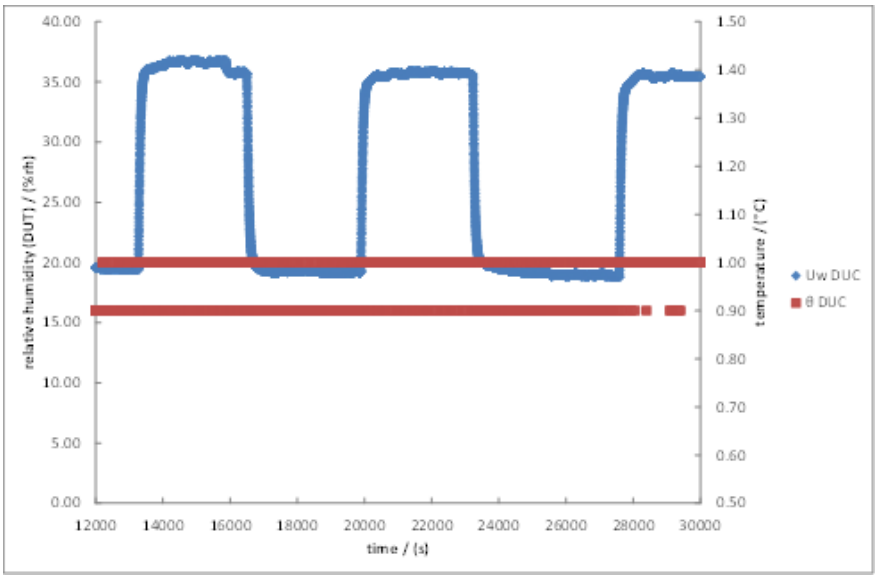

Figure 12. Humidity and temperature measured by DUC

As presented on Figure 12, humidity steps measured by DUC are recorded as well as temperature with an acquisition period of 1 point per second. Changes in humidity do not affect temperature stability, which remains within 0.1 °C. Thanks to the position transducer, it is possible to detect the time at which valves have commuted, that is to say the time at which humidity has changed from one level to another.

Table 1 presents results obtained for one hygrometer, equipped with its own filter, set at two different temperature levels: -10 °C and 10 °C. For each temperature level, measurements were repeated three times. Measurements seem to be more reproducible at higher temperature than at lower temperature. Nevertheless, the scattering could be also related to the filter surrounding the DUC or detection steady state value. From these preliminary results, it appears that response time is decreasing when surrounding temperature is increasing and response time is smaller when humidity change is increasing than when humidity change is decreasing.

Table 1. Results obtained for one hygrometer set at two different temperature levels

	Temperature -10 °C	Temperature 10 °C
$t_{90\%}$ (s) increasing humidity	324	148
	333	158
	353	158
$t_{90\%}$ (s) decreasing humidity	364	199
	380	192
	374	204

6.3.8. *Permafrost sensor dynamic*

The dynamic temperature response of permafrost sensors from different manufacturers, types and constructions is a matter of some interest. Permafrost temperature measurements are currently reported without associated uncertainties, making the information difficult to evaluate in metrological terms. Therefore, knowing the dynamic response of the sensor is relevant to complete the uncertainty budget. Sensor dynamic gives to the user valuable information, which can significantly affects the decision on frequency of recording. Overestimating or underestimating the recording times can affect temperature measurements in such a way that the daily maximum and minimum values most likely be unrecorded.

Four types of sensors were tested in laboratory conditions. The dynamic response was tested by exposition to a shock temperature change from -30 °C to 30 °C and from 30 °C to -30 °C. The test was performed in air, with no ventilation, to better represent the measurement conditions in the permafrost boreholes. The introduction of sensors to a temperature shock began after their indicated temperature was stable for a minimum of 10 min. Then, the equilibrium time was measured together with the behaviour

of the sensors temperature output and a minimum of five runs were performed. The temperature conditions were monitored by a calibrated reference PRT. The thermal shock was also conducted in a reversed order to see if there was any difference in their response time. Figure 13 shown a typical dynamic test result. It can be observed how fast the sensor achieve equilibrium and the typical curve of sensors temperature output. In general, a steeper curve is preferred, meaning a shorter equilibrium time. This predetermines the sensor for more dynamic measurements as well as for slower changing temperature processes.

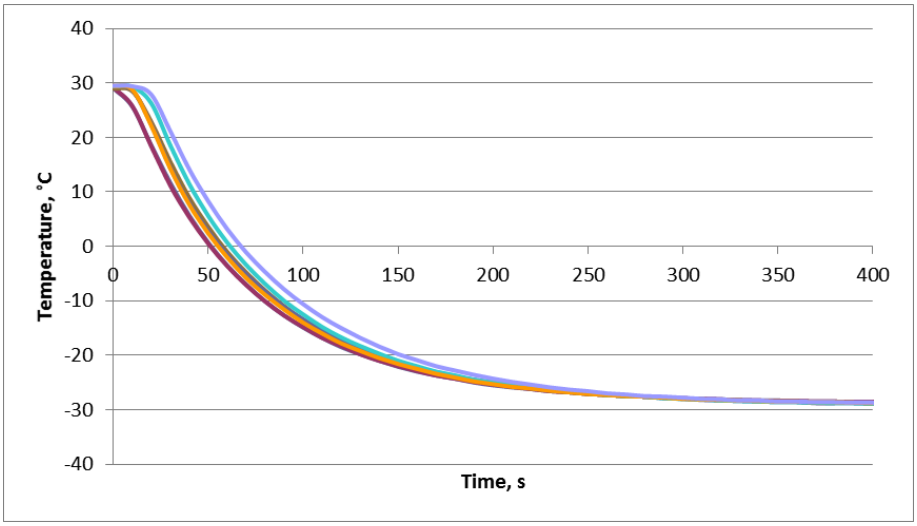

Figure 13. Repeated permafrost sensors (marked - M) reaction to a thermal shocks generated by a rapid temperature drop from 30 °C to -30 °C. According to the sampling frequency used by the involved datalogger, this curve can be used to include the sensors response time in the uncertainty budget

The measurements are still on-going and their results are intended to determine an uncertainty budget component into the permafrost measurements originating from this sensor property, in order to create a best practice document to help the end users to determine a specific permafrost sensor dynamic.

6.4. Conclusions and prospects

6.4.1. *Conclusions*

Started as a Joint Research Project, MeteoMet has extended its activities and structure, towards an established and robust collaboration among its participants. The Consortium now groups more than 50 partners: National Metrology Institute, Universities, Manufacturers and private Companies, hydro-meteo Agencies, Research Institutes, Climatologists and International Institutions. Several signs of having made this collaboration effective can be found in the numerous experiments now running and delivering scientific results, as well as in the many events held and planned by the MeteoMet Community and even in the participation of MeteoMet staff in key world institutions.

This project, which aims were to develop metrological traceability for the measurement of main ECVs defined by GCOS and the evaluation of calibration uncertainties, is structured in three work packages each covering a different area of observation: Air, Sea and Land.

The MeteoMet consortium intends to extend the investigations to other variables and at evaluating further aspects and contributions to the uncertainty. The purpose is to make a further step towards the final goal: the evaluation of the overall measurements uncertainties for the quantities involved in the meteorological observations and climate change evaluations. The improvement of quality of ECVs recorded data through the inclusion of measurement uncertainty budget will bring to possible strategies for the reduction of the uncertainty.

6.4.2. *Impact*

Beyond the MeteoMet tasks, an immediate benefit was launched organising ILC with two loops using this protocol developed within the MeteoMet2 project. The ILC protocol and Final Report on

intercomparison in the field of temperature, humidity and pressure MM-ILC-2015-THP was submitted to the WMO and published as Instruments and Observing Methods WMO-IOM report. It is now planned that the ILC will be extended also to WMO regions RA II and RA Vin 2018. The results of all potential ILCs can be linked to the results in the European region (RA-VI) enabling comparability of meteorological laboratories from different regions.

World leading manufacturers – such as Rotronic and Vaisala – will use the calibrations and tests performed within the framework of the MeteoMet project to improve their instruments. The GCOS Reference Upper-Air Network (GRUAN), WMO CIMO, WMO Commission for Climatology CCl, and the International Surface Temperature Initiative were kept regularly updated on the project results by teleconferences. Hydro-meteorological agencies and local environmental services – such as, the MeteoSwiss (Payerne research site), UK MetOffice, ARSO (Slovenia), ARPA (Piemonte, Val d'Aosta - Italy), Società Meteorologica Italiana (Italy), and European Meteorological Society – were updated on the project results by dedicated meetings.

The project International Conference on "Metrology for Meteorology and climate" (MMC), launched by MeteoMet in 2014 [30] is now recognized worldwide as a reference event in this interdisciplinary field. The MMC-2016 was held in conjunction with WMO CIMO Technical Conference (TECO) for a full week of presentations, satellite meetings and presence at the Meteorological Technology World Expo in Madrid. The MMC-2019 is already planned together with Tempmeko and Tempbeijing, in Beijing, China.

The project results are moreover expected to contribute to the improvement of:

- ISO 17714:2007 and CCT[2] Task Group for Guides on Thermometry (CCT-TG-GoTh) and Working Group for Humidity (WG-Hu);
- ISO/TS 17892-1:2004 and ISO 11271:2002 on Soil moisture;
- CIMO guide 8 revision;
- European Earth Observation Programme "Copernicus"[3];
- PermaNET network[4].

6.4.3. *Further work*

Among the numerous activities, some key studies and researches are planned to be continued by NMIs in collaboration with the key stakeholders, also beyond the official lifetime of the JRP. In particular, the studies on the full evaluation of field measurement uncertainties will be continued for cryosphere observations and extreme environmental conditions, such as high Alps and the Arctic. Measurements of ECVs in the Arctic are performed under numerous research initiatives, stations and groups, generating an increasing amount of data, recorded by a multitude of instruments and installations. For example, cryosphere systems like permafrost are very sensitive to the exchange of energy between soil and atmosphere. Homogenised and traceable procedures of measurement are desirable and needed in order to produce comparable data. The evaluation of field measurement uncertainties is also a challenging aspect, and standard calibration procedures, available from calibration services, do not fully represent real measurement conditions. In the 2015 Arctic Circle

[2] *Comité Consultatif de Thermométrie* (Consultative Committee for Thermometry)

[3] http://www.copernicus.eu/

[4] http://www.permanet-alpinespace.eu/home.html

Assembly and the 2015 NySMAC[5] meeting, the contribution from the metrology community in addressing such issues was identified to be of urgent importance, and an action towards the creation of a metrological infrastructure was included as a priority in the Flagship Programme on Atmospheric Research.

The proposed research extends the underpinning metrology developed during the MeteoMet EMRP projects, which included an "Arctic Metrology Campaign", performed in 2014 in Ny-Ålesund [14]. The benefit of having calibration devices available on site was acknowledged by the research community in Ny-Ålesund, with the proposal of starting a collaboration towards the realisation of a permanent calibration laboratory on Svalbard [31]. Beside the arctic initiatives, the activities related to supporting Global Cryosphere Watch WMO programme also include the implementation of an Alpine open-air laboratory, for testing, comparing and evaluating instrumental performances and for adopting metrology techniques to evaluate field measurement uncertainties under the harsh environmental conditions experienced across the three key climate regions. One of the goal is the study and definition of standard installations for the evaluation of glaciers mass balance.

Land ground-based stations continue to play a key role in the measurement of ECVs for the generation of data series, to detect long-term climate evolution. To reach full reliability and comparability in different places and different times, measured records need documented traceability to the SI and uncertainty evaluations. These metrological aspects are fundamental when measurement sites and stations are designed to provide

[5]Ny-Ålesund Science Managers Committee (NySMAC) was established to enhance cooperation and coordination among researchers and research activities in Ny-Ålesund – Svalbard.

reference-grade data. The MeteoMet consortium intends to promote the definition and features of reference-grade ground-based observing stations, also by comparing existing solutions, in terms of instruments capabilities, procedure to establish full documented traceability and target uncertainty. This activity will be in line with the planned creation of a Global Surface Reference Network by GCOS.

The philosophy behind the definition of the metrological requirements for a reference-level surface observing system could also be used for other purposes, and for other networks, such as the stations recognized by the WMO Global Cryosphere Watch programme or those in urban areas, or for agricultural applications.. When top-level requirements are defined, downgrading the specification to baseline networks can lead to a better classification of sites, thus improving the current siting classifications under a cost-efficient approach.

Key improvements of this proposal with respect to the state-of-the-art can be summarized as it follows:

- a unique definition of reference-grade climate records, in terms of target measurement uncertainty, measurement method and instrument characteristics, and documented traceability to SI;
- highest quality installations, as reference observing stations in distributed networks;
- improvement in site classification and sustained performances classification guides;
- a contribution in the renewal process for historical and centennial stations;
- a preliminary contribution for the definition of reference urban and agricultural stations;

- a contribution in future actions, towards the creation of a European global climate reference network.

At the time of the submission of this article, the mentioned actions are being considered, to establish continuity in this fruitful collaboration between the metrology and meteorology/climatology communities. The creation of Joint Research Units and Joint Research Laboratories is also being discussed within MeteoMet partners. Such distributed centres aim at becoming references for delivering high-quality research and services for potential stakeholders needing to deliver more robust data. Such joint initiative are being drafted by project partner and collaborators, to create consortia where all participating partners can contribute in developing specific areas of metrology to support those needs and deliver calibration services and dedicated procedures. This process will also try to avoid duplication and make well-identified distributed centres as references for data quality to be promoted within the EURAMET creation of European Metrology Networks.

The general vision of this project and the associated initiatives is to establish permanent liaisons between the involved communities, for better environmental and climate knowledge and benefit to the present and future generations of operators and scientists. It will also imply the possibility of performing stronger validation and realistic quantification of the climate models, climate change and climate predictions in a global view, as well as their use for other scientific studies related to the understanding of Earth's evolution and most importantly contributing to Earth's survival.

6.5. Acknowledgments

This work is being developed within the frame of the European Metrology Research Program (EMRP) joint research project ENV07 and ENV58

"METEOMET". The EMRP is jointly funded by the EMRP participating countries within EURAMET and the European Union.

6.6. References

[1] GCOS-184, GTOS-76, WMO-TD/No. 1523 2010 Update. Implementation plan for the Global Observing System for Climate in Support of the UNFCCC World Meteorological Organization, 2010

[2] Merlone A, Lopardo G, Antonsen I, *et al* 2012, A new challenge for meteorological measurements: The "MeteoMet" project - Metrology for meteorology, *AIP Conf. Proc.* **1552** 1030-1035; Proceedings of the International Temperature Symposium, 19–23 March 2012, Los Angeles

[3] Merlone A, Lopardo G, Sanna F, *et al*, 2015 The MeteoMet project – metrology for meteorology: challenges and results, *Meteorol. Appl.* **22** 820-829 DOI: 10.1002/met.1528

[4] Sairanen H, Heinonen M and Högström R, 2015. Validation of a calibration set-up for radiosondes to fulfil GRUAN requirements, *Meas. Sci. Technol.* **26** 105901

[5] Underwood R, Gardiner T, Finlayson A, Bell S and de Podesta M. 2017. An improved non-contact thermometer and hygrometer with rapid response. *Metrologia* **54**(1) S9-S15

[6] Guide to Meteorological Instruments and Methods of Observation, WMO-No. 8, 2008 edition, update 2010

[7] Lopardo G, Bertiglia F, Curci S, Roggero G and Merlone A 2014, Comparative analysis of the influence of solar radiation screen ageing on temperature measurements by means of weather stations, *Int. J. Climatol.***34(4)** 1297–1310, DOI: 10.1002/joc.3765

[8] Bojkovski J, Hudoklin D, Groselj D, Drnovšek J, Begeš G. 2016. How to prepare ILC - case study meteorological laboratories. V: Begeš G, et al. Book of abstracts: MMC 2016, International Conference on Metrology for Meteorology and Climate, September 26-29, Madrid, Spain, pp. 32

[9] Groselj D, Bojkovski J, Begeš G. 2016. Concept of Interlaboratory Comparison in RAVI. V: WMO TECO 2016, 27-30 September 2016, Madrid, World Meteorological Organization, pp. 1-6

10] International Organization for Standardization, 2010, ISO/IEC 17043 - Conformity assessment -- *General requirements for proficiency testing*, April 2010

[11] Lopardo G, Bellagarda S, Bertiglia F, Merlone A, Roggero G and N Jandric 2015, A calibration facility for automatic weather stations, *Meteorol. Appl.* **22** 842-846, DOI: 10.1002/met.1528

[12] Vuillermoz E, Verza G, Cristofanelli P, Bonasoni P, Roggero G and Merlone A 2014 QA/QC Procedures for in-Situ Calibration of a High Altitude Automatic Weather Station: The Case Study of the AWS Pyramid, 5050 m a.s.l., Khumbu Valley, Nepal. *Atmospheric and Climate Sciences* **4** 796-802. DOI: 10.4236/acs.2014.45070

[13] Merlone A, Roggero G and Verza G P 2015 In situ calibration of meteorological sensor in Himalayan high mountain environment, *Meteorol. Appl.* **22** 847-853, DOI: 10.1002/met.1528

[14] Musacchio C, Bellagarda S, Maturilli M, Graeser J, Vitale V, Merlone A 2015, Arctic Metrology: calibration of radiosondes ground check sensors in Ny-Ålesund, *Meteorol. Appl.* **22**854-860, DOI: 10.1002/met.1528

[15] Thorne PW, Menne, MJ, Willliams CN *et al.*, 2016 Reassessing changes in diurnal temperature range: A new data set and characterization of data biases. *J. Geophys. Res. Atmos*. **121** 5115-37 DOI: 10.1002/2015JD024583

[16] Bertiglia F, Lopardo G, Merlone A, Roggero G, Cat Berro D, Mercalli L, Gilabert A, Brunet M 2015. Traceability of Ground-Based Air-Temperature Measurements: A Case Study on the Meteorological Observatory of Moncalieri (Italy), *Int. J. Thermophys* **36(2-3)** 589-601, DOI: 10.1007/s10765-014-1806-y

[17] Sanna F, Cossu Q A, Roggero G, Bellagarda S and Merlone A. 2014 Evaluation of EPI forecasting model for grapevine infection with inclusion of uncertainty in input value and traceable calibration *Ital J Agrometeorol*, **19(3)** 33-44, DOI: 10.13140/2.1.2524.0644

[18] Sanna F, Calvo A, Deboli R, Merlone A. 2017. Vineyard diseases detection: a case study on the influence of weather instruments calibration and positioning. *Meteorol. Appl.* **25(1)** DOI: 10.1002/met.1685

[19] Santana MAA, Guimarães PLO, Lanza LG and Vuerich E 2015. Metrological analysis of a gravimetric calibration system for tipping-bucket rain gauges. *Meteorol. Appl.* **22** 879-885

[20] GCOS, 2013: The GCOS Reference Upper-Air Network (GRUAN) GUIDE Technical Report no. 2013-03, GCOS-171, version 1.1.0.3 pp. 122

[21] Lakka A, Sairanen H, Heinonen M and Högström R, 2015.Comsol-simulations as a tool in validating a measurement chamber, *Int J Thermophys.* **36** 3474–3486 DOI: 10.1007/s10765-015-2000-6

[22] Sairanen H, Heinonen M, Högström R, Lakka A and Kajastie H, 2014: A Calibration System for Reference Radiosondes that Meets GRUAN Requirements. *NCSLI Measure J. Meas. Sci.* **9** 56-60.

[23] Pavlasek P, Merlone A, Musacchio C, Olsen AAF, Bergerud RA and Knazovicka L, 2016 Effect of changes in temperature scales on historical temperature data, *Int. J. Climatol.* **36(2)** 1005-1010**,** DOI: 10.1002/joc.4404

[24] Garcia Benadí A, del Río Fernandez J, Nogueras Cervera M, Garcia Izquierdo C, del Campo D, Hernández S, 2016 Optical fibers to measure temperature vertical profile at sea. International Workshop on Marine Technology. Vilanova i la Geltrú: Sarti, 2016 p. 34

[25] C. García Izquierdo, A. Garcia-Benadí, P. Corredera, D. del Campo, S. Hernandez, J. del Río Fernandez, M. Nogueres-Cervera, C. Pulido de Torres. 2017 Traceable Sea Temperature measurements performed by Optical fibers. *IMEKO International Conference on Metrology for The Sea* (*submitted*)

[26] García Izquierdo C, del Campo D, Hernandez S, Gonzalez A, Garcia-Benadí A, del-Río-Fernández J, Nogueras-Cervera M. 2016. Calibration Uncertainties of CTDs in a large volume calibration bath. Book of abstracts: *MMC 2016*, International Conference on Metrology for Meteorology and Climate, September 26-29, Madrid, Spain, pp. 41

[27] C. García Izquierdo, L. Šindelářová, S. Hernández, A. González, R. Strnad. Evaluation of the environment and the radiation shield influence on the self-heating effect of meteorological temperature sensors. Book of abstracts: *MMC 2016*, International Conference on Metrology for Meteorology and Climate, September 26-29, Madrid, Spain, pp. 4

[28] C. García Izquierdo, S. Hernández, A. González, L. Matias, L. Šindelářová, R. Strnad, D. del Campo. 2017 Evaluation of the Self-heating effect of several resistance thermometers used in meteorological and climate applications (*submitted*).

[29] C. García Izquierdo, D. del Campo, S. Hernandez, A. González. Evaluation of the Hysteresis effect of some meteorological thermometers. Book of

abstracts: *MMC 2016*, International Conference on Metrology for Meteorology and Climate, September 26-29, Madrid, Spain, pp. 40.

[30] Merlone A, Musacchio C and Sanna F 2015. The Metrology for Meteorology Conference: MMC 2014, *Meteorol. Appl.* **22** 817-819, DOI: 10.1002/met.1548

[31] Musacchio C, Merlone A, Viola A, Vitale V and Maturilli M 2016.Towards a calibration laboratory in Ny-Ålesund, *Rend. Fis. Acc. Lincei* **27(1)** 243-49 DOI 10.1007/s12210-016-0531-9

6.7. Annex 1. MeteoMet summary data, partners and collaborators

Table 1. MeteoMet summary data

JRP start date and duration:	1 October 2011, 36 + 36 months
Budget: Number of planned deliverables Total person month equivalent (including grants)	> 11 M€ 350 Approx. 1000
JRP-Coordinator:	Dr Andrea Merlone, INRiM
JRP website address	http://www.meteomet.org

Table 2. MeteoMet Partners and Granted Institutions

Acronyms	Name	Nationality
Funded Partners		
INRiM	Istituto Nazionale di Ricerca Metrologica (acting as JRP-Coordinator for the JRP-Consortium)	Italy

BEV/PTP	Physikalisch-Technischer Pruefdienst des Bundesamt fuer Eich- und Vermessungswesen	Austria
CEM	Centro Espanol de Metrologia	Spain
CETIAT	Centre Technique des Industries Aerauliques et Thermiques	France
CMI	Cesky Metrologicky Institut Brno	Czech Republic
CNAM	Conservatoire National des Arts et Metiers	France
CSIC	Agencia Estatal Consejo Superior de Investigaciones Cientificas	Spain
DTI	Teknologisk Institut Denmark	Denmark
GUM/MG	Ministerstwo Gospodarki	Poland
IMBiH	Institut za mjeriteljstvo Bosne i Hercegovine	Bosnia and Herzegovina
INTA	Instituto Nacional de Tecnica Aeroespacial	Spain
SMU	Institut Niskich Temperatur i Badan Strukturalnych	Poland
JV	Justervesenet	Norway
MIKES/VTT	Mittatekniikan Keskus/ Teknologian tutkimuskeskus	Finland
NPL	National Physical Laboratory	United Kingdom
PTB	Physikalisch-Technische Bundesanstalt	Germany
SMD	Federale Overheidsdienst Economie, KMO, Middenstand en Energie	Belgium
SMU,	Slovensky Metrologicky Ustav	Slovakia
SP	SP Sveriges Tekniska Forskningsinstitut AB	Sweden
TUBITAK/UME	Türkiye Bilimsel ve Teknolojik Araştirma Kurumu/Ulusal Metroloji Enstitusu	Turkey
UL	Univerza v Ljubljani	Slovenia

VSL	Van Swinden Laboratorium B.V.	Netherlands
Unfunded Partners		
Chalmers	Chalmers tekniska hoegskola AB	Sweden
SHOM	Service hydrographique et océanographique de la Marine	France
UWr	Uniwersytet Wrocławski	Poland
Research Excellent Grant/ Research Mobility Grant		
REG(AU)	Aahrus Universitet,	Denmark
REG(C3)	Universitat Rovira i Virgili, Centre for Climate Change	Spain
REG(EV-K2 CNR)	EV-K2 Consiglio Nazionale delle Ricerche	Italy
REG(IMAMOTER-CNR)	Istituto per le Machine Agricole e MOvimento TERra – Consiglio Nazionale delle Ricerche	Italy
REG(KIT)	Karlsruhe Institut für Technologie	Germany
REG(UniGe)	Università degli Studi di Genova	Italy
REG(UniNa2)	Seconda Università degli Studi di Napoli	Italy
REG(UPC)	Universitat Politècnica de Catalunya	Spain
RMG(FSB)	Fakultet Strojarstva I Brodogradnje	Croatia
RMG(INBiH)	Institut za mjeriteljstvo Bosne i Hercegovine	Bosnia and Herzegovina
RMG(INTiBS)	Institut Niskich Temperatur i Badan Strukturalnych	Poland
RMG(MBM)	Montenegrin Bureau of Metrology	Montenegro
RMG(SMU)	Slovensky Metrologicky Ustav	Slovakia

7. Conclusions and future works

7.1. Conclusion

In this study, the forecasts provided by the epidemiologic model with input data inclusive of uncertainty gathered from calibrated sensors, overlapped around the estimate period of infection, confirmed that the inclusion of calibration uncertainties produces more reliable and accurate data. Moreover, the inclusion of the instrument positioning contribution affected disease prediction up to five days. This can be explained by the effect of the distance and the vine canopy's spatial arrangement, which tended to alter the vineyard's microclimate.

As far as the study on the measurement of meteorological parameters in protected cultivation is concern, the absence of UV-B radiation affects growth and leaf index area but, at the same time, it might have influenced the susceptibility of plants to mite infections. The presence of UV-B radiation, on the other hand, affects temperature and relative humidity, increasing and reducing their values respectively, that in turn affected the anthesis fruit set. Temperature values obtained from the data to which the calibration curves were applied and associated with the calibration uncertainty, were higher than the values obtained from data without application of the curve and the uncertainty, vice versa for relative humidity values. Moreover, the high temperature recorded, over 40 °C, changed the transmissive feature of the covering material and, as a consequence, the morphological characteristics of tomatoes in turn changed.

Calibration procedures and instrument positioning are important factors in agrometeorology, although further in-depth studies are needed in this field. Measurements should be based on fully documented traceability and

forecasting models should include measurement uncertainties in their input values to improve output data accuracy.

Further studies are also needed to evaluate the measurement uncertainties of meteorological parameters that can be translated in percentage uncertainties on the productivity of the agricultural products and can contribute in the assessment of the product quality, through characterization of the crop with health promoting compounds.

The positive impacts of this study were various:

- Environmental Impact: the study aimed to improve the availability of reliable data from weather observations in agricultural fields and the related studies on the epidemiological forecasting models, to contribute to the study of climate change and its impact and the adaptation of plants. This research concerned a crucial issue, given the growing attention of the international scientific community to the importance of a metrological approach as applied to agricultural needs (GCOS-200, 2016).
- Agricultural and biological impact: the study of the effect of the uncertainties in agricultural field might bring an improvement to the more widely used epidemiological forecasting models, and can lead to better adoption of measurement techniques and appropriate instruments selection.
- Financial Impact: more accurate forecasting models in conjunction with traceable meteorological data can improve the parameters for plans treatments, thus directly saving funds thanks to more reliable decision processes.

7.2. Future works

To reach full reliability and comparability in space and time, measured records need documented traceability to the SI and uncertainty evaluations. These metrological aspects are fundamental when measurement sites and stations are designed to provide reference data.

Air temperature trend analysis is mainly based on data archives, generated as temporal collection of measurements gathered from meteorological observations. For agricultural observations, obtaining meaningful values is a difficult task due to local- and micro-scale environmental variability. To date, no reference exists for a correct installation and management of agrometeorological stations and sensors.

The *Guide to Agricultural Meteorological Practices* n. 134 of the WMO (2010), gives valuable information on basic aspects of agrometeorological observations, among others, provides guidelines on preparation for agrometeorological services and information for decision-makers, on meteorological data, their collections, presentation and statistical analysis. However, there is a lack of metrological approach on data analysis, instrument calibration and traceability and uncertainty evaluations.

The establishment of the metrological requirements for the agrometeorological services and observing systems might allow to improves the accuracy in monitoring of local meteorology changes. If these metrological requirements are used in the creation of a reference surface-based observing network, the measurements performed at different times and sites would be reliably comparable since all measurements would be traceable to the SI. It will imply the possibility of performing stronger validation and realistic quantification of the

agrometeorology models and meteorological predictions in a global view, as well as its use for other scientific studies related to the agriculture.

Another field of application of metrology in the agro-food field is the accurate measurement of soil moisture as a support for irrigation. With the persistence of drought in the soil, the concentration of the abscisic acid phytohormone in the roots increases, which through the xylematic flow is translocated in the leaves and forces the stomatal openings to close. This process in the roots imposes to the plant a more economical use of water. With increasing water stress, photosynthesis is reduced, consequently vegetative growth will be reduced, as well as a reduced development of the fruit and its soluble solids composition.

Reduced or redundant supplies of water can have a negative impact on both the production and the phytosanitary status of the plant (Petroll *et al.,* 2012). The decision of what is the most appropriate time to irrigate and the amount of water needed to be made is mainly based on field observations, using various types of sensors to measure soil moisture. Various types of sensors are available to measure soil moisture, which measure the water content (% by volume) or the availability of water (matrix potential).
Taking into account the shortage in the periodic calibration of the instruments and in the evaluation of the components of the calibration uncertainties, studies are needed on the evaluation of the measuring instruments and the improvement of the measures of the soil moisture, for a better management of the water supply to the crops.
Furthermore, metrology could be a valid support for the study and the evaluation of an important parameter related the agriculture, such as the land-surface temperature and soil temperature, potential variables to be included in the list of the Essential Climate Variables (ECVs). An ECV is

a physical, chemical or biological variable or a group of linked variables that critically contributes to the characterization of Earth's climate as defined by the Global Climate Observing System (GCOS). As stated in its *Implementation Plan* (GCOS-200, 2016), GCOS is keen on observing additional parameter and addressing the new demands for climate information at a regional and local level. For land surface temperature in particular, this Plan specified that is an important variable for agriculture, vegetation and ecosystem modelling and that "*Engagement by the meteorological community with metrological institutes to improve traceability of the measurements to standards and improve uncertainty estimates is welcomed and should be maintained"*.

8. Literature cited

Actis A., Crovini L. 1982. Temperature: Its Measurement and control in Science and Industry, Ed. F. Schooley, American Institute of Physics, New York vol. 5: pp. 818-828

Adrian M., Jeandet P., Bessis R., Joubert J.M., 1996. Induction of phytoalexin (resveratrol) synthesis in grapevine leaves treated with aluminum chloride (AlCl3). *J. Agric. Food Chem*. 44: 1979-1981

Agarwal S.; Rao A.V. 2000. Tomato lycopene and its role in human health and chronic diseases. Can. Med. Assoc. J., 163: 739-744

Asami D.K., Hong Y.J., Barrett D.M., Mitchell A.E., 2003. Processing induced changes in total phenolics and procyanidins in clingstone peaches. Journal of the Science of Food and Agriculture 83: 56–63

Baldacci E., 1947. Epifitie di *Plasmopara viticola* (1941–46) nell'Oltrepò Pavese ed adozione del calendario di incubazione come strumento di lotta. Atti Istituto Botanico, Laboratorio Crittogamico, 8: 45–85

Bavaresco L., Pezzutto S., Gatti M. Mattivi F. 2007. Role of the variety and some environmental factors on grape stilbenes. *Vitis* 46 (2): 57–61

Baydar, N. G., Sagdic, O., Ozkan, G., & Cetin, S. (2006). Determination of antibacterial effects and total phenolic contents of grape (*Vitis vinifera*) seed extracts. International Journal of Food Science and Technology, 41, 799e804.

BBCH Monograph, 2001. Growth stages of mono-and dicotyledonous plants. Federal Biological Research Centre for Agriculture and Forestry, 2nd Edition, Ed. Uwe Meier, pp. 158

Benhamida A, Kaci M., Cimmino S., Silvestre C., Duraccio D. 2010. Evaluation of the Effectiveness of New Compatibilizers Based on EBAGMA-LDPE and EBAGMA-PET Master batches for LDPE/PET Blends, Macromol. Mater. Eng. 295: 222-232

BIPM, 2004. *What is metrology?* Celebration of the signing of the Metre Convention on 20 May 1875. The World Metrology Day 2004. https://web.archive.org/web/20110927012931/http://www.bipm.org/en/convention/wmd/2004

BIPM, JCGM 100:2008 Guide to the Expression of Uncertainty in Measurement. International Organization for Standardization, Geneva. ISBN 92-67-10188-9, First corrected and reprinted edition 1995. pp 134

BIPM, JCGM 200:2012. International vocabulary of metrology – Basic and general concepts and associated terms (VIM) Third Edition 2008. International Organization for Standardization, Geneva. pp. 108

Braun J., Tevini M., 1993. Regulation of UV-protective pigment synthesis in the epidermal layer of rye seedlings (*Secale cereale* L. cv. *Kustro*). Photochem. Photobiol. 57: 318–323

Briassoulis D., Waaijenberg D., Gratraud, J. von Eslner B. 1997. Mechanical Properties of Covering Materials for Greenhouses: Part 1, General Overview. Journal of Agricultural Engineering Research, 67: 81–96

Caffi, T., Rossi, V., Cossu, A., Fronteddu, F. 2007: Empirical vs. mechanistic models for primary infections of *Plasmopara viticola*. Bull. OEPP/EPPO 37, 261-271

Caldwell C.R., Britz S.J., Mirecki R.M., 2005. Effect of temperature, elevated carbon dioxide, and drought during seed development on the isoflavone content of dwarf soybean [*Glycine max* (L.) Merrill] grown in controlled environments. Journal of Agricultural and Food Chemistry 53: 1125–1129

Cao G., Sofic E., Prior R.L. 1997. Antioxidant and prooxidaant behavior of flavonoids: structure–activity relationships. Free Radic. Biol. Med. 22: 749–760

Charki A., Dollé V., Martin L., Himbert M. 2016 Metrology and quality management. In: The Mediterranean Region under Climate Change. IRD Éditions, Marseille, Sub-chapter 3.2.1 pp. 461-466

Charles M.T., Mercier J., Makhlouf J., Arul J. 2008. Physiological basis of UV-C-induced resistance to *Botrytis cinerea* in tomato fruit I. Role of pre- and post-challenge accumulation of the phytoalexin-rishitin. Postharvest Biology and Technology 47: 10–20

Chattopadhyay A, Chakraborty I., Siddique W. 2013. Characterization of Determinate Tomato Hybrids: Search for Better Processing Qualities. J Food Process Technol 4: 222

Clinton, S.K. 1998. Lycopene; chemistry, biology and implications for human health and diseases. Nutr. Rev. 56: 35–51

Crovini L., Actis A., Coggiola G., Mangano A. 1992. Temperature: Its Measurement and control in Science and Industry, Ed. F. Schooley, American Institute of Physics, New York vol. 6: 1077-1082

Del Corso G., Lercari B. 1997. Use of UV radiation for control of height and conditioning of tomato transplants (*Lycopersicon esculentum* Mill.). Scientia Horticulturae 71: 27-34

Van Ploeg D. Heuvelink E. 2005. Influence of sub-optimal temperature on tomato growth and yield: a review, The Journal of Horticultural Science and Biotechnology, 80:6, 652-659,

Dilara P.A., Briassoulis D. 2000. Degradation and Stabilization of Low-density Polyethylene Films used as Greenhouse Covering Materials. Journal of Agricultural Engineering Research, 76: 309–321

Dillard C., German B. 2000. Phytochemicals: nutraceuticals and human health. Journal of the Science of Food Agri-culture, 80: 1744–1756

Eitzinger J., Thaler S., Orlandini S., Nejedlik P., Kazandjiev V., Vucetic V., Sivertsen T.H., Mihailovic D.T., Lalic B., Dalezios N.R., Susnik A., Kersebaum C.K., Rossi F., Dalla Marta A., Nendel C., Vucetic V. 2008. In Survey of Agrometeorological practices and applications in Europe regarding climate change impact. Ed. Nejedlik and Orlandini pp 15-114

EPPO, 2000. European and Mediterranean Plant Protection Organization, EPPO standards PP 1/31(3). Guidelines for the biological evaluation of pesticides, Efficacy evaluation of fungicides & bactericides 2: 47-49

Fisher P., Runkle E. 2004. Lighting up profits, understanding greenhouse lighting. Ed. Meister Media Worldwide, USA pp. 98

Greer D.H., Weedon M.M. 2012. Interactions between light and growing season temperatures on, growth and development and gas exchange of Semillon (*Vitis vinifera* L.) vines grown in an irrigated vineyard. Plant Physiol Biochem. 54: 59-69

GCOS-200, 2016. The Global Observing System for Climate: Implementation needs. Implementation Plan. WMO, Geneva 2016 pp. 341

Giovanelli G., Lavelli V., Peri C., Nobili S. 1999. Variation in antioxidant compounds of tomato during vine and post-harvest ripening. Journal of the Science of Food and Agriculture, 79: 1583–1588

Giovannucci E., Rimm E.B., Liu Y., Stampfer M.J., Willett W.C. 2002. A prospective study of tomato products, lycopene, and prostate cancer risk. J. Natl. Cancer Inst. 94: 391–398

Hao X., Hal, B.A., Ormrod D.P., Papadopoulos A.P., 2000. Effects of pre-exposure to Ultraviolet-B radiation on responses of tomato (*Lycopersicon*

esculentum cv. *New Yorker*) to ozone in ambient and elevated carbon dioxide. Environmental Pollution 110, 217–224

Himbert M. 2009 A brief history of measurement, Eur. Phys. J. Special Topics 172, 25-35

Howard L.R., Clark, J.R., Brownmiller, C., 2003. Antioxidant capacity and phenolic content in blueberries as affected by genotype and growing season. Journal of the Science of Food and Agriculture 83: 1238–1247

IEC 60751:2008. Industrial platinum resistance thermometers and platinum temperature sensors. International Electrotechnical Commission, 2nd edition Geneva, pp. 46

ISO/IEC 17025, 2005 General requirements for the competence of testing and calibration laboratories. Italina edition. Ed. Commissione UNI-CEI Normative quadro per le attività di certificazione, pp. 36

Istat, 2017. Tavola CPOM - Superficie e produzione pomodoro, pomodoro da industria anno 2017. http://agri.istat.it/

Jagadeesh S.L., M.T. Charles, Y. Gariepy, B. Goyette, G.S. Raghavan V., Vigneault C. 2011. Influence of Postharvest UV-C Hormesis on the Bioactive Components of Tomato during Post-treatment. Handling Food Bioprocess Technol 4: 1463–1472

Javanmardi J., Kubota C., 2006 Variation of lycopene, antioxidant activity, total soluble solid and weight loss of tomato during postharvest storage. Postharvest Biol. Technol. 41: 151-155

Juran J.M. 1974. Quality-Control Handbook – Ed. McGraw Hill Higher Education, New York, 3rd edition pp. 1600

Krizek D.T., 2004. Influence of PAR and UV-A in determining plant sensitivity and photomorphogenic responses to UV-B radiation. Photochemistry and Photobiology 81: 1026–1037

Krizek D.T., Clark H.D., Mirecki R.M. 2005. Spectral Properties of Selected UV-blocking and UV-transmitting Covering Materials with Application for Production of High-value Crops in High Tunnels. Photochemistry and Photobiology 81: 1047-1051

Lafon R., Clerjeau M., 1988. Downy mildew. In: Pearson, R.C., Goheen, A.C. (Eds.), Compendium of Grape Diseases. APS Press, St. Paul, Minnesota, USA: 11–13

Lewis P., Cooke G. 2013 Developing a lean measurement system to enhance process improvement, Int. J. Metrol. Qual. Eng. 4(3): 145-151

Liu C., Jahangir M. M., Ying T. 2012. Effect of UV on chilling injury in tomatoes J Sci Food Agric 92: 3016–3022

Liu L.H., Zabaras D., Bennett L.E., Aguas P., Woonton B.W. 2009. Effects of UV-C, red light and sun light on the carotenoid content and physical qualities of tomatoes during post-harvest storage. Food Chemistry 115: 495–500

Luthria D.L., Mukhopadhyay S., Krizek D.T. 2006. Content of total phenolics and phenolic acids in tomato (*Lycopersicon esculentum* Mill.) fruits as influenced by cultivar and solar UV radiation Journal of Food Composition and Analysis 19: 771–777

Maharaj R., Arul J., Nadeau P. 1999. Effect of photochemical treatment in the preservation of fresh tomato (*Lycopersicon esculentum* cv. *Capello*) by delaying senescence. Postharvest Biology and Technology 15: 13–23

Maracchi G., Rossi F., Bogotaj L.K. Climate changes, impacts on agriculture, sustainability. In Survey of Agrometeorological practices and applications in Europe regarding climate change impact. Ed. Nejedlik and Orlandini pp 3-13

McBratney A., Whelan B., Ancev T., Bouma J. 2005. Future directions of precision agriculture. Precision Agriculture, 6, 7–23

Merlone A., Sanna F., Bell S., Beges G., et al., 2018. The MeteoMet2 Project–Highlights and Results. Measurement Science and Technologies 29 025802 pp. 17pp

Monteith, J.L., 2000. Agricultural Meteorology: evolution and application. Agric. For. Meteorol. 103:5–9

Monteith, J.L. and M.H. Unsworth, 2007: Principles of Environmental Physics. Plants, Animals, and the Atmosphere. Third edition. London, Edward Arnold, pp. 422

Mori K., Goto-Yamamoto N., Kitayama M., Hashizume K. 2007. Loss of anthocyanins in red wine grape under high temperature. J. of Experimental Botany. 58 (8): 1935-1945

Mukhopadhyay S., Luthria D.L., Robbins R.J., 2006. Optimization of extraction process for phenolic acids from black cohosh (*Cimicifuga racemosa*) by pressurized liquid extraction. Journal of the Science of Food and Agriculture 86: 156–162

Obande M.A., Tucker G. A., Shama G. 2011. Effect of pre-harvest UV-C treatment of tomatoes (*Solanum lycopersicon* L.) on ripening and pathogen resistance. Postharvest Biology and Technology 62: 188–192

Orlandini S., Dalla Marta A., D'Angelo I., Genesio R., 2003. Application of fuzzy logic for the simulation of *Plasmopara viticola* using agrometeorological variables. Bulletin OEPP/EPPO Bulletin 33: 415-420

Osseni L., Charki A., Kebe F., Calchera G., Martin L. 2015. Quality management: the challenges of regional governance in West Africa, Int. J. Metrol. Qual. Eng. 6(4): 404-410

Pertoll G., Pedri U., Raifer B. 2012. Effetti dell'irrigazione sulla crescita vegetativa, sulla produzione e sulla qualità del vino: risultati di prove pluriennali. Acta Italus Hortus. 3: 475-480

Prior R.L., Cao G., Martin A., Sofic E., McEwen J., O'Brien C., Lischner N., Ehlenfeldt M., Kalt W., Krewer G., Mainland C.M., 1998. Antioxidant capacity as influenced by total phenolic and anthocyanin content, maturity, and variety of *Vaccinium* species. J. Agric. Food Chem. 46: 2686–2693

Ranieri A., Giuntini D., Lercari B., Soldatini G.F. 2004. Light influence on antioxidant properties of tomato fruits. Progress in Nutrition 6: 44-49

Rossi V., Caffi T., Giosuè, S., Bugiani R., 2008. A mechanist model simulating primary infections of downy mildew in grapevine. Ecol. Modelling, 212: 480-491

Rossi V., Caffi T., Salinari F. 2012. Helping farmers face the increasing complexity of decision-making for crop protection. Phytopathologia Mediterranea 51(3): 457−479

Rippin, D. W. T. (1978), Parameter estimation in engineering and science, by James V. Beck and Kenneth J. Arnold, published by John Wiley and Sons, 1977. 501 + XIX pages. AIChE Journal, 24: 367. doi:10.1002/aic.690240233

Rozema J., Staaij JvD, Bjorn L.O., Caldwell M., 1997. UV-B as an environmental factor in plant life: stress and regulation. Trends Ecol. Evol. 12: 22–28

Sanna F, Cossu QA, Bellagarda S, Roggero G, Merlone A, 2014. Evaluation of EPI forecasting model with inclusion of uncertainty in input value and traceable calibration, Italian Journal of Agrometeorology, 12(3): 33-44

Santana M.A.A., Guimarães P.L.O., Lanza L.G., Vuerich E. 2015. Metrological analysis of a gravimetric calibration system for tipping-bucket rain gauges. Meteorological Application 22: 879–885

Siegfried W., Viret O., Bloesch B., Bleyer G. Kassemeyer H., 2004. VitiMeteo Plasmopara ein neues Prognosemodell für den Echten Mehltau. Schweizerische Zeitschrift für Obst- und Weinbau 140(23): 10-13

Stapleton A.E., 1992. Ultraviolet radiation and plants: burning questions. Plant Cell 4: 1353–1358.

Sullivan J.H., 2007. Possible impacts of changes in UV-B radiation on North American trees and forests. Environmental Pollution 137, 380–389

Todorov A. V., 1982. Lecture notes for training class IV. Agricultural meteorological personnel. WMO, Geneva, N. 593

Toor R.K., Savage G.P. 2005. Antioxidant activity in different fractions of tomatoes. Food Research International 38: 487–494

Tsormpatsidis E. Henbest R.G.C., Davis F.J., Battey N.H., Hadley P., Wagstaffe A. 2008UV irradiance as a major influence on growth, development and secondary products of commercial importance in Lollo Rosso lettuce 'Revolution' grown under polyethylene films. Environmental and Experimental Botany 63: 232–23

Turunen M., Heller W., Stich S., Sandermann H., Sutinen M.L., Norokorpi Y., 1999. The effects of UV exclusion on the soluble phenolics of young Scots pine seedlings in the subarctic. Environmental Pollution 106, 219–228

UNI EN 13206:2017. Materie plastiche - Film termoplastici di copertura per uso in agricoltura ed orticoltura. Ed. UNIPLAST - Ente Italiano di Unificazione nelle Materie Plastiche ICS. Milano pp. 56

Vakalounakis D.J. 1991. Control of early blight of greenhouse tomato, caused by *Alternaria solani*, by inhibiting sporulation with ultraviolet-absorbing vinyl film. Plant Disease, 75: 795- 797

Wang H., Cao G., Prior R.L., 1996. Total antioxidant capacity of fruits. J. Agric. Food Chem. 44: 701–705

WMO no. 134. 2010. Guide to Agricultural Meteorological Practices. Ed. 2010 update 2012 Geneva pp. 799

Wohlfahrt G., Gu L. 2015. The many meanings of gross photosynthesis and their implication for photosynthesis research from leaf to globe. Plant, Cell and Environment 38, 2500–2507

Acknowledgement

I would like to thanks the INRiM thermodynamic division research group (or Metrology for the Quality of Life), Graziano Coppa, Fabio Bertiglia, Chiara Musacchio and in particular Andrea Merlone for his friendly and scientific guidance, without him, this project would not have been possible.

Angela Calvo, my tutor and supervisor from the University of Turin, Deparment of Agricultural, Forest and Food Science (DiSAFA), for her advices and for the good job done together.

Roberto Deboli for his technical support, patience and comprehension, and Donatella Duraccio for her contribution on the analysis of the covering materials, both from IMAMOTER-CNR. Elena Zocca and Caterina Perrone from IPSP-CNR for their plants assistances and to let me use the IPSP's greenhouse.

At this point, some personal considerations are needed, in Italian is better.

Superata la soglia dei 40 anni mi trovo a raggiungere un altro traguardo. Come tutte le sfide, anche questa non è stata priva di difficoltà. I momenti di cedimento sono stati tanti così come i "ma chi me l'ha fatto fare". Ciò che mi ha fatto andare avanti, oltre agli incoraggiamenti delle persone a me care, è stata sicuramente la passione per la scienza e la voglia di migliorare nel mio piccolo questo strano mondo in cui stiamo vivendo.

Detto questo, alla classica domanda "Se potessi tornare indietro rifaresti questo percorso?" è difficile dare una risposta... se potessi tornare indietro non rifarei tante cose, ma sicuramente rifarei gli studi che ho fatto, magari con maggior impegno e in tempi più brevi!

Non posso non citare le mie care sorelle Alessia e Cristina e il mio papà, a loro va un grosso abbraccio.

Il pensiero più forte va a mia madre, che è stata sempre orgogliosa di me e dei miei successi nonostante tutto, e che per pochi mesi non ha avuto modo di starmi accanto per l'ennesima volta e festeggiare questo momento. Sarai sempre nei miei pensieri.